

2003

Subcellular Localization and Activity of the Multidrug Resistance Protein 1

Asha Rajagopal

Follow this and additional works at: http://digitalcommons.rockefeller.edu/student_theses_and_dissertations



Part of the [Life Sciences Commons](#)

Recommended Citation

Rajagopal, Asha, "Subcellular Localization and Activity of the Multidrug Resistance Protein 1" (2003). *Student Theses and Dissertations*. 327.
http://digitalcommons.rockefeller.edu/student_theses_and_dissertations/327

This Thesis is brought to you for free and open access by Digital Commons @ RU. It has been accepted for inclusion in Student Theses and Dissertations by an authorized administrator of Digital Commons @ RU. For more information, please contact mcsweej@mail.rockefeller.edu.

LD
444.5
R166
2003



THE LIBRARY

Rockefeller University Library
1230 York Avenue
New York, NY 10021-6399



**Subcellular Localization and Activity of the multidrug resistance
protein 1**

A thesis presented to the faculty of
The Rockefeller University
in partial fulfillment of the requirements
for the Degree of Doctor of Philosophy

by
Asha Rajagopal

April 21, 2003
The Rockefeller University
New York

TABLE OF CONTENTS

TABLE OF FIGURES.....	v
ACKNOWLEDGMENTS	viii
LIST OF ABBREVIATIONS	ix
ABSTRACT.....	1
CHAPTER ONE: A BRIEF INTRODUCTION TO MULTI-DRUG RESISTANCE AND THE ABC TRANSPORTER FAMILY	2
1.1 MULTI-DRUG RESISTANCE DEFINED	2
1.2 ABC TRANSPORTERS AND MULTI-DRUG RESISTANCE.....	4
1.3 MRP1	5
1.4 CONTEXTUALIZING OUR PRESENT STUDY	6
CHAPTER TWO: MATERIALS AND METHODS.....	9
2.1 Tissue culture	9
2.1.1 Cell lines	9
2.1.2 Transfections.....	9
2.2 DNA constructs.....	10
2.3 Western blot analysis	11
2.4 Fluorescence microscopy.....	11
2.5 Activity Assays and Fluorescence Quantification	13
2.5.1 Fluorescent chemotherapeutic reagents	13
2.5.2 Non-fluorescent chemotherapeutic reagents	13
2.5.3 Assays for speculated MDR modulators	14
2.6 Immunocytochemistry.	14

2.7	Crosslinking	14
2.8	Fluorescent labeling of subcellular compartments.	15
2.9	Glutathione assays.	15
2.10	Flow cytometry	16

CHAPTER 3 ASSESSMENTS OF MRP1-EGFP EXPRESSION AND

ACTIVITY..... 17

3.1	Generation of MRP1-EGFP	17
3.2	Expressing the construct in HeLa cells	17
3.3	MRP1-EGFP is expressed in cells as a full-length protein.....	19
3.4	Fluorescent MRP1 activity assays	21
3.5	Weak bases doxorubicin, daunorubicin, and mitoxantrone	23
3.6	Microtubule-disrupting agents.	26
3.7	Overview	29

CHAPTER 4 LOCALIZATION OF MRP1..... 42

4.1	Expression in Polarized Cells	42
4.2	Perinuclear localization of MRP1-ECFP in multiple cell lines	43
4.3	Characterizing the sub-cellular distribution of MRP1	44
4.4	Quantifying co-localization	50

CHAPTER 5 SUBCELLULAR ACTIVITY OF MRP1 68

5.1	Drug sequestration	68
5.2	Doxorubicin localizes to MRP1-ECFP containing vesicles	70
5.3	Doxorubicin sequestration in MRP1-vesicles is dependent on MRP1 activity	72

5.4	BM[PEO] ₄ and BMH cross-link MRP1-ECFP	77
5.5	BM[PEO] ₄ and BMH do not increase cell permeability to MRP1 substrates	78
5.6	Expression of Pgp and BCRP also results in analogous doxorubicin sequestration	79
5.7	Discussion	80
CHAPTER 6 MRP1 ACTIVITY AND GLUTATHIONE.....		97
6.1	Glutathione co-transport model	97
6.2	Glutathione co-transport: evaluating the data	99
6.3	Methods of studying glutathione dependence <i>in vivo</i>	101
6.4	Testing human MRP1 activity in mouse.....	103
6.5	MRP1 is active in GCS2-NAC cells, in the absence of glutathione.....	103
6.6	MRP1 is active in cells depleted of glutathione.....	105
6.7	BSO increases cell permeability to MDR substrates	107
6.8	Discussion	108
CHAPTER 7 CONCLUSION.....		128
BIBLIOGRAPHY		134

TABLE OF FIGURES

- Figure 3-1 Proposed topology of MRP1 and MRP1-EGFP
- Figure 3-2 Endogenous expression of MRP1 in HeLa cells
- Figure 3-3 HeLa cells MRP1-EGFP transfected HeLa cells over-express full length MRP1-EGFP
- Figure 3-4 MRP1-ECFP is active against the MDR substrate TMRE
- Figure 3-5 MRP1-EGFP has activity against weakly basic chemotherapeutic agents
- Figure 3-6 FACS analysis of MRP1-EGFP activity
- Figure 3-7 Methods of visualizing the microtubule cytoskeleton.
- Figure 3-8 Assaying MRP1 transport of microtubule depolymerizing agents.
- Figure 4-1 MRP1-ECFP is sorted to the baso-lateral membrane
- Figure 4-2 MRP1-ECFP localization in four cell types
- Figure 4-3 Localizing organelles using wide field epi-fluorescence microscopy
- Figure 4-4 MRP1-ECFP does not localize to the recycling endosomes
- Figure 4-5 MRP1-ECFP does not localize to the Golgi or the ER
- Figure 4-6 MRP1-ECFP does co-localize with a lysosomal marker
- Figure 4-7 MRP1-EYFP co-localizes with synaptotagmin VII
- Figure 4-8 Wild-type MRP1 co-localizes with synaptotagmin VII
- Figure 4-9 Wild-type MRP1 co-localizes with the lysosomal marker cathepsin D
- Figure 4-10 Pgp-ECFP can also be found in vesicles positive for a lysosomal marker
- Figure 4-11 BCRP-ECFP is found in lysosomes

Figure 4-12 CFTR-ECFP is not found in lysosomes.

Figure 4-13 Co-localization of MRP1-EYFP and MRP1-ECFP, and Golgi-EYFP with Cy3-Transferrin.

Figure 4-14 Correlation Coefficients permit quantification of protein co-localization

Figure 5-1 Doxorubicin sequestration in MCF7-Adr cells.

Figure 5-2 The expression of MRP1 in drug sensitive MCF7 cells.

Figure 5-3 Doxorubicin redistribution upon the expression of MRP1.

Figure 5-4 Doxorubicin localizes to MRP1-ECFP-positive vesicles.

Figure 5-5 Accumulation of doxorubicin in MRP1-positive regions is dependent on MRP1 activity, and not pH.

Figure 5-6 Crosslinking MRP1-ECFP interferes with its ability to transport substrates at the plasma membrane, as assayed by TMRE accumulation.

Figure 5-7 MRP1-ECFP actively sequesters doxorubicin in internal compartments.

Figure 5-8 The effect of crosslinking on the electrophoretic mobility and transport activities of MRP1-ECFP.

Figure 5-9 Pgp and BCRP co-localize with a lysosomal marker and accumulate doxorubicin in regions positive for Pgp or BCRP.

Figure 6-1 Glutathione bio-synthetic pathway and generation of a glutathione deficient mouse line.

Figure 6-2 Confirmation of the disruption in γ -GCS in GCS2-NAC cells.

Figure 6-3 MRP1-ECFP is expressed, properly targeted, and functional in a mouse cell line.

Figure 6-4 MRP1 is active in GCS2-NAC cells.

Figure 6-5 Quantification of MRP1-dependent drug transport in glutathione depleted cells.

Figure 6-6 BSO incubation depleted intracellular glutathione stores by more than 80%.

Figure 6-7 MRP1 is active in HeLa cells depleted of cellular glutathione via BSO.

Figure 6-8 MRP1 is active against daunorubicin in HeLa cells depleted of cellular glutathione via BSO.

Figure 6-9 Quantification of MRP1-dependent drug transport in HeLa cells depleted of glutathione via BSO.

Figure 6-10 Evaluation of the effect of BSO on cells expressing varied levels of MRP1.

Figure 6-11 BSO increases cellular drug accumulation and has cytotoxic effects in NIH3T3 cells.

Acknowledgments

If this dissertation is small in scope, the intellectual guidance that fostered it is by no means so. Through the course of my studies here at Rockefeller, and elsewhere, many have taught me, and many have cultivated, by their example, a curiosity for the mechanism, and art, of living things. For their support, and encouragement, I am grateful.

Specifically, I would like to thank David Gadsby, Tarun Kapoor, and Kathleen Scotto, the members of my committee, for taking the time to help. I would like to thank the members of my lab, past and present, for all their years of support. And I would like to thank my teachers: Collin and Dr. Dauwalder, for sharing with me their love of living things; Yu and Martin, for always listening and helping; and Sandy, for his patience, his interest, and, most of all, for his kindness.

List of Abbreviations

ABC	ATP-binding cassette protein
Adr	adriamycin (aka doxorubicin)
ATP	adenosine triphosphate
BFA	Brefeldin A
BSO	buthione sulfoximine
CFTR	cystic fibrosis transmembrane conductance regulator
CMV	cytomegalovirus
DMEM	Dulbecco's Modified Eagle Medium
DMSO	dimethyl sulfoxide
DNA	deoxyribonucleic acid
ECFP	enhanced cyan fluorescent protein
EDTA	ethylenediaminetetraacetic acid
EGFP	enhanced green fluorescent protein
ER	endoplasmic reticulum
EYFP	enhanced yellow fluorescent protein
FACS	fluorescence-activated cell sorting
GCS	glutamyl cysteine synthetase
GSH	reduced glutathione
GST	glutathione-S-transferase
HBSS	Hanks buffered saline solution
HHBSS	Hanks buffered saline solution with Hepes
HPLC	high performance liquid chromatography
kDa	kilodalton

LP	long pass
MDCK	Madin-Darby canine kidney
MDR	multidrug resistance
MDR1	Multidrug resistance 1 (encodes Pgp)
MRP1	Multidrug resistance protein 1
MTOC	microtubule organizing center
NAC	N-acetyl cysteine
NHDF	normal human dermal fibroblast
NNAL	4-(methylnitrosamino)-1-(3-pyridyl)-1-butanol
PBS	phosphate buffered saline
PCR	polymerase chain reaction
Pgp	P-glycoprotein
Tfn	transferrin
TLC	thin layer chromatography
TMRE	tetramethyl rhodamine ester
YCF1	yeast cadmium factor protein 1

Abstract

Multi-drug resistance or MDR is a major impediment to the successful administration of chemotherapy. Broadly defined, the term MDR applies to any mechanism the cell uses to counter the effects of chemotherapeutic agents, protecting the cell at once against the toxicity of many, structurally dissimilar compounds. There are several routes to MDR for a cell, and they include everything from decreasing intracellular drug concentrations to increasing rates of drug metabolism. The study presented here focuses on the role of drug transporters in conferring drug resistance. MDR transporters are traditionally thought to extrude cytotoxins from the cell at the plasma membrane, and they thereby serve as a permeability barrier for drug entry into the cell. Several MDR transporters have been cloned to date, but this study focuses on the functional characterization of one of these proteins, the human multidrug resistance protein 1 or MRP1.

MRP1, like other members of the MDR transporter family, is thought to be expressed at the plasma membrane and decrease the intracellular accumulation of many different chemotherapeutic compounds. Unlike other MDR transporters, however, MRP1 is thought to require reduced glutathione to enable the transport of most of its chemotherapeutic substrates. Using a fluorescently tagged MRP1 protein, we make two novel demonstrations: that MRP1 can contribute to a drug resistance phenotype from intracellular membranes, as well as from the plasma membrane; and two, that MRP1 is active in the absence of glutathione.

Chapter One: A Brief Introduction to Multi-drug Resistance and the ABC transporter family

1.1 Multi-drug Resistance Defined

Cellular multi-drug resistance or MDR is a significant obstacle to the successful administration of chemotherapy. Broadly defined, the term MDR applies to any mechanism the cell uses to counter the effects of chemotherapeutic agents, protecting the cell at once against the toxicity of many, structurally dissimilar compounds. There are several routes to MDR for a cell, and they include everything from decreasing intracellular drug concentrations to increasing rates of drug metabolism (see two recent reviews (Gottesman, 2002; Gottesman *et al.*, 2002)). I will briefly give an overview of the cellular mechanisms of acquiring drug resistance, organizing the discussion under two general subheadings: one, diminishing drug availability to cellular targets, and two, altering drug sensitivity.

Decreasing the availability of drugs to their cellular targets can occur simply by reducing the rates of drug entry. For drugs that enter cells by passive diffusion, for example, structural changes at or near the plasma membrane can alter rates of drug entry. Recent research into drug resistance in polarized epithelial cells, for example, suggests that barriers to drug diffusion are created in an “entrance compartment” by micro-villi and an associated actin cytoskeleton (Lange and Gartzke, 2001). For those drugs that enter cells by utilizing existing cellular machinery, decreases in drug uptake can occur either as a result of changes in the endocytic pathway or in plasma membrane receptors. Resistance to the anti-folate drug methotrexate, for example, often occurs as a result of mutations in the two transporters responsible for folate uptake, transporters co-

opted by the drug to enter the cell (for a review, see *Cancer, Principles and Practices of Oncology*). Decreased drug presentation can also occur if the drug is sequestered away from cellular targets once it has entered the cell. The chemotherapeutic doxorubicin, for instance, accumulates in the lysosomes of drug resistant cells, and is thus kept from the nucleus, where it is known to induce apoptosis by damaging DNA (Schindler *et al.*, 1996; Hurwitz *et al.*, 1997). Finally, drugs can be less available at their cellular targets because they are effluxed from the cell upon entry. Drug efflux pumps like the well studied P-glycoprotein are expressed at the plasma membrane and actively extrude chemotherapeutics in an ATP-requiring transport event. Transporters like P-glycoprotein will be the subject of this study and will be discussed subsequently in further detail.

Under the second subheading of acquiring MDR, we find all the methods available to the cell to reduce cellular sensitivity to MDR agents. Increasing rates of DNA repair, for example, or inhibiting apoptosis, both increase survival rates in response to chemotherapeutics. Drugs can also be metabolized, thereby altering their toxicity. Cisplatin resistance, for example, is associated with increases in the expression of the gene encoding glutathione-S-transferase π (GST). Moreover, GST-mediated glutathione conjugation is frequently associated with drug resistance to alkylating compounds like melphalan (Yokomizo *et al.*, 1995), as well as many other electrophilic chemotherapeutics (Morrow *et al.*, 1998). Other detoxification pathways exist, and are broadly classified under two general categories: Phase I detoxification, in which a functional group is added or exposed (usually via a cytochrome P-450 enzyme) or Phase II detoxification, in which drugs undergo conjugation reactions via

glutathionation, sulfonation, acetylation or methylation (see *Cancer, Principles and Practices of Oncology*). Finally, cells can become MDR by altering their sensitivity to the anti-proliferative nature of chemotherapeutic agents, with less stringent cell cycle regulation, for example.

1.2 ABC transporters and Multi-drug resistance

To date, 48 human transporters belonging to the ATP-binding cassette (ABC) family of proteins have been identified (Muller, 2003), and a number of them have been implicated in the development of multi-drug resistance. These transporters confer drug resistance by actively extruding chemotherapeutic compounds from the cell, in an ATP-dependent manner. The first and probably most well characterized ABC protein involved in acquiring MDR is P-glycoprotein, encoded by the multidrug resistance 1 (MDR1) gene. Over-expression of the cDNA encoding P-glycoprotein is sufficient to confer drug resistance to many structurally unrelated cytotoxins, including those administered in chemotherapy, like the anthracyclines, the vinca-alkaloids, and colchicine (Gros *et al.*, 1986; Chen and Simon, 2000). P-glycoprotein (Pgp) is a 170-kDa protein, expressed in the apical membrane of polarized cells, whose expression can be inversely correlated with the successful administration of chemotherapy (Chan *et al.*, 1991). Structurally, Pgp and other members of the ABC family generally consist of a core of 12 transmembrane domains and two nucleotide binding domains, although there are some notable exceptions (Borst and Elferink, 2002). The breast cancer resistance protein or BCRP, for example, is a half transporter, and consists of only 6 transmembrane domains and one nucleotide binding domain. The multi-drug resistance protein 1, as well as other members of

the MRP family, have a core structure similar to Pgp, with a 280 amino acid N-terminal extension (Bakos *et al.*, 1998). However, what these MDR-conferring ABC proteins all share is the ability to significantly reduce the intracellular concentration of many structurally unrelated compounds when over-expressed at the cell surface.

1.3 MRP1

Human MRP1, or the multidrug associated protein 1, is a 190-kDa member of the ABC family of transporters. The gene encoding MRP1 is to be found on chromosome 16; it spans 200 kb minimally and includes 31 exons, as well as multiple class 0 introns (Grant *et al.*, 1997). As its name suggests, the protein is thought to be responsible for conferring multidrug resistance in a variety of cancers and has, like Pgp, become a major obstacle to the successful administration of chemotherapy. First cloned in 1992 from a daunorubicin resistant lung cancer cell line (Cole *et al.*, 1992), MRP1 has since been associated with increased resistance to doxorubicin, vincristine, VP16, and colchicine. MRP1 is expressed ubiquitously throughout the body (Borst *et al.*, 2000), and MRP1 mRNA has been found in a large variety of tumor types (Hipfner *et al.*, 1999). Moreover, increased expression of the transporter has been shown to correlate with poor clinical outcomes (Hipfner *et al.*, 1999).

Physiologically, MRP1 is thought to extrude the cysteinyl leukotriene LTC₄ from the cell, as well as other conjugated organic anions. Its ability to transport LTC₄ has suggested a role for MRP1 in mediating the migration of dendritic cells to the lymph nodes, as extrusion of LTC₄ in these cells is necessary for chemotaxis to the chemokine CCL19 (Robbiani *et al.*, 2000). Its transport of

LTC₄ has also implicated MRP1 in regulating inflammation in tissues, as MRP1 null mice were deficient in both LTC₄ transport, as well as LTC₄-dependent inflammatory responses (Wijnholds *et al.*, 1997). Additionally, MRP1-mediated LTC₄ transport has been found to correlate with increased sensitivity to *Streptococcus pneumoniae*, as increased intracellular concentrations of LTC₄ negatively regulate LTC₄ biosynthesis, and thereby increase production of another cysteinyl leukotriene LTB₄, an important elicitor of microbiocidal responses in phagocytic cells (Schultz *et al.*, 2001).

Despite these physiological roles, *mrp1* null mice are viable, fertile, and show no developmental phenotypes or discernable changes in body or organ morphology (Wijnholds *et al.*, 1997). However, these mice have substantially increased sensitivities to MDR drugs like VP16 and vincristine (the latter only in isolated bone marrow derived mast cells). As a result of exposure to etoposide-phosphate, *mrp1* null mice show extensive damage in the oropharyngeal mucosal layer, the testicular tubules, and the choroid plexus epithelium, suggesting that the protein actively protects against xenobiotic agents in these tissues (Wijnholds *et al.*, 1998; Wijnholds *et al.*, 2000). Mouse *mrp1* is also thought to contribute to the blood brain drug permeability barrier (Wijnholds *et al.*, 2000).

1.4 Contextualizing our present study

Despite these many and substantial advances in our understanding of MRP1 activity, both in normal and in patho-physiology, many avenues still remain open for MRP1 studies. Previous biochemical and whole cell investigations of MRP1, for example, have produced a number of inconsistent reports of MRP1 substrate specificity and activity in general. Some *in vivo*

studies have found MRP1 to be functional in intracellular compartments (Tommasini *et al.*, 1996), while others have seen MRP1 active primarily at the plasma membrane. Some studies have suggested MRP1 to be active against mitoxantrone, cadmium, vinblastine, and colchicine (Tommasini *et al.*, 1996), while others have found MRP1 to confer no increased resistance to these compounds. Some of these inconsistencies may be due to the different cell lines used to study MRP1; many no doubt are due to the culture conditions used to model *in vivo* MRP1 activity. Cells are either continuously cultured in chemotherapeutic agents or selected in antibiotics to ensure MRP1 expression. These culture conditions have been shown to result in massive physiological changes in the cell, including the up-regulation of DNA repair enzymes, the down-regulation of apoptotic machinery, resulting in the generation of multifactorial drug resistance (Chen and Simon, 2000). Therefore, the changes induced by drug selection could not be distinguished from the effect of MRP1 expression.

For all these reasons, we have developed a means of studying MRP1 activity in whole cells without protracted drug selection. We have created a GFP fusion construct which tags the C terminus of MRP1 and permits easy identification of MRP1 expression in cells. The fusion protein additionally allows us to correlate degrees of MRP1 expression with GFP fluorescence, and thereby makes direct studies of MRP1 activity possible. By comparing cells transiently transfected with the MRP1-EGFP fusion construct to their non-transfected counterparts, we can assess the immediate effect that MRP1 introduction has on a cell's drug resistance properties. Transient transfection with the MRP1-EGFP fusion construct obviates the need for protracted propagation in antibiotics and

product guidelines. To increase the transfection efficiencies of primary and embryonic stem cell lines, endotoxin free DNA was used; endotoxin-free DNA was purified using the Endo-free plasmid purification kit from Qiagen.

2.2 DNA constructs.

The plasmid encoding synaptotagminVII-ECFP was a gift from Norma Andrews, Yale University, New Haven, Connecticut (Litman *et al.*, 2000). The plasmid encoding ECFP-CFTR was a gift of David Gadsby, Rockefeller University, New York, New York. The pEYFP-ER and the pEYFP-Golgi vectors were purchased from BD Biosciences Clontech, Palo Alto, California.

The construction of the pMDR1-ECFP plasmid has been previously described (Chen and Simon, 2000). Briefly, the MDR1-EGFP fusion vector was made using site-directed mutagenesis to replace the 3' stop codon with a SalI site. The MDR1 open reading frame was then inserted into pEGFP-N1 (Clontech). The EGFP coding region was then excised and replaced with ECFP, using ApaI and BsrGI restriction enzymes.

BCRP cDNA was a generous gift of Doug Ross, University of Maryland, Baltimore, Maryland (Doyle *et al.*, 1998); it was subcloned into the EGFPc1 plasmid (Clontech) between the *EcoRI* and *XhoI* sites. The pECFP-BCRP plasmid was made by replacing the EGFP coding sequence with the sequence of ECFP.

Human MRP1 cDNA was obtained in the cloning vector pGEM-11Zf (gift of Gary Kruh, Fox Chase). To generate an expression plasmid for wild-type MRP1, designated pMRP1, MRP1 cDNA was subcloned between the SacI and XbaI sites of pEGFP-N1 (Clontech, Palo Alto, CA), a step that excised the EGFP

coding sequence and created a pEGFP-N1-backbone plasmid with MRP1 placed under the control of the CMV promoter. To generate the MRP1-EGFP fusion protein, standard mutagenesis techniques were used on pMRP1 to replace the MRP1 stop codon with an AgeI site, the site at which GFP was introduced. pMRP1-ECFP and pMRP1-EYFP were created by replacing EGFP with ECFP or EYFP (Clontech).

2.3 Western blot analysis

MRP1 and MRP1-EGFP transfected cells were dissociated with Cell Stripper (Cellgro) and solubilized with 1% Triton X-100. The nuclear debris was removed by a low speed centrifugation and the supernatant was resolved on a 4-20% gradient gel, using SDS PAGE. After electro-transfer onto a membrane (Amersham Pharmacia Biotech, Piscataway, NJ) using a semi-dry electro-blotter, proteins were immunoblotted with either the MRPr1 anti-MRP1 rat monoclonal antibody (Alexis Biochemicals, San Diego, CA) and an alkaline phosphatase conjugated anti-rat IgG antibody (Sigma) or directly with the alkaline phosphatase conjugated Living Colors Peptide Antibody (Clontech).

2.4 Fluorescence microscopy

Cells were observed by fluorescent microscopy on fibronectin-coated (Sigma) glass bottom culture dishes (MatTek, Ashland, MA). Wide field fluorescence microscopy was performed with an IX-70 Olympus microscope using a 1.4 N.A. X60 oil-immersion objective, and an ORCA cooled CCD camera (Hamamatsu Photonics, Hamamatsu City, Japan) as previously described (Chen and Simon, 2000). Wide field fluorescence microscopy with deconvolution was

performed using a DeltaVision deconvolution microscope with a 1.4 N.A. oil-immersion 60X objective. The following excitation and emission filters were used for wide-field fluorescent microscopy: CFP: $\lambda_{\text{ex}} = 400\text{-}430\text{ nm}$, $\lambda_{\text{em}} = 460\text{-}500\text{ nm}$; GFP: $\lambda_{\text{ex}} = 480\text{-}490\text{ nm}$, $\lambda_{\text{em}} = 500\text{-}550\text{ nm}$; TMRE: $\lambda_{\text{ex}} = 530\text{-}560\text{ nm}$, $\lambda_{\text{em}} = 570\text{-}650\text{ nm}$. Confocal microscopy was performed on either an upright AxioPlan 2 microscope or an inverted Axiovert 100 microscope, each with an LSM 510 confocal attachment (Carl Zeiss, Thornwood, NY), using a 1.2 N.A. water-immersion 63X objective. The following excitation laser lines and emission filters were used: GFP: $\lambda_{\text{ex}} = 488\text{ nm}$, $\lambda_{\text{em}} = 500\text{-}530\text{ nm}$; daunorubicin, doxorubicin: $\lambda_{\text{ex}} = 488\text{ nm}$, $\lambda_{\text{em}} = 580\text{ nm}$ long pass (LP); and mitoxantrone: $\lambda_{\text{ex}} = 633\text{ nm}$, $\lambda_{\text{em}} = 650\text{ nm}$ LP.

Fluorescent images were analyzed using MetaMorph software (Universal Imaging, Downingtown, Pennsylvania). To quantify fluorescence intensities on a cell-by-cell basis, bright field images were used to acquire the cell boundary, and MetaMorph software was used to calculate the average intensity within the cellular boundary for each fluorophore. The mean of these averages was calculated, along with the standard error. Data was collated and graphed using software from Sigma Plot (SPSS Science, Chicago, IL). The degree to which different fluorescent markers were said to correlate was determined by the correlation co-efficient for any two given fluorophores, where the correlation co-efficient is an expression of the degree to which the pixel intensities of two different fluorophores deviate from each other for a given area within a micrograph. Correlation co-efficient calculations were performed using MetaMorph software.

2.5 Activity Assays and Fluorescence Quantification

2.5.1 *Fluorescent chemotherapeutic reagents*

Tetramethyl rhodamine ester or TMRE was purchased from Molecular Probes, Eugene, Oregon. Mitoxantrone was purchased from Sigma. Doxorubicin and daunorubicin were purchased from Calbiochem, La Jolla, California.

MRP1, BCRP, and Pgp activity assays were conducted similarly. 24-48 hours after transfection, cells expressing fluorescent conjugates of the transporter of interest were washed in HHBSS, incubated in either 50 nM TMRE, 1-10 μ M daunorubicin, 1-10 μ M doxorubicin, or 1-10 μ M mitoxantrone for 15 minutes in a 5% pCO₂ incubator, and observed by fluorescent microscopy. All chemotherapeutic reagents, with the exception of TMRE, were washed out prior to observation.

2.5.2 *Non-fluorescent chemotherapeutic reagents*

Vincristine, vinblastine, and colchicine were purchased from Calbiochem. Cells expressing fluorescent conjugates of the transporters of interest were washed in HHBSS, incubated in 100-600nM vincristine, 100-600nM vinblastine, or 2 μ M colchicine for different time intervals in a 5% CO₂ incubator, then washed in HHBSS, and subsequently fixed and immunostained to visualize the microtubule cytoskeleton. To visualize microtubules, cells were washed in chilled phosphate buffered saline (PBS), permeabilized with ice-cold methanol for 10 min at 20 °C, washed in ice cold PBS, and immuno-labeled with Cy3-labeled anti- β tubulin antibody (Sigma) according to manufacturer's instructions.

2.5.3 Assays for speculated MDR modulators

Verapamil was used to inhibit MRP1 transport activity at 50 μ M. Buthione sulfoximine (BSO) was purchased from Sigma. Cells were incubated in 25 μ M BSO for 24 hours prior to assays of MDR transport or intracellular glutathione concentration, and was present during all transport assays.

2.6 Immunocytochemistry.

For fixation, cells were washed with chilled phosphate buffered saline (PBS), permeabilized with ice-cold methanol for 10 min at 20 °C, and rinsed twice with cold PBS. To detect MRP1 or cathepsin D, fixed cells were then incubated with the anti-MRP1 antibody MRP1r1 at 1:200 or with the anti-cathepsin D antibody cathepsin D (Ab-2) (Oncogene Research Products, San Diego, California) at 1:20 for one hour. Cells were subsequently washed and incubated for one hour in anti-rat Alexa594 (Molecular Probes) 1:1,000 for MRP1 or anti-rabbit fluorescein for cathepsin D imaging.

To visualize microtubules, MRP1-CFP transfected cells were fixed in 95% ethanol for 10 minutes at –20°C, washed in ice cold PBS, and immuno-labeled with Cy3-labeled anti- β tubulin antibody (Sigma) according to manufacturer's instructions.

2.7 Crosslinking

BM[PEO]₄ stock was prepared at 28mM in water and used at a hundred fold dilution in Hanks buffered saline solution with 10mM Hepes, pH 7.3 (HHBSS). Cells were exposed to the reagent at 37 °C for 10 minutes. The crosslinking reaction was quenched with 50mM L-cysteine in HHBSS (quenching

buffer) for 5 minutes at room temperature. Cells were subsequently washed with HHBSS and then assayed for MRP1 activity. Crosslinking with BMH was performed with a 90mM DMSO stock used at 1/1000X. Once again, cells were exposed to BMH for 10 minutes at 37 °C, then resuspended in quenching buffer for 5 minutes at room temperature, washed in HHBSS, and then assayed for MRP1 activity.

2.8 Fluorescent labeling of subcellular compartments.

In order to label the recycling endosome, cells were incubated with cy3-transferrin, as previously described (Lampson *et al.*, 2001). In order to label the lysosomes, cells were transfected with synaptotagmin VII-ECFP or were probed with an anti-cathepsin D antibody. Additionally, Texas Red dextrans were chased into the lysosomes as follows: cells were incubated in dextrans for 1 hour at 37 °C, washed in culture medium, washed again 1 hour later, and then allowed to remain in culture medium for 8-12 hours.

2.9 Glutathione assays.

Glutathione assays were performed using the FluoReporter Glutathione/Glutathione S-Transferase Assay Kit from Molecular Probes (Eugene, Oregon) according to manufacturer's instructions. Briefly, confluent cells were dissociated with Cell Stripper (Cellgro) and lysed in a solution containing 1% Triton X-100, protease inhibitor and 1mM EDTA. Cell lysates were then incubated in reaction buffer with kit-provided glutathione S-transferase enzyme and pentafluorobenzyl fluorescein for 30 minutes in a 37°C water bath. Reaction products were then assessed for fluorescent glutathione adducts using

thin layer chromatography (TLC). Samples were dotted onto TLC silica gel 60 F₂₅₄ plates (EM Science, Merk, Darmstadt, Germany), and then these plates were placed in a TLC chamber containing 60% 1-butanol, 20% methanol, and 20% water. Fluorescent adducts were detected and analyzed using standard techniques. This assay is advertised to be sensitive to within 10 μ M GSH.

2.10 Flow cytometry

Flow cytometry was performed on a FACSort (Becton Dickinson, San Jose, CA). Adherent cells were non-enzymatically dissociated using Cell Stripper, resuspended in Opti-MEM with fluorescent drugs and incubated at 37 °C for 30 min, and stored on ice until sample acquisition (not more than 30 min). The cells were harvested and resuspended in ice-cold PBS with a DNA stain to label dead cells [either 10 nM TOTO-3 iodide (Molecular Probes) or 1 μ M propidium iodide (Sigma)] immediately before data acquisition. The lasers and filters used were: GFP: λ_{ex} = 488 nm, λ_{em} = 500-520 nm; daunorubicin, doxorubicin, TMRE, propidium iodide: λ_{ex} = 488 nm, λ_{em} = 564-606 nm; and mitoxantrone, TOTO-3 λ_{ex} = 633 nm, λ_{em} = 650 nm LP.

3 Chapter 3 Assessments of MRP1-EGFP expression and activity

3.1 Generation of MRP1-EGFP

In the first chapter, we discussed some of the different approaches available to the study of multiple drug resistance, and particularly, that mediated by MRP1. The method that we have chosen to employ, fluorescence-based *in vivo* analysis of protein function, requires fluorescent labeling of both MRP1 and its drug substrates. A number of MRP1 substrates are naturally fluorescent and therefore could be used to monitor the drug transport activity of the protein. To label MRP1 itself with a fluorescent tag, we chose to add the enhanced green fluorescent protein to the C-terminus of MRP1 (Fig. 3-1). Using site-directed mutagenesis, we replaced the stop codon of the MRP1 cDNA with a restriction site that facilitated the addition of the enhanced green fluorescent protein or EGFP (see Materials and Methods). Once the EGFP tag was added to the C-terminus of MRP1, substitutions of the EGFP coding region were made which replaced the EGFP with the enhanced cyan fluorescent protein (ECFP), the enhanced yellow fluorescent protein (EYFP), or Ds Red.

3.2 Expressing the construct in HeLa cells

To determine whether the protein would be functional with a fluorescent tag, we transfected the MRP1-EGFP cDNA into HeLa cells, a cell line derived from a human, cervical adenocarcinoma. This cell line is easily transfected, adheres well to fibronectin-coated glass cover-slips, and, when adherent, exhibits a flattened morphology that makes it a good choice for epi-fluorescent microscopy. Although HeLa cells do express MRP1 endogenously, this

expression is not sufficient to confer drug resistance. For instance, non-transfected HeLa cells are 5 to 15 fold more sensitive to doxorubicin, daunorubicin, vincristine, and VP16 than HeLa cells transfected with, and over-expressing, MRP1 (Cole *et al.*, 1994). In our own investigations of non-transfected HeLa cells, we found that endogenously expressed MRP1 migrated as a doublet near the 250 kDa protein marker, a finding in keeping with the 190kDa molecular weight reported for MRP1 (Fig. 3-2, a). A similar MRP1 doublet has been seen in cells transfected with MRP1 cDNA reference, and this doublet most probably represents different glycosylation states of the protein (Bakos *et al.*, 1996).

Immunocytochemistry revealed the protein to be at the plasma membrane, and in another sub-cellular compartment, a distribution that has also been previously reported for the protein (Chang *et al.*, 1997). (Fig. 3-2, b). The sub-cellular distribution of the protein will be the subject of future chapters. Despite this endogenous expression of MRP1, the HeLa cell line remains sensitive to the addition of chemotherapeutics, and exogenous over-expression of the protein confers drug resistance and supports enhanced transport of various chemotherapeutic agents (Grant *et al.*, 1994). Of course, drug resistance is a relative term, and the sensitivity of non-transfected HeLa cells is simply a comparative assessment of drug toxicity. Endogenous MRP1 is most probably functional in HeLa cells, and the over-expression of this protein confers increased drug resistance. Moreover, because the HeLa cell line has been used frequently to examine the effects of MRP1 over-expression, both *in vivo* and *in vitro*, the cell line was an ideal starting point for our own investigations of MRP1-EGFP activity (Leier *et al.*, 1994; Cole *et al.*, 1994; Grant *et al.*, 1994; Leier *et al.*, 1996; Loe *et al.*,

1996a; Loe *et al.*, 1996b; Ito *et al.*, 2001; Qian *et al.*, 2001; Rybczynska *et al.*, 2001).

3.3 MRP1-EGFP is expressed in cells as a full-length protein

HeLa cells were therefore transfected with the MRP1-EGFP construct and examined first for protein expression. As with any fluorescent protein conjugate, we had to confirm that the observed fluorescence was from the EGFP-MRP1 fusion protein rather than a proteolytically cleaved fragment which contained just EGFP. In this way, we could ensure that we would not mistake free EGFP or partially proteolyzed protein for a full-length construct. We used two methods to ascertain whether the EGFP tag could be a reliable marker for MRP1: immunocytochemistry and Western blot. For the latter, cells were first transfected with MRP1-EGFP or wild-type MRP1, lysed, and then probed on immunoblots for the expression of MRP1 and EGFP (Fig. 3-3, a-b). Once again, over-expressed wild-type MRP1 was found to run as a doublet, near the 250-kDa marker, much like endogenously expressed MRP1 did (compare Fig 3-2 a, and Fig. 3-3, a, left lane). Likewise, the MRP1-EGFP protein band was also found to run as a doublet, but its electrophoretic mobility was slightly retarded relative to wild-type MRP1, a finding in keeping with the addition of a 27-kDa EGFP tag to MRP1 (Fig. 3-3, a, right lane). Protein fragments were not detectable in either lane, suggesting that there was very little protein degradation of either MRP1 or MRP1-EGFP. Probing cell lysates with an anti-EGFP antibody (an anti-Living colors peptide antibody) yielded similar results: no protein fragments were detectable in MRP1-EGFP transfected cells, and MRP1-EGFP ran as a doublet near a 250-kDa protein marker (Fig. 3-3, b).

Immunocytochemistry of MRP1-EGFP transfected cells also suggested that the EGFP fluorescent marker remained closely associated with MRP1. We found nearly identical fluorescence distributions for EGFP fluorescence as for immunofluorescence against MRP1, when cells were transfected with MRP1-EGFP, and then fixed and labeled with fluorescent anti-MRP1 secondary antibodies (Fig. 3-3, c-f). There was no evidence of free EGFP, for there was no EGFP fluorescence in the nucleus of MRP1-EGFP transfected cells (Fig. 3-3, c, truncated arrow), nor was there any cytosolic fluorescence. Free EGFP is known to accumulate in the nucleus and the cytosol when it is expressed in cells. However, EGFP fluorescence in MRP1-EGFP transfected cells remained primarily at the surface of the cell on the plasma membrane and in a region adjacent to the nucleus, a pattern very similar to that seen with endogenously-expressed, wild-type MRP1 (Fig. 3-2, b). In addition, the anti-MRP1 label in MRP1-EGFP expressing cells mirrored EGFP fluorescence: the MRP1 label was also at the plasma membrane and adjacent to the nucleus (Fig. 3-3, d). The merge of anti-MRP1 fluorescence (red) and EGFP fluorescence (green) revealed the extent of their co-localization; the two signals overlapped closely and created a more or less yellow image (Fig. 3-3, e). A line-scan of the merged image demonstrated the extent to which the two fluorophores had similar distributions across a given cell (Fig. 3-3, f). Further investigations of the sub-cellular localization of MRP1-EGFP were conducted, but discussion of this will be saved for the following chapter. For now, it is sufficient for us to note that two independent assays suggested that the N and C termini of MRP1-EGFP were always expressed in conjunction, the amino-terminal region of MRP1 being identified by the MRPr1 antibody (at amino acids 238-247 (Flens *et al.*,

1994;Chang *et al.*, 1997)) and the C-terminus by EGFP fluorescence.

Thus, it was most likely that MRP1-EGFP was being expressed in cells as a full length protein.

3.4 Fluorescent MRP1 activity assays

We now wanted to transfect the fluorescent MRP1 construct into cells and assay its transport activity. Our first activity assay was with TMRE, a fluorescent MRP1 substrate that enters the mitochondria of living cells. Because the fluorescence spectra of TMRE overlaps that of EGFP, we chose to transfect cells with MRP1-EGFP for our initial assessments of protein activity. Transient transfection with MRP1-EGFP resulted in a mixed population of cells: cells that expressed MRP1-EGFP to various degrees (high to low), as well as cells that did not express the protein at all. The latter population of cells served as an internal control. Relative to this control, the expression of MRP1-EGFP would result in decreased drug accumulation if the protein were active. Cells that expressed the fusion protein would be easily detectable by their ECFP fluorescence; if ECFP-positive cells consistently showed decreased TMRE fluorescence, we would judge the transporter to be functional against this substrate. When MRP1-EGFP transfected cells were loaded with TMRE, we found that the protein substantially reduced the intracellular accumulation of TMRE at steady-state (Fig. 3-4). In a field of transfected cells loaded with TMRE, the cell expressing MRP1-EGFP and visible by ECFP fluorescence (Fig. 3-4, a) was not visible under TMRE fluorescence (Fig. 3-4, b). Only the non-MRP1 expressing cells in the field, those not detectable by ECFP fluorescence, were illuminated under TMRE fluorescence (Fig. 3-4, b). The merge of the two fluorescent images made this drug

accumulation pattern clear: where there was ECFP fluorescence (green), there was no TMRE fluorescence (red), and where there was TMRE fluorescence, there was no ECFP fluorescence (Fig. 3-4, c).

Because TMRE is a live stain dye, we wanted to be sure that the absence of TMRE fluorescence in MRP1-EGFP expressing cells was not the result of compromised cell viability. We chose therefore to pre-incubate cells with verapamil, a known inhibitor of MRP1 activity, and then assay its effect on TMRE accumulation in transfected cells. If MRP1-EGFP expression were simply causing cell death, then the addition of verapamil should have no effect on TMRE exclusion in these cells; on the other hand, if TMRE exclusion in MRP1-EGFP expressing cells had been the result of MRP1-mediated transport, then the inhibition of MRP1 transport activity by verapamil would promote TMRE accumulation in these cells. When MRP1-EGFP transfected cells were pre-incubated in verapamil, we saw that MRP1-EGFP expressing cells (Fig. 3-4, d) were no longer able to exclude TMRE (Fig. 3-4, e-f), while non-expressing cells still accumulated the drug (Fig. 3-4, e-f). This experiment suggested active transport of TMRE by MRP1-EGFP.

Once we had established that MRP1-EGFP was both fully expressed and functional, we could now test the activity of the protein against substances that were more disputed substrates of MRP1. For example, previously published reports have suggested MRP1 to be active against the MDR substrates mitoxantrone (Morrow *et al.*, 1998), vinblastine, and colchicine, while others have found MRP1 to confer no increased resistance to these compounds (Cole *et al.*, 1994; Litman *et al.*, 2000). Studies involving the anthracyclines doxorubicin and daunorubicin have also suggested seemingly conflicting assessments of MRP1

transport. Although MRP1 expression has been associated with the efflux of daunorubicin from cells, MRP1-expression has not been associated with the cellular efflux of doxorubicin, despite the observation that MRP1 expression is sufficient to confer doxorubicin resistance (Cole *et al.*, 1991). If MRP1 is not conferring cellular resistance against doxorubicin by mediating its transport from the cell, then what other resistance mechanisms could it be promoting? We chose to investigate these questions next using our fluorescence-based *in vivo* transport assays.

3.5 The Weak bases doxorubicin, daunorubicin, and mitoxantrone

We began first with the chemotherapeutic agents daunorubicin, doxorubicin, and mitoxantrone. These weakly basic MDR substrates intercalate between the bases of DNA, inhibit topoisomerase II activity, and disrupt cellular replication (Vincent De Vita *et al.*, 2001). All three compounds are naturally fluorescent, and each has been suggested as an MRP1 substrate. In keeping with previous reports, we found that MRP1-EGFP expression substantially reduced the intracellular accumulation of daunorubicin. HeLa cells transfected with MRP1-EGFP and examined under confocal microscopy showed MRP1-mediated reduction in daunorubicin accumulation (Fig. 3-5, a-c), with MRP1-expressing cells (a) almost undetectable under daunorubicin fluorescence (b-c). However, drug efflux assays of doxorubicin were more difficult to interpret. The MRP1-EGFP expressing cells that were exposed to doxorubicin showed no significant reduction in drug accumulation relative to non-expressing cells (Fig. 3-5, d-f). The three cells in the center of the field in Fig. 3-5 (d), for example, were positive for both EGFP and doxorubicin fluorescence (Fig. 3-5, e-f). It is interesting to

note, though, that the nuclei of all three of these MRP1-positive cells showed almost no doxorubicin fluorescence. (Fig. 3-5, f, white arrow), while the nuclei of non-expressing cells showed a predominantly nuclear accumulation of the drug (Fig. 3-5, f, yellow arrow). Since MRP1-expressing cells have been reported to be resistant to the cytotoxic effects of doxorubicin, this decreased sensitivity may be the result of altered patterns of drug distribution in these cells, rather than the result of increased drug efflux. The nucleus is, after all, the primary sub-cellular target of doxorubicin toxicity. This question of MRP1-mediated drug resistance will be discussed in greater detail in chapter 5.

Transiently transfected HeLa cells were next incubated in 2 μ M mitoxantrone. Cells with elevated MRP1-EGFP levels (Fig 3-5, g, cell in the upper center with an arrow), showed diminished levels of mitoxantrone accumulation (Fig. 3-5, h). However, cells with lower levels of MRP1 (bottom center of Fig. 3-5, g), had levels of mitoxantrone that were indistinguishable from non-expressing cells (Fig. 3-5, h). In the merged image (Fig. 3-5, i), we can clearly distinguish a spectrum of drug accumulation that corresponds to the degree of MRP1-EGFP expressed in the cell. This pattern suggests that MRP1 is indeed active against mitoxantrone, if not quite as active as against daunorubicin, where EGFP fluorescence always correlated with drug exclusion. However, these comparisons of MRP1 activity are over-simplified, based on limited cell samples, and highly dependent upon the viewer's visual interpretation of the data. In order to facilitate more rigorous comparisons of MRP1 activity on different substrates, we decided to employ another fluorescence-based assay of drug transport, fluorescence activated cell sorting or FACS. With FACS, fluorescence

measurements are automated, and sample sizes are thereby increased many orders of magnitude above those permitted by fluorescence microscopy.

When FACS-based analyses of MRP1 activity were conducted on daunorubicin, we found that the expression of MRP1, represented by EGFP fluorescence, was associated with decreased drug fluorescence (Fig. 3-6, a). The range of MRP1-EGFP fluorescence varied over 100-fold, and over this range of expression, we saw drug reduction that, at its maximum, was slightly greater than 10 fold over background. Examinations of Pgp-mediated daunorubicin transport revealed a nearly identical activity range (Fig. 3-6, b). We next examined MRP1-mediated doxorubicin transport by FACS, and surprisingly enough, found that MRP1 expression had little effect on the total intracellular accumulation of doxorubicin (Fig. 3-6, c). This finding is in keeping with our studies of doxorubicin transport under confocal microscopy (Fig. 3-5, d-f), and support our preliminary hypothesis that MRP1 is altering patterns of intracellular drug accumulation, rather than contributing to drug efflux from the cell. Moreover, examinations of Pgp found a similar relationship: expression of the transporter did not contribute to decreased drug accumulation (Fig. 3-6, d). These data, along with the hypothesis that MDR transporters promote drug resistance by means other than drug efflux, will be discussed in subsequent chapters.

Finally, flow cytometry revealed that MRP1 activity against mitoxantrone (Fig. 3-6, e) was considerably diminished when compared to daunorubicin (Fig. 3-6, a). Cells expressing the highest level of MRP1-EGFP showed considerably less than a ten-fold reduction in drug accumulation (Fig. 3-6, e), an activity comparable to Pgp-EGFP expressing cells (Fig. 3-6, f). This weak activity may account for the differing assessments of mitoxantrone as a substrate of MRP1.

3.6 Microtubule-disrupting agents.

Thus far, we had seen that the expression of MRP1 was capable of decreasing the steady-state accumulation of fluorescent chemotherapeutic agents, as assayed by their fluorescence. We next wanted to determine whether these transport activities would also be able to reduce the cytotoxic effects of chemotherapeutic agents and thereby contribute to drug resistance. For this line of investigation, we chose to study another class of MDR substrates, microtubule depolymerizing reagents like the vinca alkaloids and colchicine. If MRP1-EGFP expression alone mitigated the depolymerizing effects of these reagents, then there would be a direct link between the expression of our fluorescent MRP1 construct and drug resistance. Moreover, we could also try to resolve for ourselves the previous controversy in the field regarding the substrate status of these drugs.

In order to proceed with these investigations, we needed a way of making the cytotoxic effects of these reagents amenable to fluorescence-based assays of MRP1 activity. In short, we needed a reliable method of visualizing microtubules after drug incubation. At first, we attempted co-transfections of MRP1-EYFP and tau-ECFP, the latter having been used as an indicator of microtubule structure in cells previously (Schmoranzner and Simon, *Mol. Biol. Cell*, in press). However, we needed long expression times (24-48 hours post transfection) to ensure functional MRP1. Unfortunately, these expression times resulted in the severe over-expression of tau-CFP; the protein was no longer reliably associated with the cytoskeleton and poorly represented the structure of microtubules (Fig. 3-7, a). We next chose to fix cells and probe them with an anti-tubulin antibody, a method

which yielded more reliable representations of the microtubule cytoskeleton. This latter method was sensitive enough to detect elaborate microtubule structures, including the microtubule organizing center or MTOC (Fig. 3-7, b arrow), a sensitivity necessary for assaying degrees of microtubule depolymerization in response to drug addition. In addition, immunocytochemistry allowed us to augment our fluorescent assays of MRP1 activity with another fluorescent protein: instead of co-transfecting with MRP1-EYFP and tau-ECFP, we could now follow the fluorescence of MRP1-EYFP and Pgp-ECFP and compare in this way the cyto-protective effects each protein afforded.

For these assays, then, one set of HeLa cells was transfected with MRP1-EYFP, another set was transfected with Pgp-ECFP, and these two sets were plated on the same dish for visualization. Cells either expressed MRP1-EYFP, or Pgp-ECFP, or they expressed no exogenous drug transporter and were therefore our control population of cells. When cells transfected and plated in this way were exposed to vincristine, and then examined for microtubule depolymerization, we found that both MRP1 and Pgp provided substantial chemo-protection against the cytotoxicity of vincristine (Fig. 3-8, a-e). The field of cells in Figs. 3a-e shows one cell strongly expressing MRP1-EYFP (Fig. 3-8, a), two cells strongly expressing Pgp-ECFP (Fig. 3-8, b), and a number of surrounding cells expressing neither protein (Fig. 3-8, d). The microtubules of non-expressing cells were severely disrupted by vincristine incubation, so much so that they had altered cell morphology (Fig. 3-8, d). These cells were round and considerably smaller than their MRP1-EYFP or Pgp-ECFP-tagged counterparts. However, the cell expressing MRP1-EYFP and the two cells expressing Pgp-ECFP showed

relatively little microtubule depolymerization; each cell had an intricate microtubule network. The microtubule-organizing center was intact in Pgp-ECFP expressing cells but not in the MRP1-EYFP expressing cells. Therefore, MRP1 provided some protection against the depolymerizing effects of vincristine, if not as much as Pgp.

Next, we assayed the effect of MRP1-EYFP and Pgp-ECFP on colchicine toxicity (Fig. 3-8, f-j). Cells incubated in 2 μ M colchicine were unable to maintain microtubule integrity in the absence of either multidrug resistance protein (Fig. 3-8, i). These cells were only diffusely stained with the anti-tubulin antibody, and they showed no discernable microtubule structure. The expression of Pgp-ECFP, however, prevented this loss; the ECFP-tagged cell (Fig. 3-8, g) had relatively undamaged microtubules, with the MTOC still intact (Fig. 3-8, h). Similarly, the two MRP1-EYFP expressing cells (Fig. 3-8, f) had a complex network of microtubules with the MTOC quite evident (Fig. 3-8, j).

Lastly, we examined the effect of expressing MRP1-EYFP on vinblastine toxicity, once again in the presence of ECFP-tagged Pgp. The field of cells in Figs. 3-8, k-n contained one MRP1-expressing cell (Fig. 3-8, k), four Pgp-ECFP expressing cells (Fig. 3-8, l) and a number of cells expressing neither protein (Fig. 3-8, n). Cells lacking both multidrug resistance proteins had clearly been affected by vinblastine; they had no extant MTOC and considerably disrupted microtubules (Fig. 3-8, n). All four cells expressing Pgp-ECFP showed relatively undisrupted microtubule structures, with a MTOC somewhat visible in each cell (Fig. 3-8, m). In contrast, the cell expressing MRP1-EYFP could not be distinguished from the non-expressing cells (Fig. 3-8, o). As evident in the detail of the anti-tubulin stained field (Fig. 3-8, o), the center cell with the least

microtubule structure was the one transfected with MRP1. The adjacent cell had only a slightly disrupted MTOC and was also faintly labeled with ECFP-tagged Pgp. The surrounding cells, which expressed neither MDR protein, had microtubules that had been severely damaged by vinblastine. It seems therefore, that MRP1, unlike Pgp, provides little to no protection against the effects of vinblastine. This differential effect of MRP1 expression on vincristine and vinblastine had been previously reported (Cole *et al.*, 1994).

3.7 Overview

In this chapter, we have seen that MRP1-EGFP can be used as a reliable indicator both of MRP1 localization and activity. The fusion construct allowed us to determine if the immediate introduction of MRP1 altered the cellular response to a chemotherapeutic challenge, and it did so in a way that correlated levels of MRP1-EGFP expression to the intracellular concentration of fluorescent substrates. After brief incubations in compounds previously reported to be MRP1 substrates, HeLa cells expressing MRP1-EGFP were examined for their ability either to affect intracellular drug distribution or to mitigate cytotoxic damage. In accordance with previous findings, MRP1-EGFP expression resulted in substantially diminished accumulation of TMRE and daunorubicin, and somewhat reduced levels of mitoxantrone. However, MRP1-EGFP had little effect on total doxorubicin concentrations inside the cell. Surprisingly, though, cells expressing the fusion construct did have significantly lowered doxorubicin fluorescence inside the nucleus, a reduction which may be responsible for MRP1-mediated resistance against this chemotherapeutic. Whether this altered nuclear distribution points to functional MRP1 away from the plasma membrane will be discussed in

subsequent chapters. When MRP1 expression was assayed for its ability to protect against the microtubule-depolymerizing effects of three chemotherapeutic agents, the protein was found to substantially attenuate the damage caused by colchicine, somewhat guard against vincristine-induced microtubule disruption, and have no detectable effect against vinblastine.

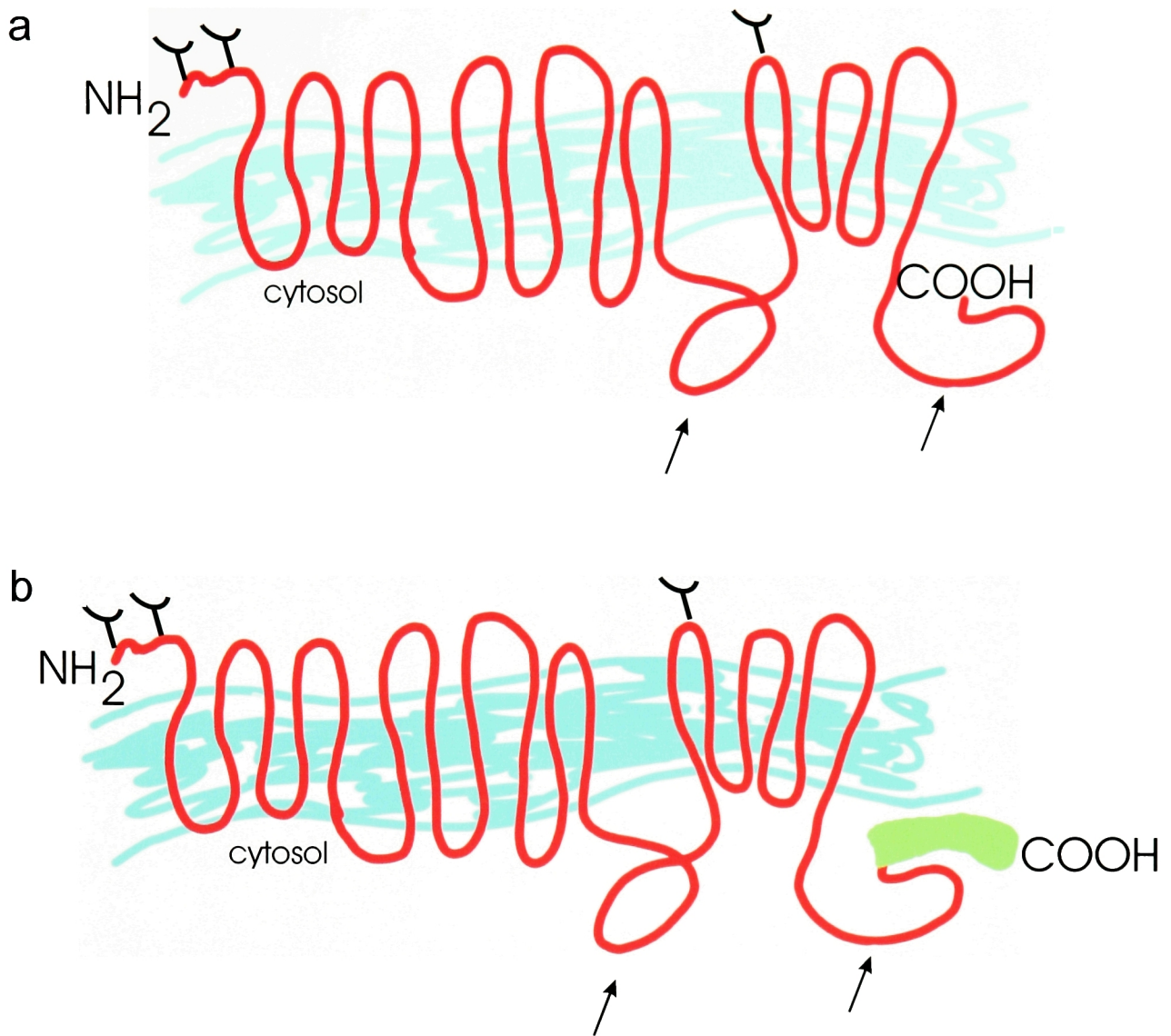


Figure 3-1 Proposed topology of MRP1 and MRP1-EGFP

a. A proposed topology of MRP1 is presented, showing the five trans-membrane (TM) domains thought to characterize its N-terminus, the remaining twelve TM domains with their nucleotide binding domains (indicated with arrows), and the three proposed glycosylation sites at Asn 19, Asn 23, and Asn 1006 (indicated by branched symbols). b. A sketch of the protein now with EGFP (in green) added to its C-terminus.

a

b

— — 250
— 105
— — 75
— 50
— — 35
— 30
— 25

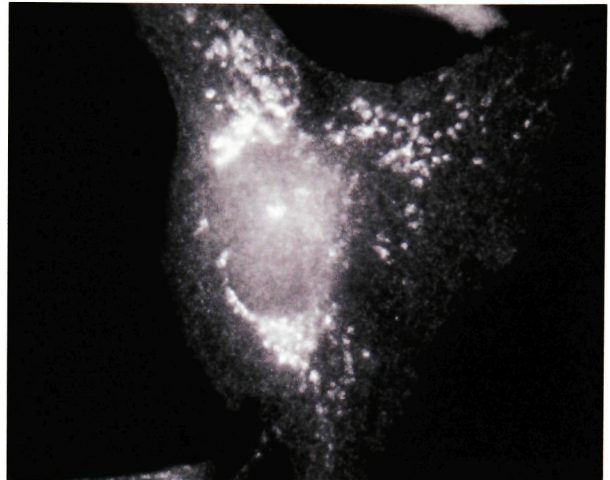
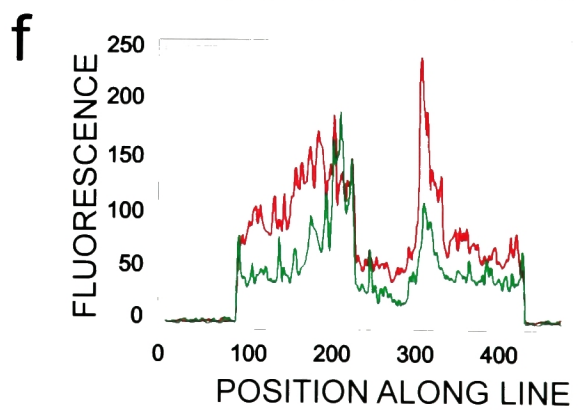
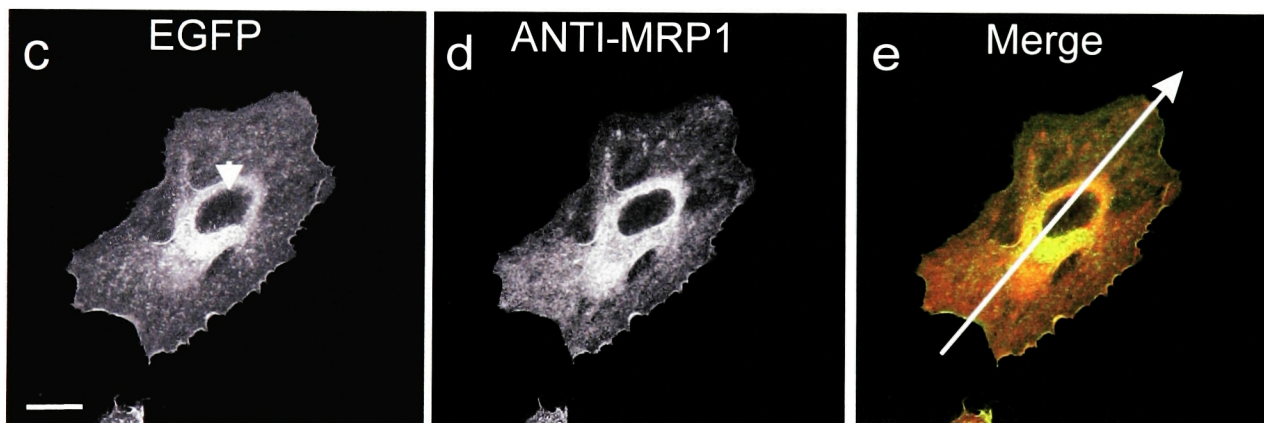
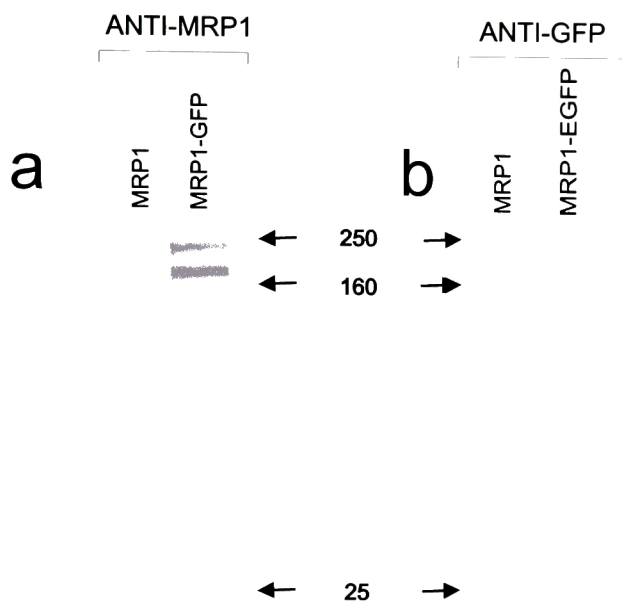


Figure 3-2 Endogenous expression of MRP1 in HeLa cells.

a. HeLa cell lysates were probed after SDS page for the expression of endogenous MRP1 on an immunoblot with the MRP1 antibody MRPr1. Two bands were detected near the 250 kDa protein marker, a result consistent with the reported 190 kDa mass for MRP1. The two fragments are thought to represent different glycosylation states of the protein. b. HeLa cells were probed for the subcellular distribution of endogenous MRP1 with the MRPr1 antibody. MRP1 was found at the plasma membrane and in a sub-cellular compartment.

Figure 3-3 MRP1-EGFP transfected HeLa cells over-express full length MRP1-EGFP. a-b. In lanes loaded with MRP1-EGFP transfected cell lysates, both an anti-MRP1 and an anti-GFP antibody recognized a doublet of reduced electrophoretic mobility, a doublet that would correspond to the addition of a 30 kDa EGFP to MRP1. No proteolysis products were recognized by either antibody. c-d. MRP1-EGFP transfected cells were probed with an anti-MRP1 antibody and examined under confocal microscopy to determine the extent of co-localization between the EGFP (c) and anti-MRP1 (d) fluorescent signals. EGFP fluorescence was merged with the fluorescence derived from labeled MRP1 (e) to demonstrate the extent of the colocalization. f. The relative fluorescence intensities of both labels were plotted in a line scan of the merged image. The scale bar for the micrographs is 20 μ m.



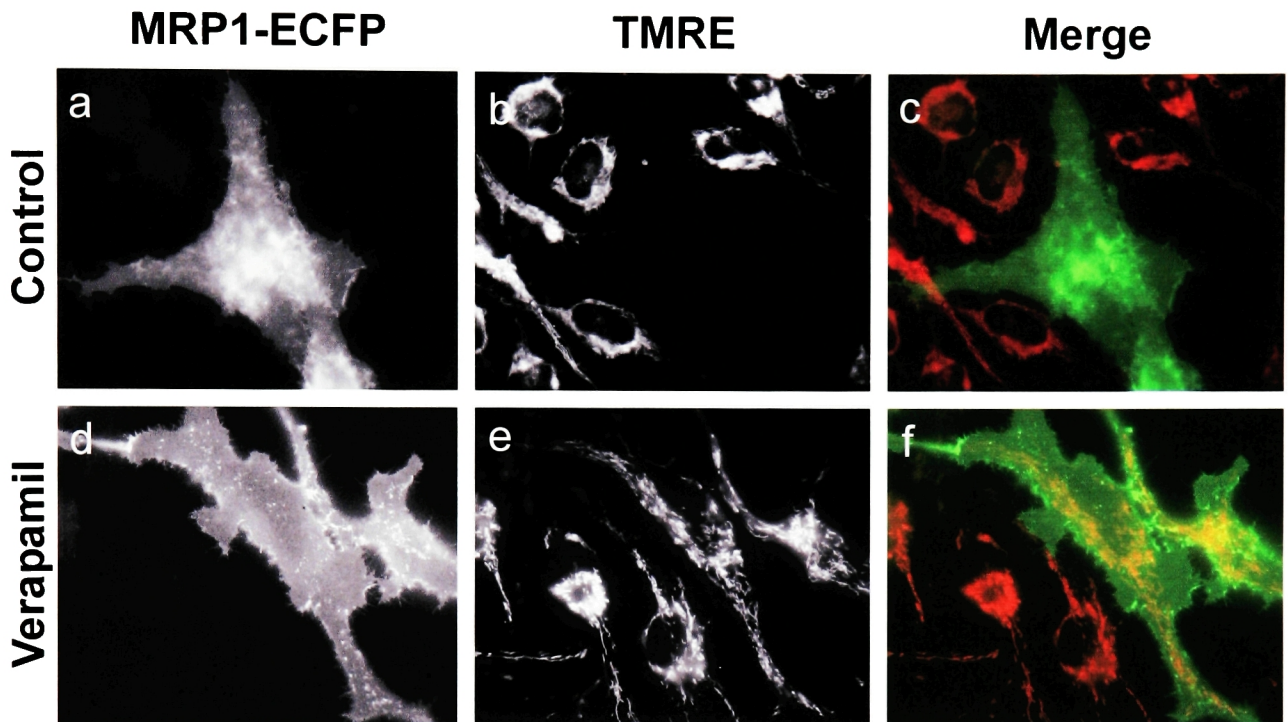


Figure 3-4 MRP1-ECFP is active against the MDR substrate TMRE.

a-c. MRP1-ECFP transfected HeLa cells were assayed for protein transport activity with TMRE, a live-stain dye which is also a known MRP1 substrate. The cell positive for MRP1-ECFP expression (a) showed reduced TMRE accumulation (b-c) compared to its non-MRP1-ECFP expressing counterparts (b-c). d-e. To determine whether the reduction in TMRE accumulation was as a result of loss of cell viability or active, MRP1-mediated transport, cells were treated with the MRP1 inhibitor verapamil prior to the TMRE assay. MRP1-ECFP expressing cells (d) now accumulated TMRE (e-f), suggesting that MRP1-ECFP was capable of active transport.

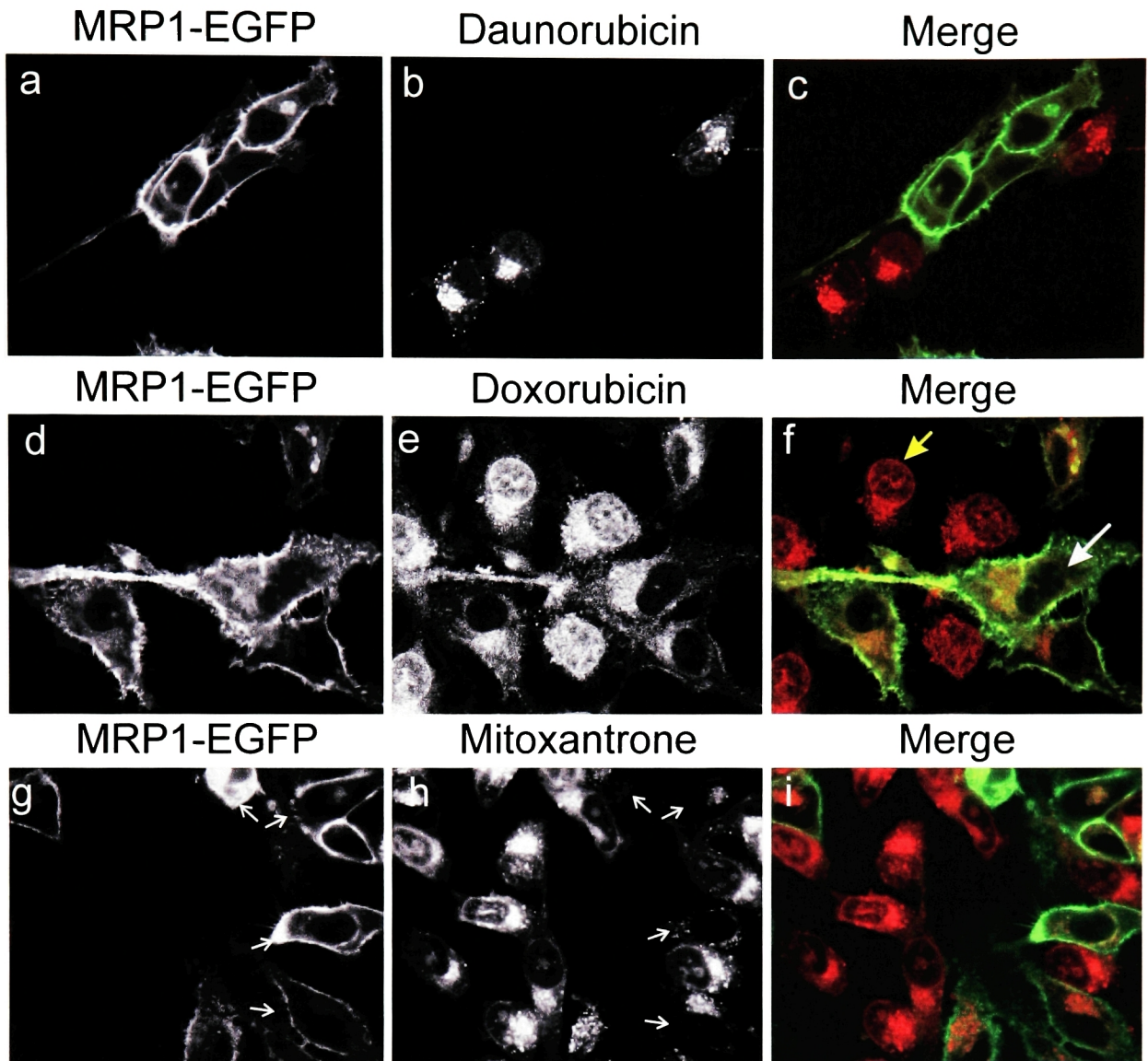
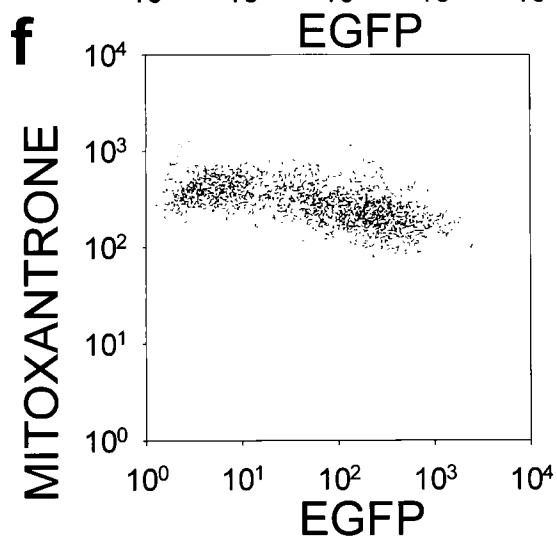
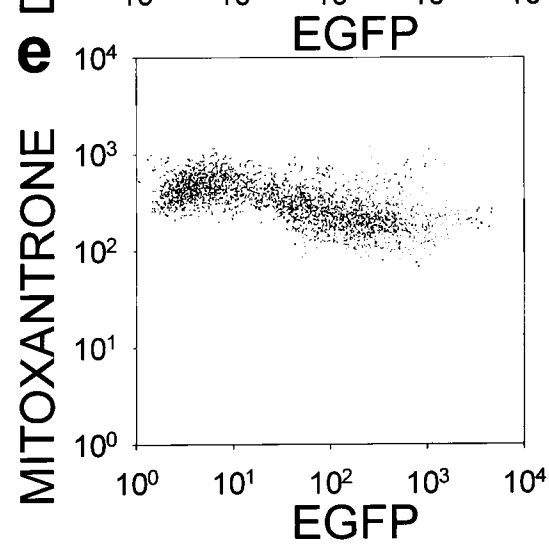
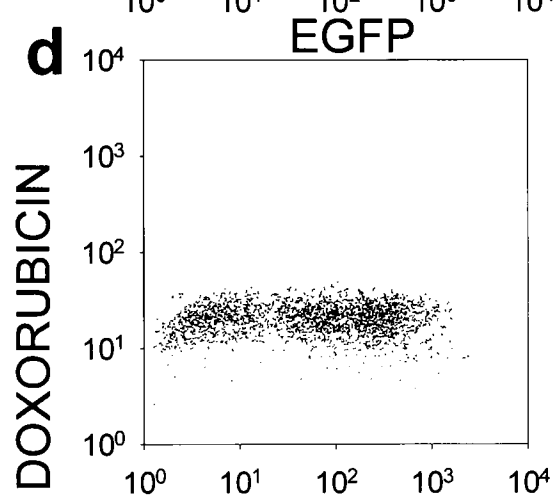
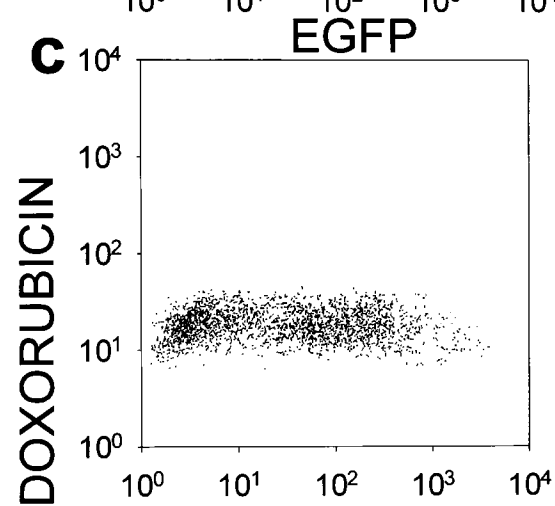
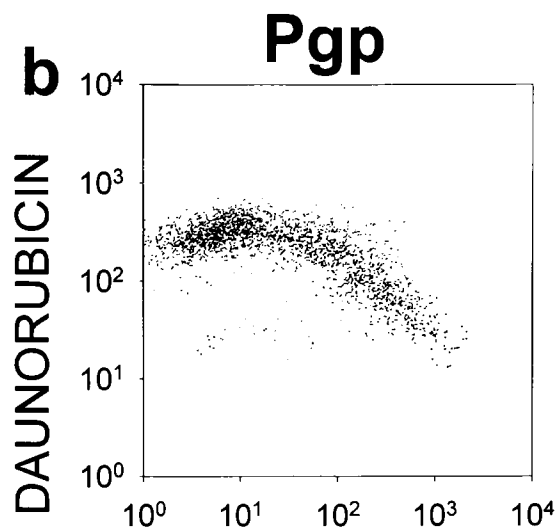
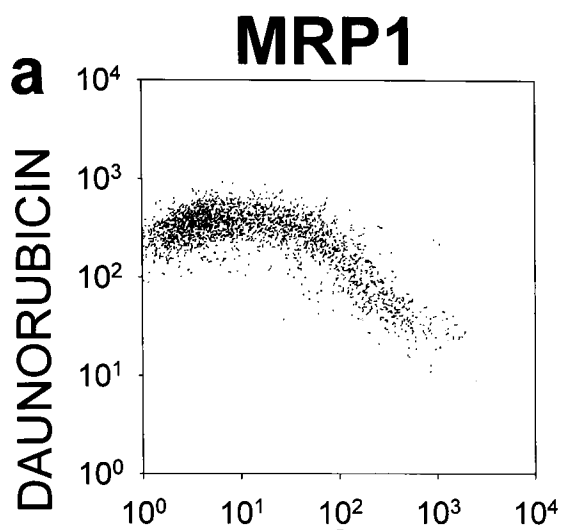


Figure 3-5 MRP1-EGFP has activity against weakly basic chemotherapeutic agents. HeLa cells were transiently transfected with MRP1-EGFP and observed 48 hours after transfection for the accumulation of fluorescent chemotherapeutic drugs. Cells incubated in 10 mM daunorubicin (a-c) showed nuclear and preinuclear accumulation of the drug after 15 minutes (b); however, expression of MRP1-GFP (a) substantially diminished the intracellular accumulation of daunorubicin, a pattern made evident in the merged image (c). When transiently transfected HeLa cells were incubated in doxorubicin (d-e), the expression of MRP1 (d) was able to alter the intracellular distribution of the drug so that it was no longer present in the nucleus (e). The merged image (f) makes this pattern clear. Finally, cells were incubated in 2 mM mitoxantrone and observed for MRP1-mediated changes in drug accumulation (g-i). MRP1 expression (g) resulted in a slight decrease in mitoxantrone accumulation (h), an observation made clear in the merged image (i).

Figure 3-6 FACS analysis of MRP1-EGFP activity.

a. The expression of MRP1-EGFP substantially diminished the intracellular accumulation of daunorubicin, a reduction that was greater than 10 fold when EGFP fluorescence was 100 fold over background. b. FACS was also performed of daunorubicin accumulation in Pgp-GFP transfected cells for comparison. c. When transiently transfected HeLa cells were incubated in doxorubicin, no change in the total intracellular accumulation of the drug was observed under FACS for MRP1-GFP expressing cells over the entire range of EGFP fluorescence. d. A FACS analysis of Pgp-EGFP expressing cells incubated in doxorubicin was conducted for comparison. e. Cells were incubated in 2 μ M mitoxantrone and observed for MRP1-mediated changes in drug accumulation. MRP1 expression only resulted in a slight decrease in mitoxantrone accumulation in cells with the greatest EGFP fluorescence. f. Pgp activity on mitoxantrone was used as a point of comparison.



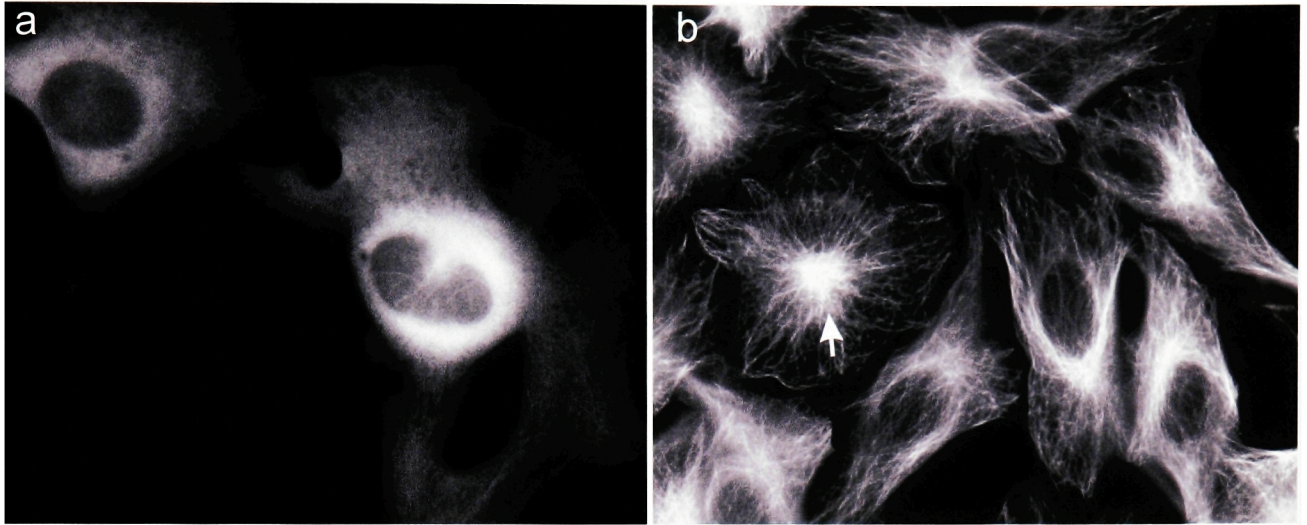
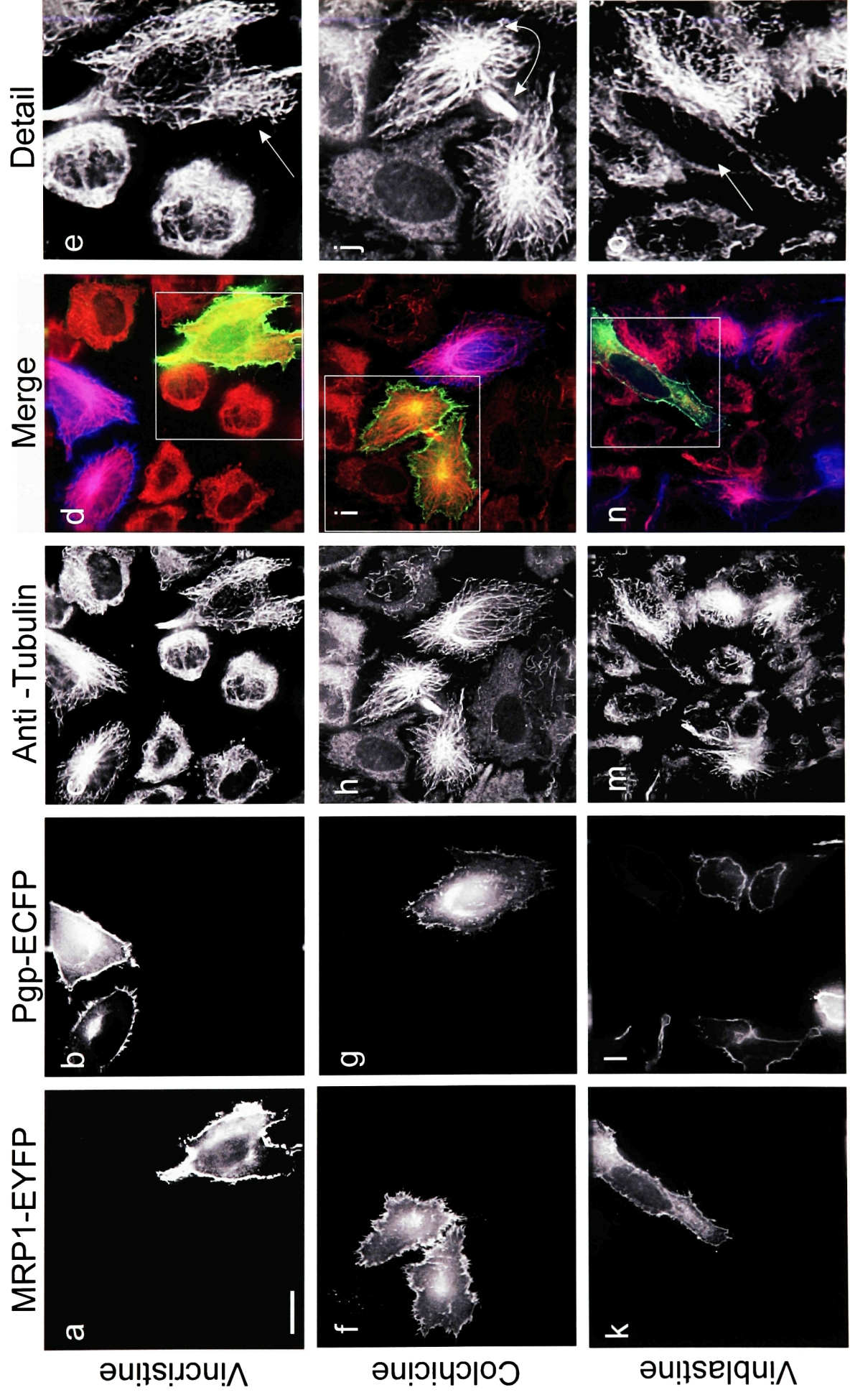


Figure 3-7 Methods of visualizing the microtubule cytoskeleton.

a. HeLa cells were transfected with tau-ECFP and examined 24-48 h. later for microtubule structure. b. HeLa cells were fixed and probed with a Cy3-labeled anti- β tubulin antibody and then examined for microtubule structure.

Figure 3-8 Assaying MRP1 transport of microtubule depolymerizing agents.

HeLa cells were separately transfected with MRP1-EYFP or Pgp-ECFP; cells were plated together, and incubated in a microtubule-disrupting agent, and examined for the extent of microtubule damage with a fluorescent anti-tubulin antibody. a-e. An incubation in 600 nM vincristine resulted in substantial microtubule disruption in cells that did not express either MDR protein (c). Cells expressing MRP1-EYFP (a) were afforded some chemo-protection against vincristine-mediated cytotoxicity (c, e), and cells with Pgp-ECFP (b) were relatively unaffected (c, d). f-j. Cells incubated in 2 mM colchicine were examined for microtubule damage. MRP1-EYFP expressing cells (f), as well as Pgp-ECFP expressing cells (g), maintained a complex microtubule structure in the presence of colchicine (i), while non-expressing had almost completely depolymerized microtubules (h,i,j). k-o. Incubating cells in 600nM vinblastine resulted in almost complete depolymerization of both MRP1-EYFP expressing cells (k, o) and non-expressing cells (m, n, o), whereas cells expressing Pgp-ECFP (l) were much less affected by the drug (m-o).



4 Chapter 4 Localization of MRP1

In the previous chapter, we demonstrated that the MRP1-EGFP fusion protein is functional, localizes to the plasma membrane, and has an activity profile analogous to wild-type MRP1. We also saw that a fraction of the total MRP1 pool localized to a region within the cell and adjacent to the nucleus, and another fraction to the plasma membrane. We next wanted to examine the sub-cellular distribution of MRP1, within two particular contexts. First, we wanted to determine whether MRP1-ECFP would undergo polarization-dependent sorting to the plasma membrane in cells capable of polarization. Second, we wanted to identify the sub-cellular organelles within which MRP1 might be found. Given the fluorescent nature of the MRP1-ECFP construct, live cell-examinations of MRP1 localization would be possible using fluorescence microscopy in conjunction with live-cell fluorescent markers for sub-cellular organelles. Several such markers are commercially available and include reporters for the ER, the Golgi, the recycling endosomes, and the lysosomes. Considering the peri-nuclear localization of MRP1, these particular markers would be helpful in determining the organelle or organelles in which MRP1 might be found.

4.1 Expression in Polarized Cells

To determine whether MRP1-ECFP would be expressed in a polarized fashion in epithelial cells, polarized MDCK cells were transfected with MRP1-ECFP and visualized 24 hours later, using deconvolution microscopy. This technique collects light from multiple sections of a sample at specified distances in the Z plane, in our case every 1.5 μm , and using a nearest neighbor deconvolution algorithm, reallocates out of plane fluorescence. Deconvolution

microscopy thereby allows for a more direct sampling of cell sections, and minimizes the contribution of fluorescent signals from other focal planes. When MRP1-ECFP transfected MDCK cells were examined in this fashion, MRP1-ECFP was found at the basal membrane (Fig. 4-1 a) and at the lateral membrane (Fig. 4-1 b), but the protein was not present at the apical surface (Fig. 4-1 c). This distribution is in contrast to the localization of MRP1-ECFP in non-polarized cells. HeLa cells, for example, express the protein at the basal surface (Fig. 4-1 d), the lateral surface (Fig. 4-1 e, arrow), as well as the apical surface (Fig. 4-1 f). Baso-lateral localization for wild-type MRP1 has been previously reported (Evers *et al.*, 1996).

4.2 Perinuclear localization of MRP1-ECFP in multiple cell lines

In HeLa cells, MRP1-ECFP fluorescence was evident adjacent to the nucleus. To ensure that this localization pattern was not specific to one cell type, a number of other cell types were transfected with MRP1-ECFP and examined under wide-field epi-fluorescence microscopy for the sub-cellular distribution of the protein. In the mouse embryonic stem cell line BDC1, for example, fluorescence from MRP1-ECFP was present in a region surrounding the nucleus (Fig. 4-2 a, arrow), as well as at the plasma membrane. In this micrograph, the rim-staining that generally characterizes plasma membrane-localized markers was less visible. However, the apparent sub-cellular distribution of MRP1-ECFP was highly dependent upon the focal plane visualized for all the cells and cell types used in this study. Depending upon the cell and the focal plane chosen, MRP1-ECFP was more or less evident at the plasma membrane or the peri-nuclear region for BDC1 cells (Fig. 4-2 a), for the immortalized mouse line NIH 3T3 (Fig. 4-2

b), for the primary human fibroblast NHDF (Fig. 4-2 c), and for the glutathione mutant mouse embryonic stem cell line GCS2-NAC (Fig. 4-2 d). Hence, while peri-nuclear staining was clear in the micrograph of the NHDF cell (Fig. 4-2 c), rim-staining was less evident. In the same fashion, the rim-staining of the NIH 3T3 cell was clear, while the peri-nuclear staining was not (Fig. 4-2 b). In some cases, the relative distribution of the organelles in a cell made a rim-stain and a peri-nuclear stain both evident (Fig. 4-2 d). Nevertheless, in all cells examined for the sub-cellular distribution of MRP1-ECFP, the protein was found both at the plasma membrane and in a peri-nuclear compartment.

4.3 Characterizing the sub-cellular distribution of MRP1

Since a significant fraction of the total MRP1 expressed in a cell localized to an intracellular compartment, we next wanted to determine which organelle or organelles were constituents of this compartment. To establish whether MRP1 resided in a particular organelle, we used fluorescent markers for organelles found in the peri-nuclear region of the cell, and we determined the degree of spatial correlation between the fluorescent signal of the marker and the fluorescent signal of MRP1. We began our search with fluorescent reporters for the Golgi and the recycling endosomes. For *in vivo* labeling of the Golgi, we used a fluorescently-tagged, truncated version of human Golgi resident protein beta 1,4-galactosyl-transferase, a commercially available reporter (Clontech) shown to be a specific marker for the trans Golgi compartment (Llopis *et al.*, 1998). For the recycling endosomes, we used cy-3 labeled transferrin, a protein which binds the transferrin receptor and is in this way internalized by the cell to label the recycling endosomes (Lampson *et al.*, 2001).

HeLa cells were transfected with both MRP1-ECFP and Golgi-EYFP and then loaded with cy3-labeled transferrin. When cells were next visualized using epi-fluorescent microscopy, we found that all three fluorescent labels accumulated in a peri-nuclear region (Fig. 4-3, a-d). We could not easily distinguish the degree to which MRP1-ECFP signal derived from the Golgi or the recycling endosomes, as the markers themselves overlapped. Moreover, because the images represented light collected from the entire sample, we were not able to distinguish localization patterns in the Z plane. In an attempt to spatially segregate these markers, we treated cells with BFA, a reagent which induces retrograde transport from the Golgi to the ER, and thus has the effect of collapsing the Golgi apparatus back into the ER (Lippincott-Schwartz *et al.*, 1990). If the MRP1-ECFP signal emanated from the recycling endosomes, it would not be affected by the addition of BFA. However, if peri-nuclear MRP1-ECFP resided primarily in the Golgi, we would expect to see a more reticulate distribution for the transporter upon BFA addition. When we added BFA to these cells, we were not able to make a reliable assessment of the effect of BFA on MRP1 localization, even after comparing cells in the same field before and after the addition of the drug (Fig. 4-3, a-d vs. e-h). Cell movements between these two visualization times made comparisons of cells pre-and-post BFA treatment difficult, as we could not account for the changes in organellar distribution caused by cell movement. Moreover, the addition of BFA did not completely collapse the Golgi into the ER in every cell, and therefore the problem of overlapping signals in the Z plane was not resolved.

In order to improve our resolution in the Z plane, and thereby distinguish over-lapping markers in the peri-nuclear region, we decided to use deconvolution

microscopy once again. HeLa cells transfected with MRP1-ECFP were incubated in cy3-transferrin to label the recycling endosomal compartment and then sections of cells were examined for co-localization of the two markers. Deconvolution microscopy enabled us to visualize individual MRP1-ECFP vesicles in the peri-nuclear region (Fig. 4-4 a), as well as individual vesicles of the endosomal compartment (Fig. 4-4, b). The merge of these two fluorescent signals (Fig. 4-4 c), as well as an enlarged image of the peri-nuclear region (Fig. 4-4 d-f) demonstrated that very little of the MRP1-ECFP signal emanated from the recycling endosomes. Vesicles contained either MRP1-ECFP or cy3-transferrin. Few, if any, contained both.

We decided next to determine whether MRP1 might reside in the Golgi, by transfecting cells with MRP1-ECFP and Golgi-EYFP, and once again examining cells using deconvolution microscopy. Individual cell sections revealed vesicles labeled with either MRP1-ECFP (Fig. 4-5, a,d) or Golgi-EYFP (Fig. 4-5, b,e), but rarely were there ever vesicles that expressed both fluorescent markers together (Fig. 4-5, c, f). Similar results were obtained when cells were transfected with MRP1-ECFP and a fluorescent marker for the ER (Fig. 4-5, g-l). Both MRP1-ECFP and ER-EYFP were found in peri-nuclear vesicles, but there was very little co-localization of these markers in these vesicles.

MRP1-ECFP might also reside in the lysosomes. ABC proteins are known to be expressed in the vacuole of non-mammalian systems (Li *et al.*, 1996; Lu *et al.*, 1997), and in mammals, proteins that are not part of the ABC family do confer drug resistance from lysosomes (Cabrita *et al.*, 1999). Moreover, lysosomes may promote drug detoxification and in this way provide a link between two distinct multidrug resistance pathways. We decided to test this

possibility by chasing fluorescently-labeled dextrans into the lysosomes of MRP1-ECFP transfected cells. Fluorescent dextrans are routinely employed to label the different stages of the endocytic pathway of living cells. When incubated in fluorescent dextrans, cells will endocytose these particles, and depending upon the length of the chase, the dextrans will reside in the early or late endosomes, or if given enough time, in the lysosomal compartment. The lysosomes of MRP1-ECFP transfected HeLa cells were labeled in this fashion, and then examined for the degree to which the ECFP signal emanated from regions of the cell that were positive for Texas-Red dextrans. Once again, MRP1-ECFP fluorescence was evident at the plasma membrane and in a peri-nuclear compartment (Fig. 4-6, a, d). Fluorescence from lysosomes (Fig. 4-6, b,e) correlated spatially with that from MRP1-ECFP (compare Fig. 4-6, d, with Fig. 5-6, e), and these two signals appeared to emanate from the same vesicles. To verify these results with another marker for the lysosomes, we chose to co-express MRP1 with synaptotagmin VII, a lysosomal membrane protein that is also found in some cell types at the plasma membrane. When HeLa cells were co-transfected with MRP1-EYFP and synaptotagmin VII-ECFP, we found that these cells had vesicles positive for both fluorescent proteins (Fig. 4-7, vesicles of note are circled for ease of identification).

These co-localization studies suggested that MRP1-ECFP resides in the lysosomes during some time in its trafficking history. As plasma membrane proteins are routed to the lysosomal compartment for degradation, we became concerned that the MRP1-ECFP present in this compartment may represent an aberrant localization pattern, one introduced solely by the ECFP tag, perhaps as a result of a protein misfolding event that targeted MRP1-ECFP for proteolysis.

However, if the peri-nuclear fluorescence represented degraded protein, it should have been detectable by Western blot, as intracellular MRP1 constituted a considerable fraction of the total protein expressed. Our previous investigations of MRP1-EGFP expression indicated that the large fraction of MRP1-EGFP being expressed by the cell was not proteolyzed (Chapter 3). On the other hand, it is possible that the lysosomal localization of the protein was an artifact of the ECFP tag, effecting the trafficking dynamics of the protein in way that misrepresented the localization of wild-type MRP1. To determine if the fluorescent tag was responsible for aberrant localization of MRP1, synaptotagmin VII was transfected into HeLa cells along with wild-type MRP1, and immunocytochemistry was performed using the MRP1 antibody MRPr1. We found that wild-type MRP1 co-localized with synaptotagmin VII in a region adjacent to the nucleus (Fig. 4-8, a-c). Under deconvolution microscopy, we could distinguish vesicles which contained both MRP1 (Fig. 4-8, d, f circles) and synaptotagmin VII (Fig. 4-8, e-f circles). As an added assurance, we wanted to determine whether MRP1 would co-localize with another lysosomal marker. As our fluorescent dextrans would not withstand the fixation process, we chose another lysosomal resident protein for our studies, cathepsin D. In accordance with our previous findings, wild-type MRP1 was found to co-localize with this lysosomal marker as well (Fig. 4-9).

We next wanted to determine whether this lysosomal localization pattern of MRP1 would be exhibited by other ABC proteins, particularly those involved in conferring drug resistance. We therefore transfected HeLa cells with fluorescent conjugates of other MDR proteins, in particular, Pgp and BCRP, both of which have been implicated in the acquisition of drug resistance in a clinical

setting. As with MRP1, we used fluorescent conjugates of Pgp and BCRP to examine the sub-cellular localization of these proteins. Both fluorescent proteins have been examined in detail and have been found to be reliable markers of wild-type Pgp and BCRP. Neither fluorescent conjugate is subject to extensive proteolysis, as determined by Western Blot, and both proteins reduce the intracellular accumulation of chemotherapeutic agents (Kartner *et al.*, 1983). When the lysosomes of Pgp-ECFP transfected HeLa cells were labeled with fluorescent dextrans, we found that both fluorescent signals emanated from the peri-nuclear region of the cell. Moreover, individual vesicles that contained both Pgp and the lysosomal marker were easily detected (Fig. 4-10, circles). In the same fashion, we found BCRP-ECFP also to localize to lysosomal vesicles within the perinuclear region of HeLa cells (Fig. 4-11).

However, when we examined an ABC protein not implicated in the acquisition of multi-drug resistance, we found that the protein did not localize to the lysosomes. CFTR, like MRP1, Pgp, and BCRP, was studied as a protein conjugate of ECFP, and its subcellular distribution was determined by employing fluorescent dextrans chased into the lysosomes. The intracellular localization of CFTR varied from cell to cell in each round of transfection, from a primarily reticulate, intracellular distribution (Fig. 4-12, a) that most resembled the distribution of an ER protein (Fig. 4-12, g), to a primarily plasma membrane-localized protein (Fig. 4-12, b). However, at no point did CFTR-ECFP co-localize with lysosomal dextrans (Fig. 4-12, b, e), as evident in the merge of the two fluorescent signals (Fig. 4-12, c, f). This data is suggestive of a functional relationship between drug resistance proteins and lysosomal targeting, a pattern that we will discuss further in the next chapter.

4.4 Quantifying co-localization

Thus far, determinations of co-localization had been performed entirely by visual inspection. We now wanted to quantify the degree to which MRP1, or any other fluorescent ABC protein, could be said to reside in one organelle, or another, and thereby remove the arbitrary nature of visual assessments. Moreover, quantification of visual data would enable us to compare the results of different experiments and enable us to assess relative degrees of correlation between different fluorescent markers. In order to do this, we used a correlation algorithm available to us from MetaMorph software. For a given micrograph, this algorithm determines the degree to which distinct fluorophores vary their intensities through a two-dimensional space in a coordinated fashion, and represents this information in a “correlation coefficient.” Correlation coefficients are expressed on a scale of -1 to 1, with -1 representing no correlation whatsoever, and 1 representing identity. To better understand the nature of this quantification, we wanted to test the scaling system by acquiring correlation coefficients for either end of the spectrum: for proteins that should co-localize entirely and therefore represent identity, and for proteins that should share very little in their sub-cellular distribution.

To test the former, we began by transfecting cells with two versions of the same protein, MRP1-EYFP and MRP1-ECFP. Differing only in their fluorescent tags, these proteins should share similar localization patterns and set the upper limit of co-localization. When HeLa cells were co-transfected with MRP1-EYFP and MRP1-ECFP, we found that the two proteins did share very similar distributions; again both were targeted to the plasma membrane and a peri-nuclear region (Fig. 4-13 a-c). Closer inspection of the peri-nuclear region revealed individual vesicles

that shared the two fluorophores (Fig. 4-13, d, e; for example, circle 1).

However, there were also a number of vesicles that contained predominantly one fluorophore over another (Fig. 4-13, d,e; for example, circle 2). Indeed, there were surprising differences in the vesicular distribution of these two proteins, differences which would make a correlation co-efficient of 1 less likely (Fig. 4-13, d,e, other circles). When these images were analyzed for correlation coefficients, we found an average assignment of 0.7677 for MRP1-EYFP and MRP1-ECFP.

To find the lower limit of co-localization, we chose to examine Golgi-EYFP transfected cells whose recycling endosomes were labeled with cy-3 transferrin (Fig. 4-13, f-h). The correlation coefficient for this pair was 0.2699, suggesting that even distinct organelles are characterized by overlapping pixels. This correlation co-efficient may represent patterns of vesicular exchange between the organelles, or it may be an artifact of pixel density and distribution in the confined space of a cell. Nevertheless, we allowed this correlation co-efficient, along with that found for the doubly transfected MRP1 expressing cells, to define the limits of our quantification.

With these limits in mind, we then generated correlation co-efficients for the micrographs analyzed thus far for co-localization, and plotted them on a line graph (Fig. 4-14, a-c). These numerical assessments of co-localization supported our previous understanding of MRP1 localization. MRP1, like MRP1-ECFP, localizes primarily to the lysosomal compartment 24-48 hours after transfection (Fig. 4-14 a,b). Very little of the protein is found in the ER, the recycling endosomes, or the Golgi (Fig. 4-14, a). Analysis of the localization of Pgp-ECFP and BCRP-ECFP suggest a similar pattern; both proteins can be found primarily in the lysosomal compartment 48 hours after transfection, while CFTR-ECFP, a non-MDR ABC protein, is not to be found there (Fig. 4-14, c).

The demonstration of a lysosomal distribution for MRP1, Pgp, and BCRP, does not preclude sub-cellular localization elsewhere. Indeed, this intracellular distribution may be a factor of cell cycle or trafficking history, and these proteins may present themselves in other locations under different conditions, or at different times. MRP2, for example, has been found in a novel subcellular organelle in nonpolarized hepatic cells (Tuma *et al.*, 2002). However, it would not be unprecedented to propose that MRP1, BCRP, and Pgp all reside in the lysosomes. ABC proteins are known to be expressed in the vacuole of non-mammalian systems (Li *et al.*, 1996; Lu *et al.*, 1997), and in mammals, proteins that are not part of the ABC family do confer drug resistance from lysosomes (Cabrita *et al.*, 1999). Moreover, lysosomes may promote the detoxification of the drug and in this way provide a link between two distinct multidrug resistance pathways. Whether this sub-cellular localization pattern of these MDR transporters is a result of over-expression is not known. In so far as multidrug resistant cancer cells are known to over-express ABC transporters like MRP1, the over-expression system used in this study models itself after a patho-physiological state. However, predominantly intracellular localization patterns for MRP1 have been reported for many normal tissues (Flens *et al.*, 1996; Wioland *et al.*, 2000). Moreover, we found that cells expressing even low levels of MRP1-CFP were characterized by primarily intracellular versions of the protein, suggesting that vesicular MRP1 may not be the result of over-expression.

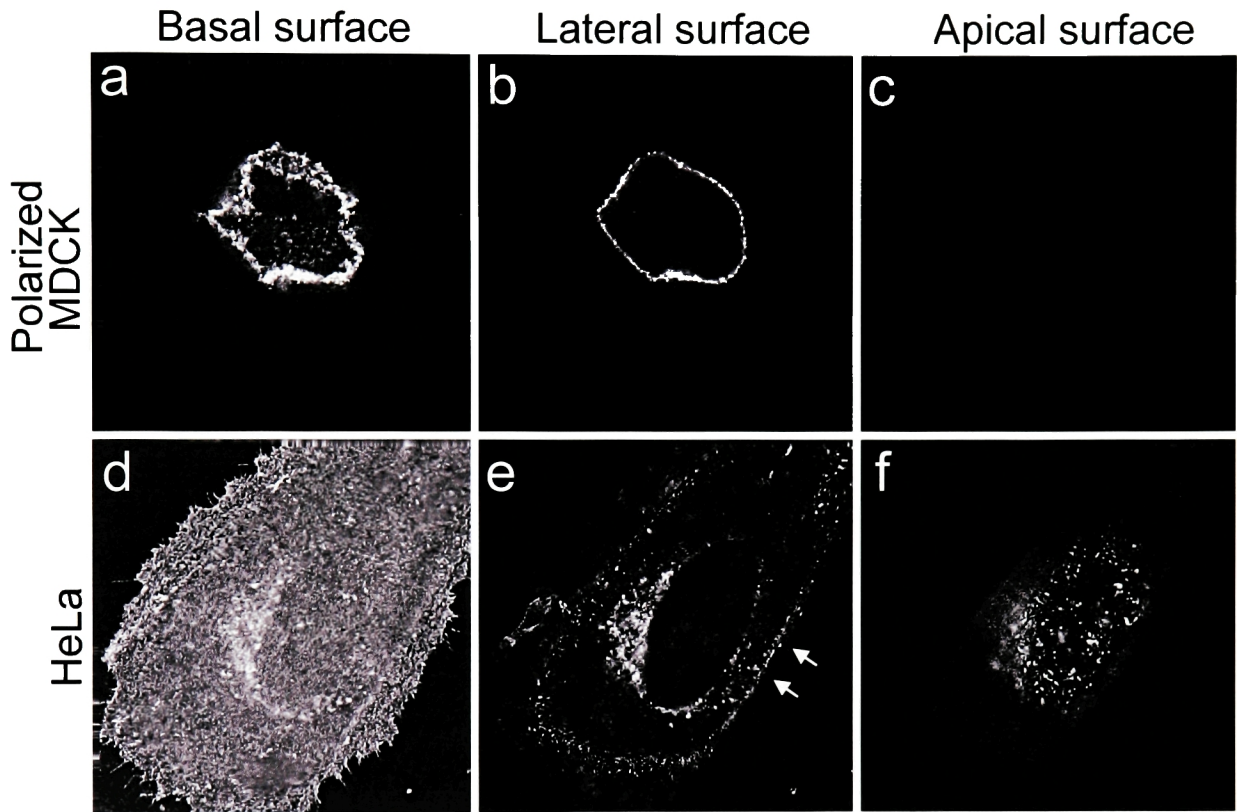


Figure 4-1 MRP1-ECFP is sorted to the baso-lateral membrane.

a-c. MRP1-ECFP was transfected into MDCK epithelial cells after polarization and examined 24-48 hours later. MRP1-ECFP was observed at the basal surface and the lateral surface, but not the apical surface in these cells. d-f. Non-polarized cells transfected with MRP1-ECFP expressed the protein at the plasma membrane. Arrows indicate lateral surface.

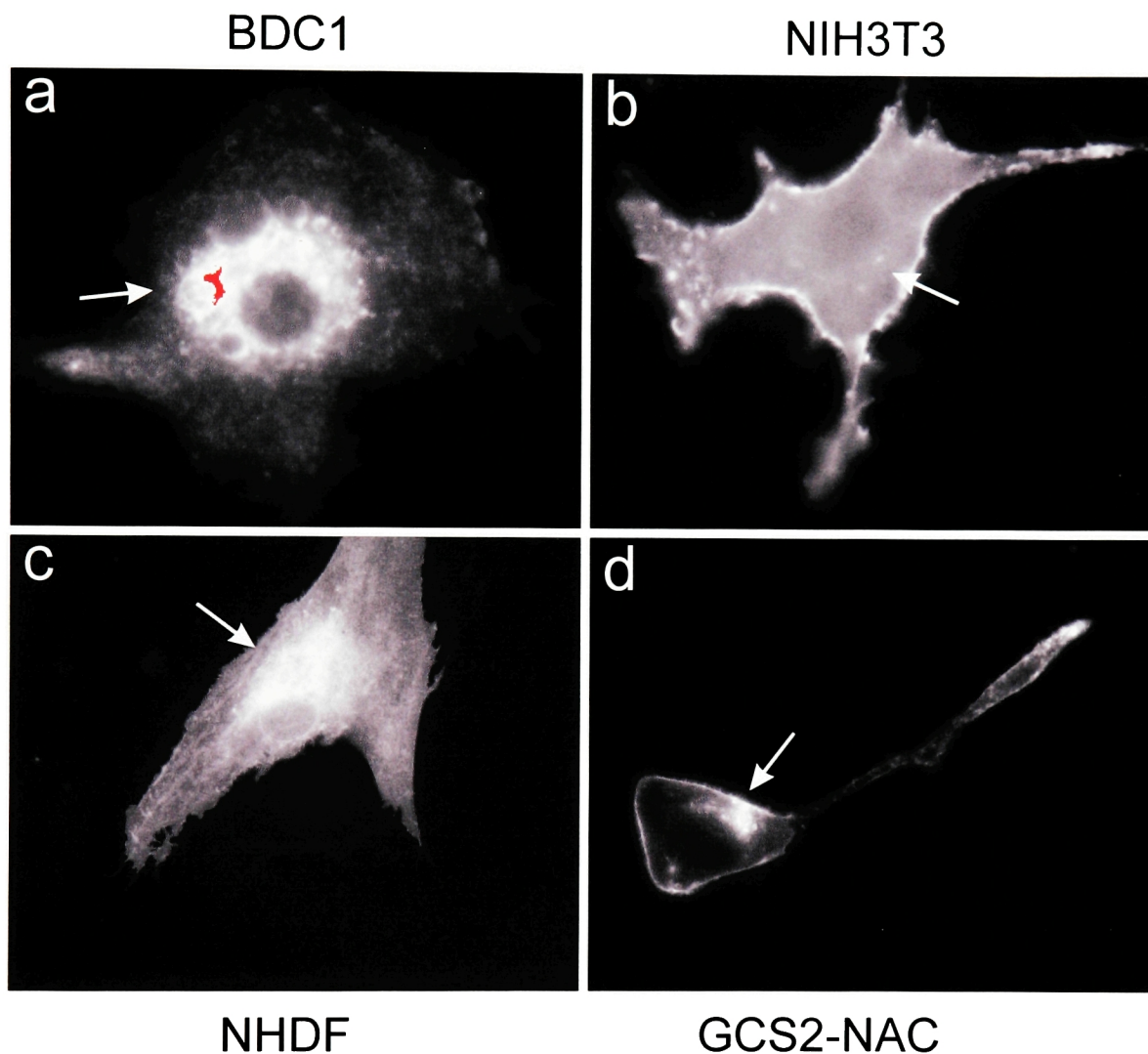
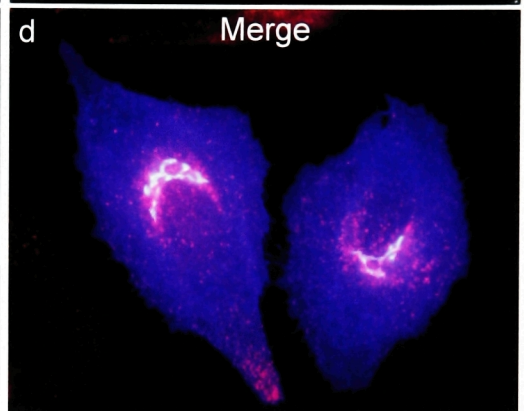
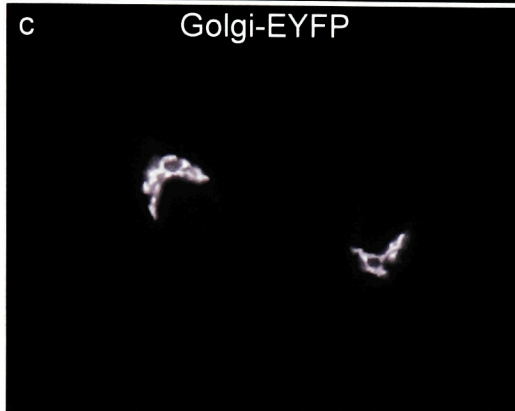
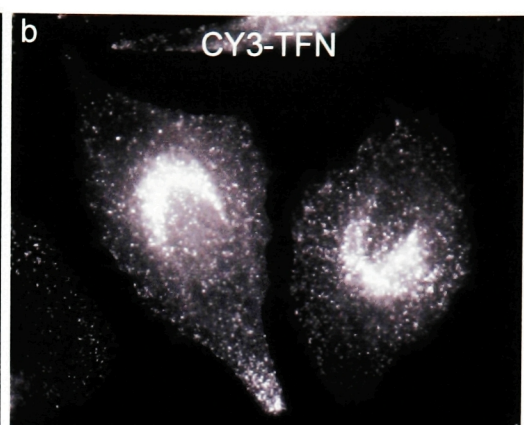
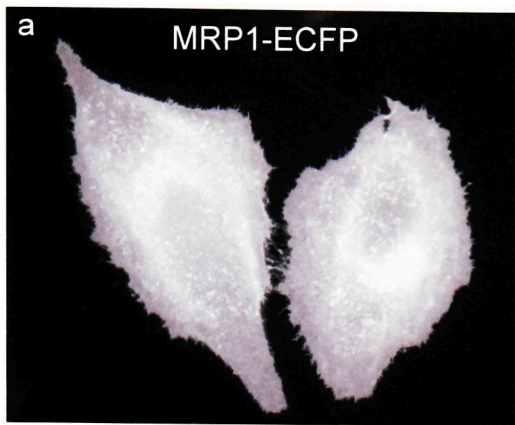


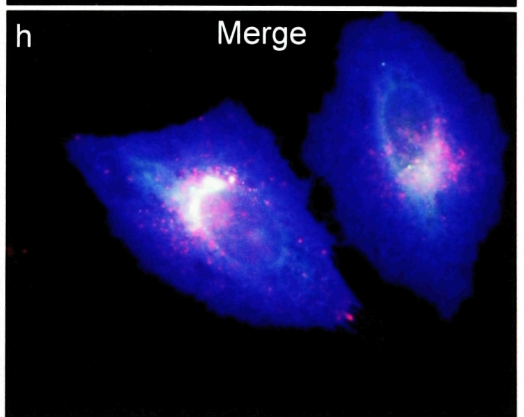
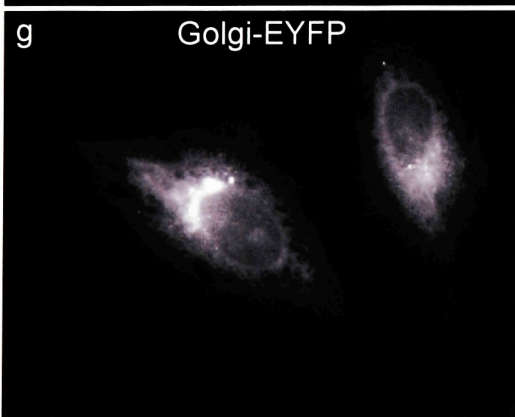
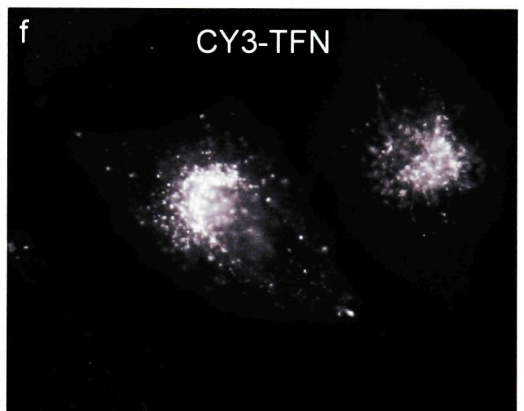
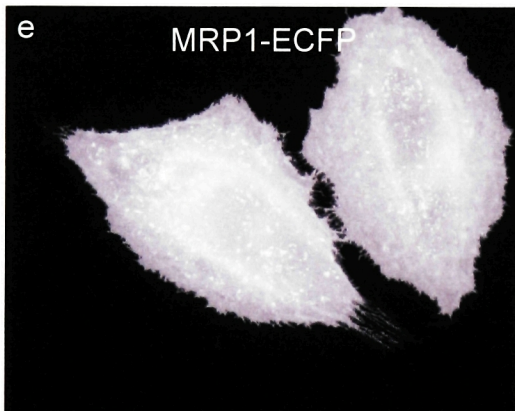
Figure 4-2 MRP1-ECFP localization in four cell types. MRP1-ECFP localizes to the plasma membrane and, to varying degrees, a peri-nuclear region, as seen in four different cell types. Cell types are as follows: a. a mouse embryonic cell line; b. an immortalized mouse cell line; c. a primary, human fibroblast line; and d. a mouse embryonic cell line incapable of glutathione production. Arrows indicate the peri-nuclear region.

Figure 4-3 Localizing organelles with epi-fluorescent microscopy a-d. HeLa cells transfected with MRP1-ECFP and Golgi-EYFP were labeled with Cy3-Tfn to visualize recycling endosomes. Cells showed a perinuclear staining for all three fluorescent signals, making sub-cellular determinations of MRP1-ECFP localization difficult. e-h. The addition of BFA did not clarify MRP1-ECFP distribution patterns, as cell movement made comparisons between pre-and-post BFA addition difficult.

-BFA



+ BFA



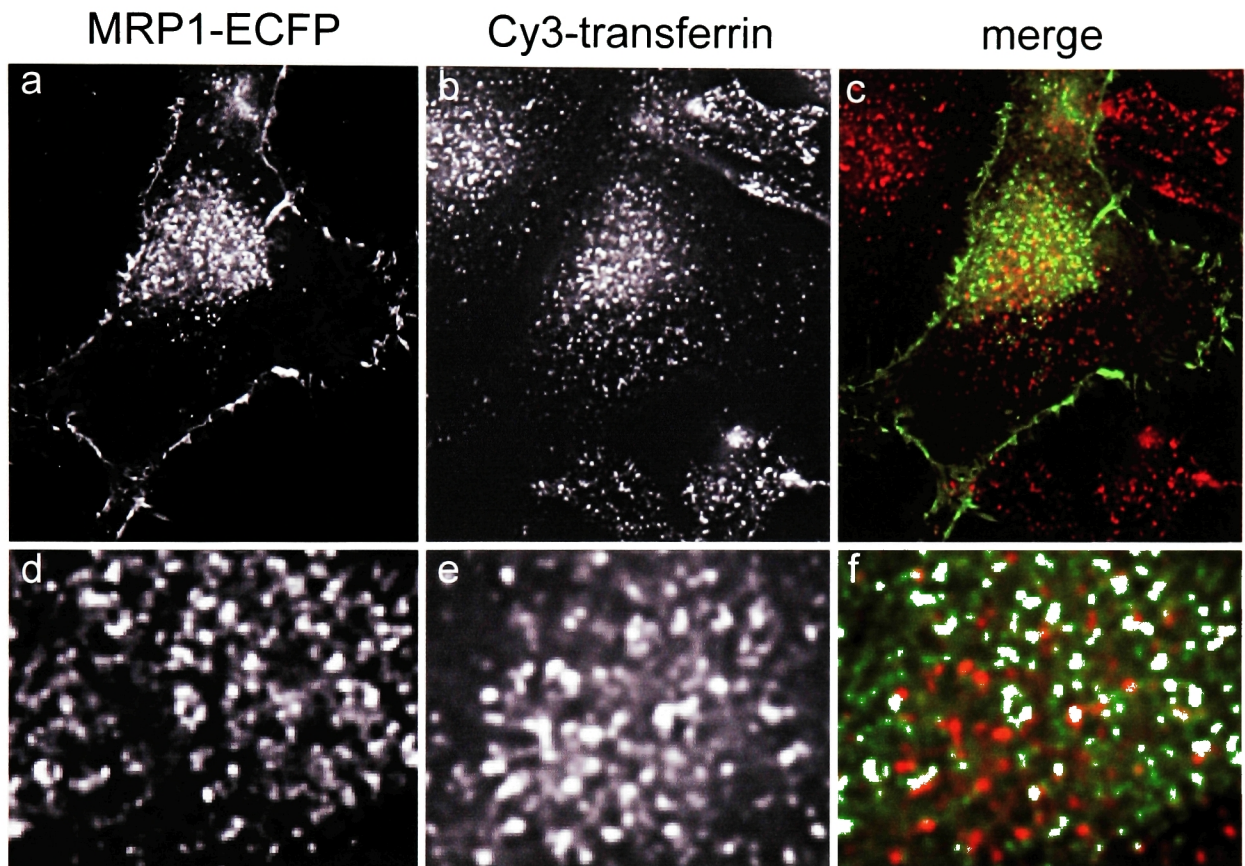


Figure 4-4 MRP1-ECFP does not localize to the recycling endosomes.

a-c. MRP1-ECFP transfected cells were loaded with cy3-transferrin and examined with a deconvolution fluorescent microscope to determine the degree to which the MRP1-ECFP signal (a) co-localized with the recycling endosomes (b). One section of the cell is presented. d-e. An enlarged image of the cell depicted in (a-c) makes evident the degree to which MRP1-ECFP does not co-localize with the recycling endosomal compartment. The vesicles containing each fluorescent signal are distinct.

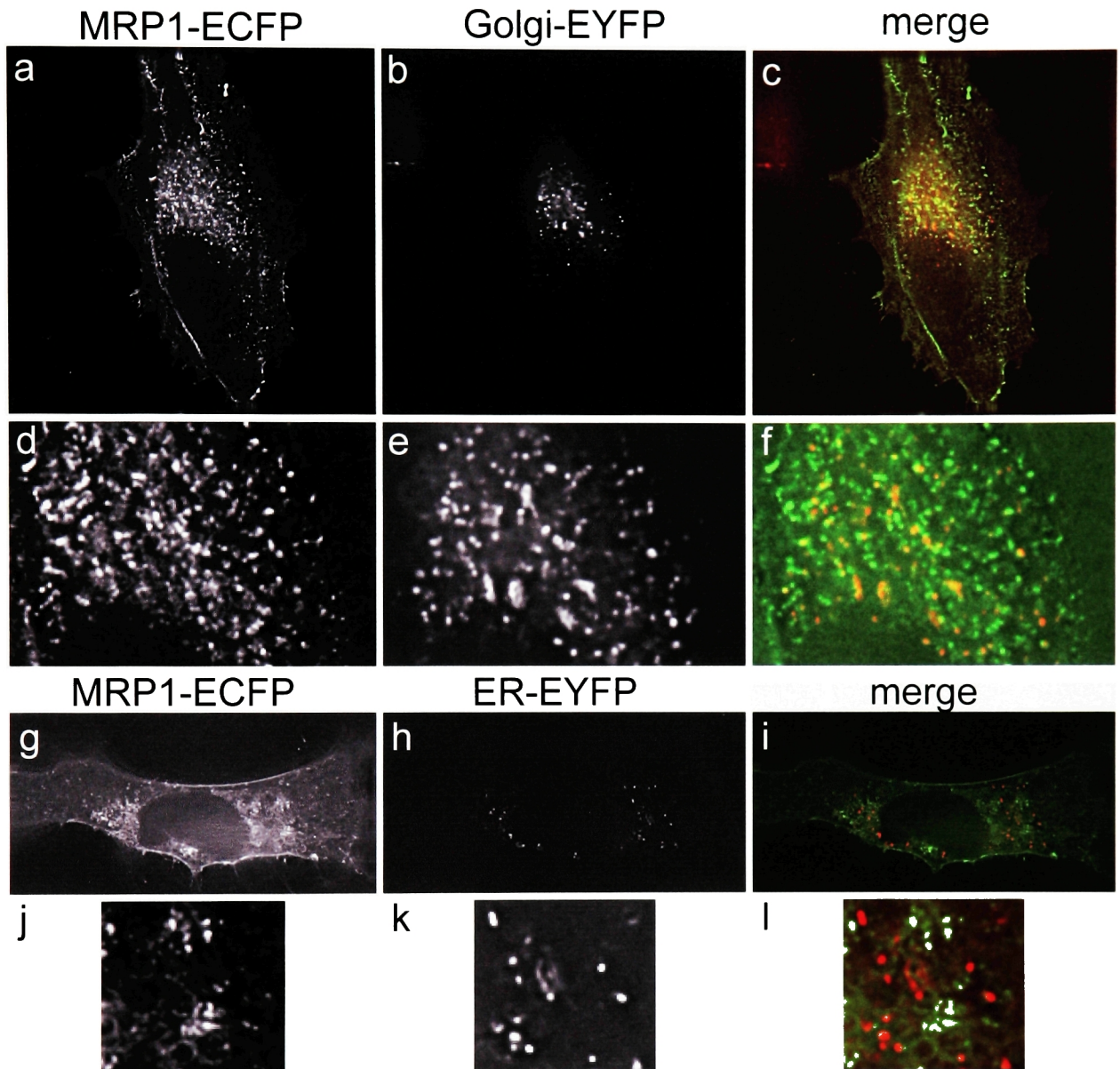


Figure 4-5 MRP1-ECFP does not localize to the Golgi or the ER

a-c. HeLa cells were transfected with both MRP1-ECFP (a) and Golgi-EYFP (b), and examined with a deconvolution fluorescent microscope to determine the extent of the colocalization. d-e. An enlarged image of the cell above in which vesicles containing one or the other of the two fluorescent markers are clear. g-l. HeLa cells were transfected with MRP1-ECFP (g, j) and ER-EYFP (h, k) to determine the extent of the co-localization. Few vesicles, if any, were simultaneously labeled with two fluorescent signals.

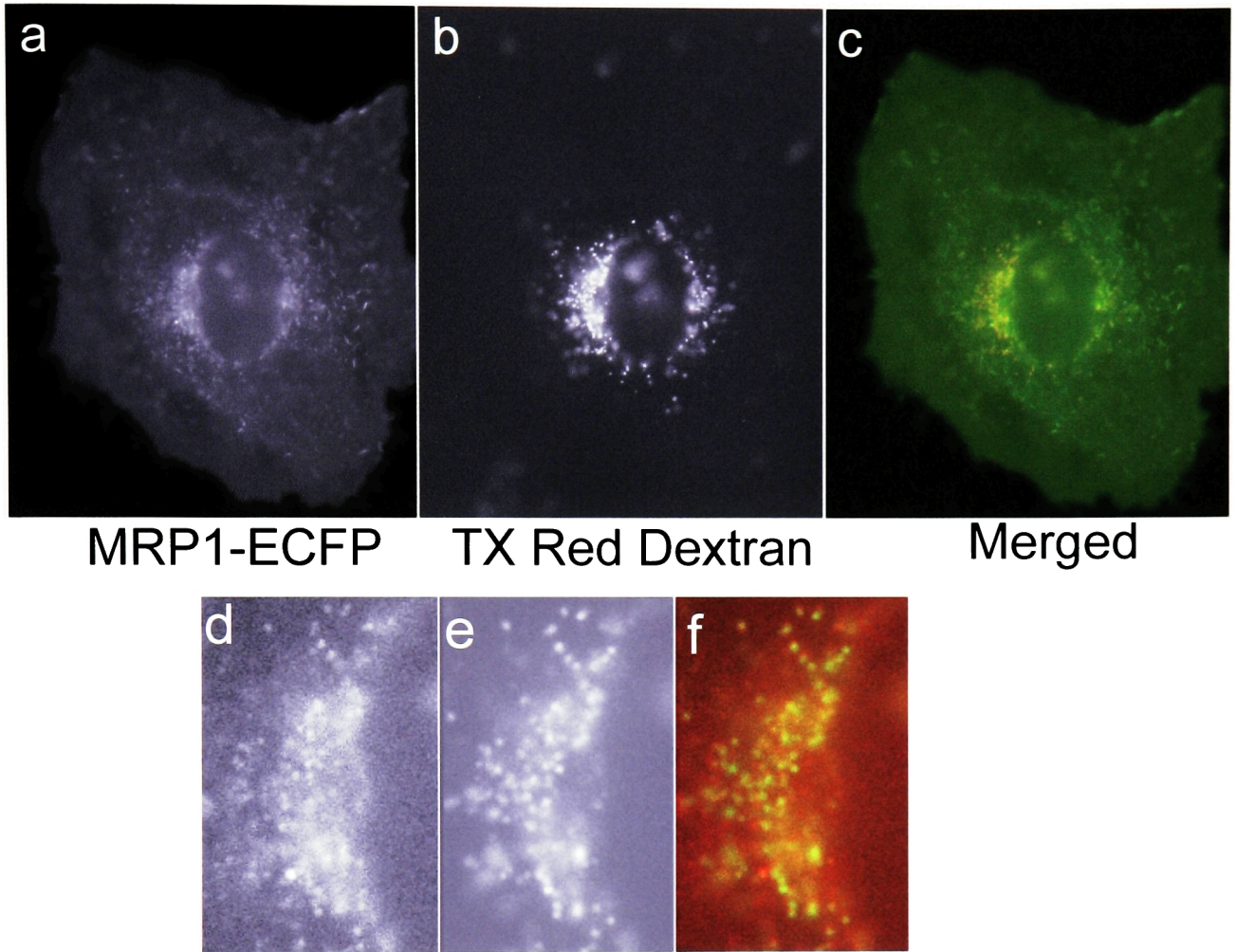


Figure 4-6 MRP1-ECFP co-localizes with a lysosomal marker

a-c. MRP1-ECFP transfected Hela cells were incubated with fluorescent dextrans that were chased into the lysosomes. The MRP1-ECFP signal (a, d) correlated with that of the lysosomal marker (b, e), as seen in the merged image (c, f). Three second time delays occurred between image acquisitions, during which time, vesicular movement precluded absolute spatial resolution of the two fluorophores.

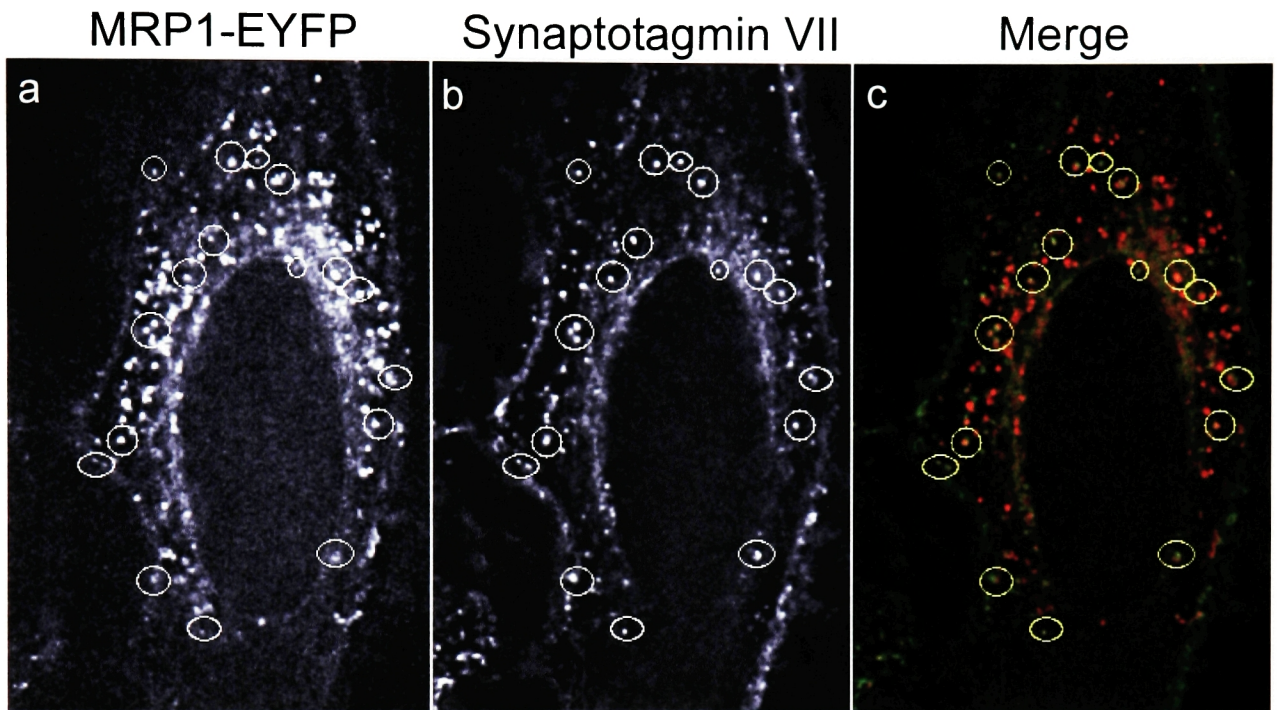


Figure 4-7 MRP1-EYFP co-localizes with synaptotagmin VII

a-c. Hela cells were transfected with MRP1-EYFP (a) and synaptotagmin VII (b), a lysosomal membrane marker, and then were imaged using deconvolution microscopy. A section of a cell is presented in which some of the vesicles that clearly express both proteins are circled.

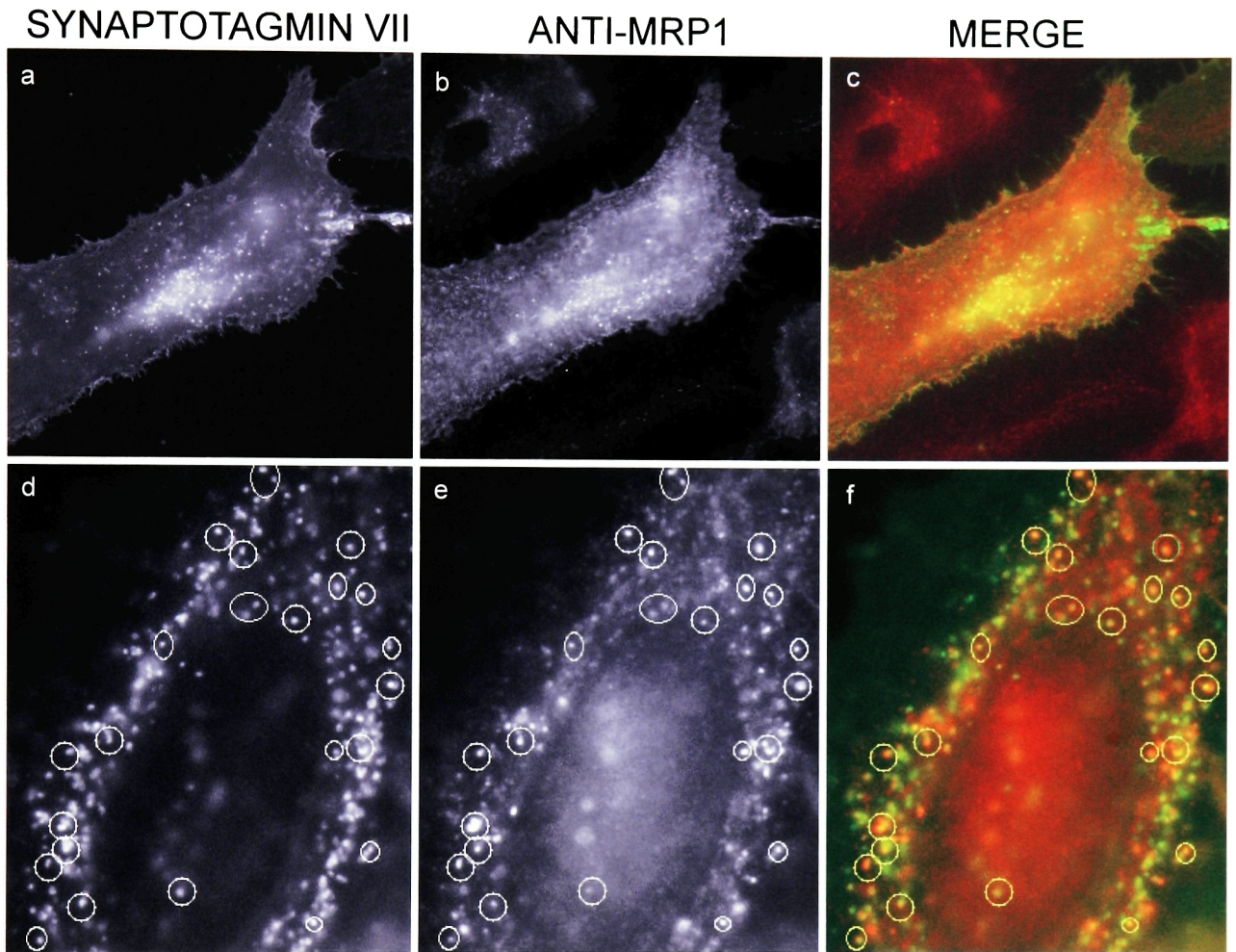


Figure 4-8 Wild type MRP1 co-localizes with synaptotagmin VII

a-c. HeLa cells were transfected with MRP1 and synaptotagmin VII (a) and then probed with the anti-MRP1 antibody MRPr1 for the presence of wild type MRP1 (b) in lysosomes. d-f. An enlarged section of a cell co-transfected with wild-type MRP1 and synaptotagmin VII. Circles indicate vesicles that are positive for both proteins.

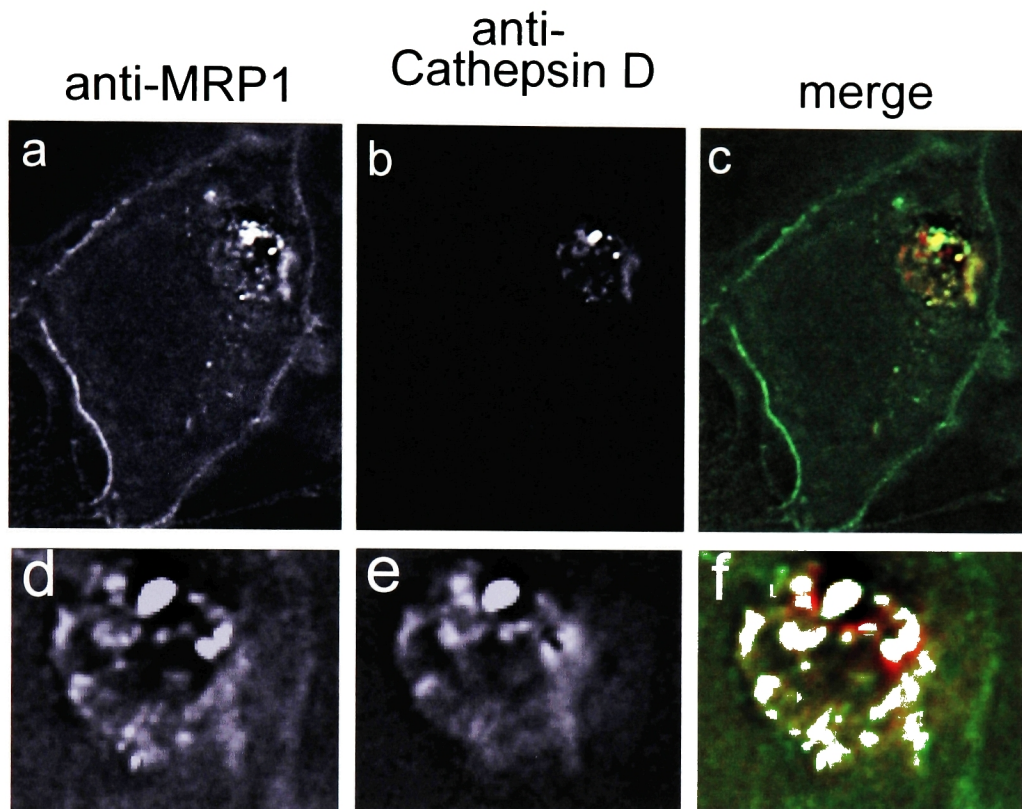


Figure 4-9 Wild-type MRP1 co-localizes with the lysosomal marker cathepsin D

a-c. MRP1 transfected HeLa cells were fixed and probed for wild-type MRP1 (a) as well as the lysosomal resident protein cathepsin D (b). Once cell section is represented. d-f. An enlarged image of another section of the same cell presented in a-c.

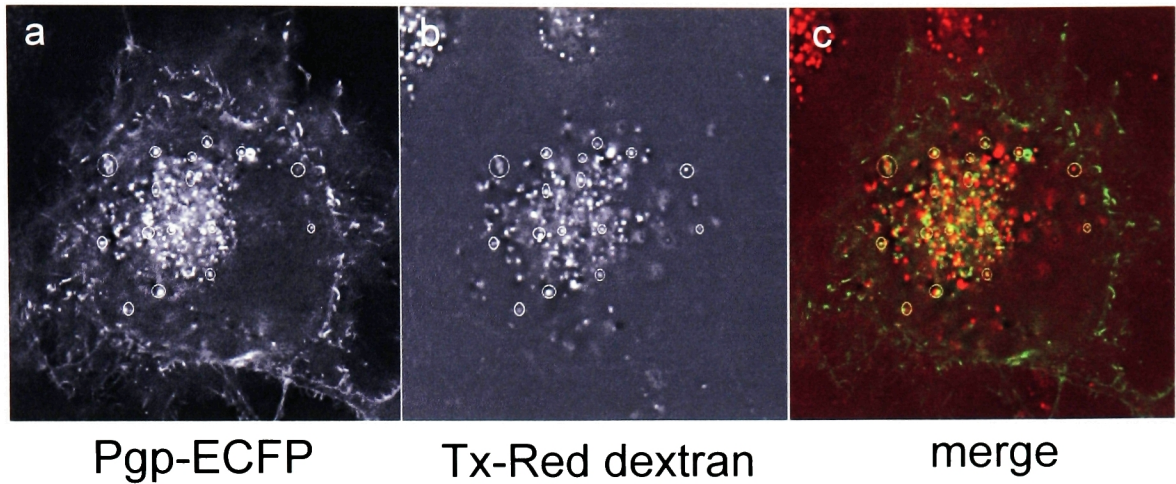


Figure 4-10 Pgp-ECFP can also be found in vesicles positive for a lysosomal marker

a-c. A HeLa cell was transfected with Pgp-ECFP (a) and then labeled with fluorescent dextrans chased into the lysosomes (b). Circles call attention to vesicles containing both fluorescent signals.

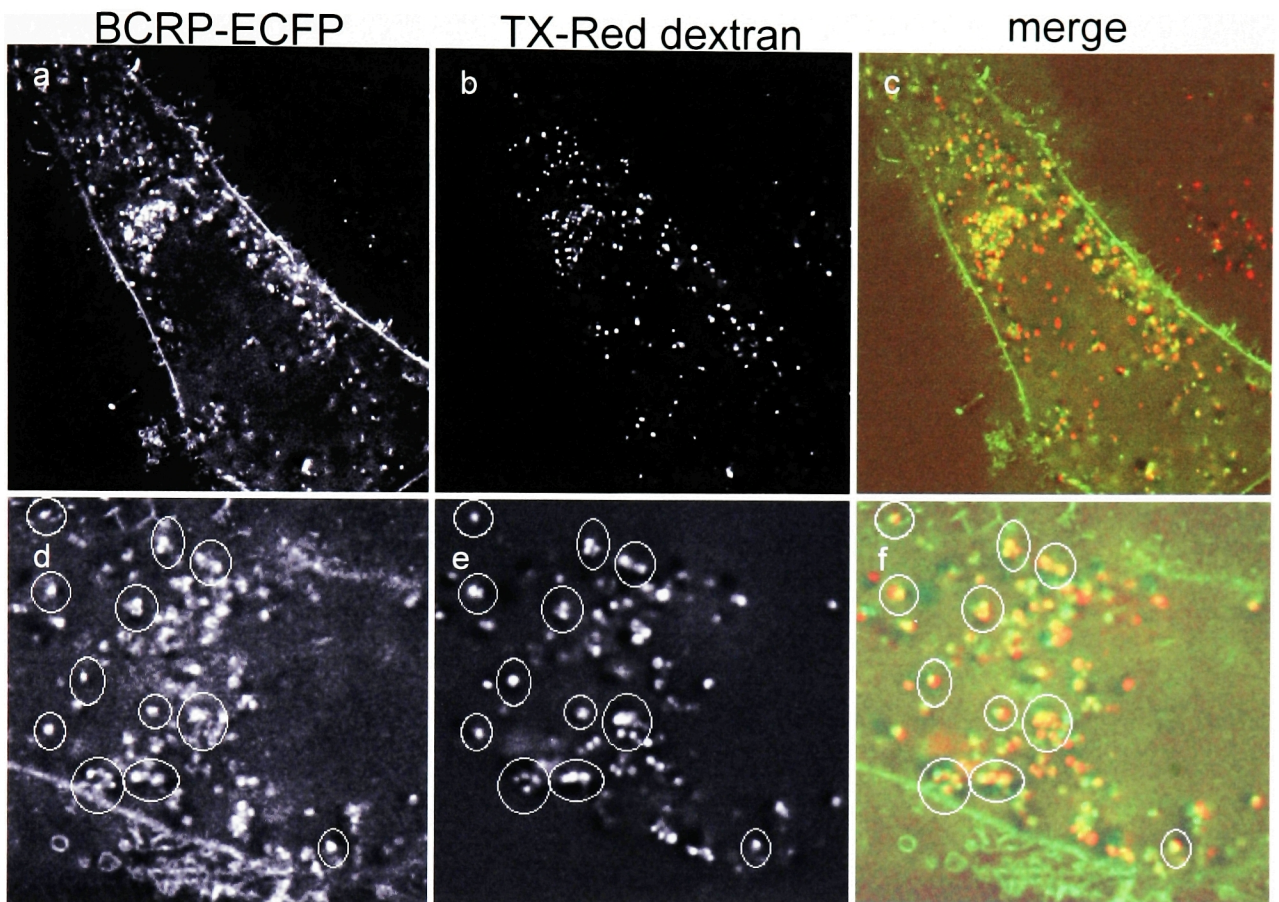


Figure 4-11 BCRP-ECFP is found in lysosomes

a-c BCRP-ECFP transfected cells were loaded with fluorescent dextrans to label the lysosomes. BCRP-ECFP (a) was found in vesicles in the peri-nuclear region of cells, and these vesicles were positive for fluorescent dextrans (b), as seen in the merge (c). d-f. An enlarged region of a BCFP-ECFP transfected cell in which vesicles positive for BCRP (d) and fluorescent dextrans (e) are apparent (circles, f)

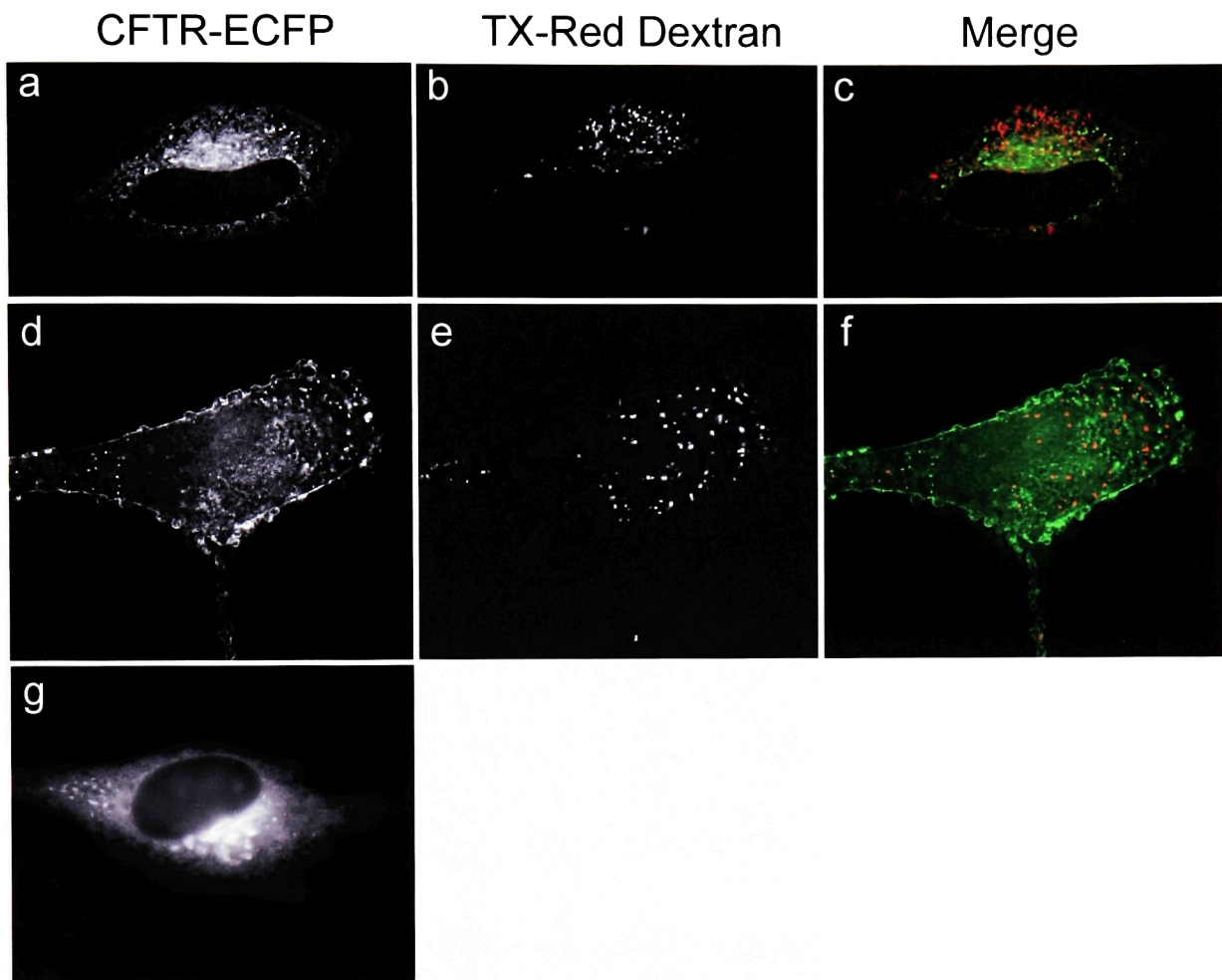


Figure 4-12 CFTR-ECFP is not found in lysosomes.

a-f. The lysosomes of HeLa cells transfected with CFTR-ECFP (a, d) were labeled with fluorescent dextrans to determine whether CFTR could be found in the lysosomes. g. A HeLa cell transfected with ER-EYFP is shown as a point of comparison.

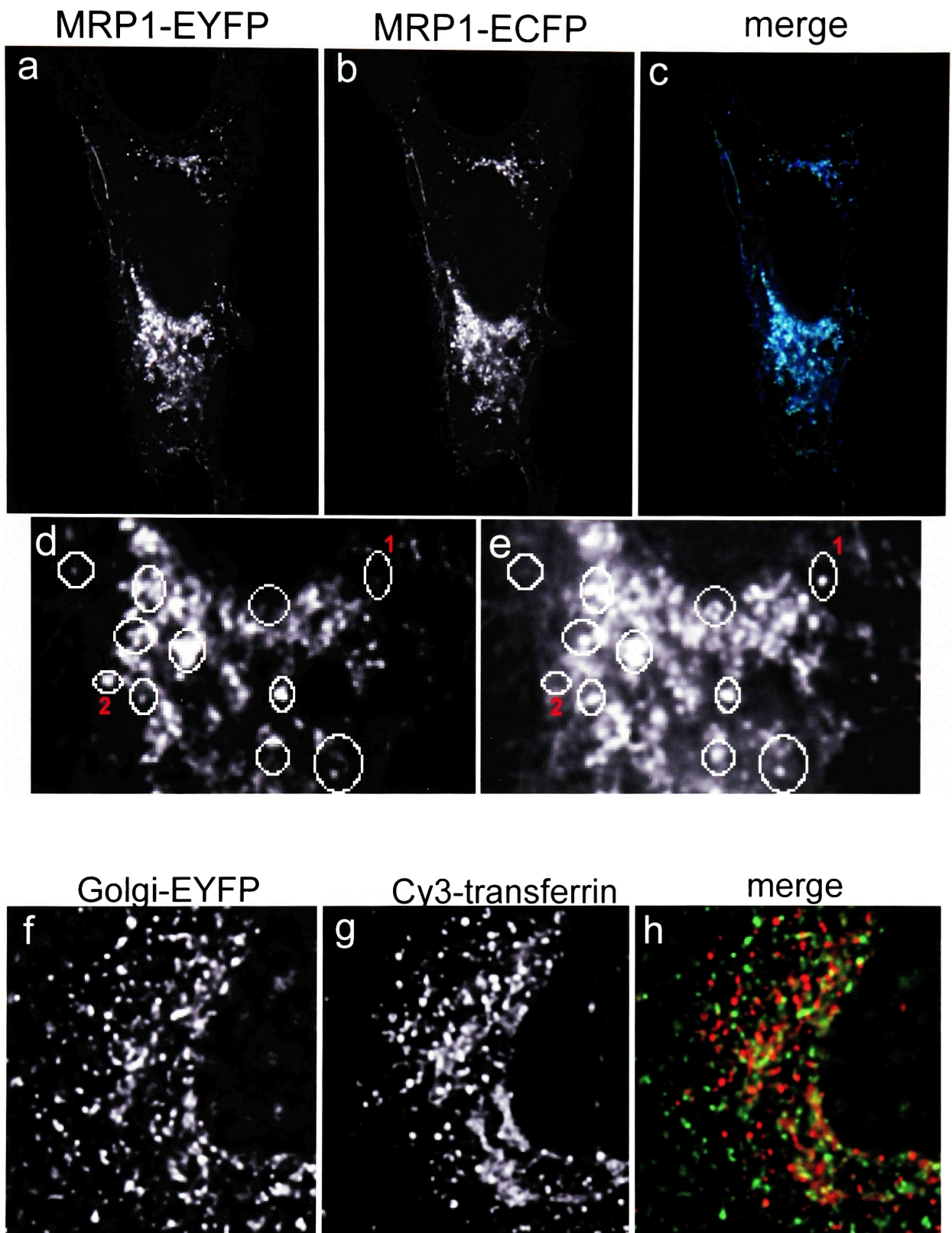


Figure 4-13 Determining the limits of co-localization.

a-c. HeLa cells were transfected with MRP1-EYFP and MRP1-ECFP to determine the extent of the co-localization of the two markers. d-e. An enlarged image of the cell presented in a-e, in which vesicles containing the two fluorophores are visible. Circles indicate variability in co-localization in a positive control. f-h. The Golgi apparatus and the recycling endosomal compartment were labeled in HeLa cells to determine the extent of their co-localization.

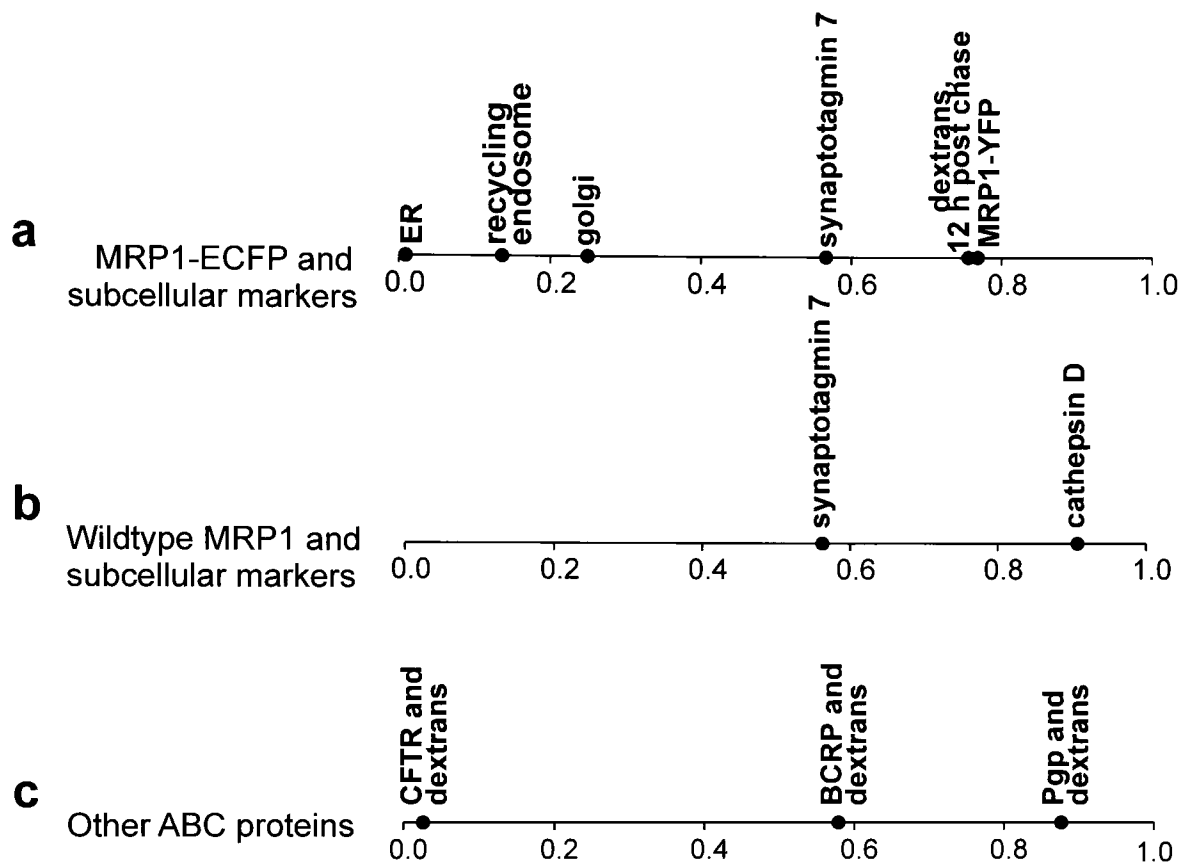


Figure 4-14 Correlation Coefficients permit quantification of protein co-localization studies. a. Correlation coefficients for MRP1-ECFP and various subcellular markers are plotted. Correlation coefficients for wild-type MRP1 and the lysosomal compartment are plotted. c. Correlation coefficients for other ABC proteins and the lysosomal compartment are plotted.

5 Chapter 5 Subcellular activity of MRP1

5.1 Drug sequestration

In the last chapter, we determined that MRP1 localizes both to the plasma membrane and to an intracellular compartment that is positive for at least three different lysosomal markers. We found that this distribution pattern characterized the expression of MRP1-ECFP, as well as the expression of wild-type MRP1.

We also discovered that this subcellular localization pattern was shared by other MDR-conferring proteins, transporters like P-glycoprotein and BCRP, but not by other ABC proteins, like CFTR. We now wanted to determine whether this intracellular distribution was of any physiological relevance to the cell. In particular, we wondered whether these MDR proteins could be active in these compartments, and whether this activity could contribute to drug resistance.

There is some precedence for suggesting that these proteins might be functional within sub-cellular compartments. Non-mammalian members of the ABC family, for example, are known to be active in intracellular compartments. The yeast cadmium factor 1 (YCF1) and plant homologues of the human MRP1, *Arabidopsis thaliana* MRP1 and MRP2, are all thought to transport substances from the vacuolar membrane into the vacuole (Li *et al.*, 1996; Lu *et al.*, 1997; Lu *et al.*, 1998). As the storage compartment for toxins of varied sources, the vacuole serves in a drug resistance capacity, sequestering everything from herbicides and anti-microbial agents to oxidizing metabolites from the rest of the cell. In a similar fashion, the lysosomal compartment, where we have found human MRP1 to reside, has been implicated in an analogous role: providing drug resistance by sequestering toxins away from the rest of the cell (Hurwitz *et al.*, 1997). The

MCF7-Adr cell line, for example, is a multidrug resistant line whose drug resistance is in main part due to the sequestration of drug away from the nucleus in lysosomes, as well as other intracellular organelles (Altan *et al.*, 1998) (Fig. 5-1, a). In contrast, the parental line, MCF7, is sensitive to chemotherapeutic agents like doxorubicin which accumulates in the nucleus, the site of doxorubicin toxicity (Fig. 5-1, b).

Drug sequestration is a well-characterized mechanism of conferring drug resistance, and it is thought to be mediated by altered intracellular pH. Drug resistant cells frequently have intracellular compartments that are acidified and therefore more likely to accumulate weakly basic drugs like doxorubicin. Disrupting cellular acidification with the addition of concanamycin A, for example, results in the redistribution of chemotherapeutics into the nucleus of some drug resistant cell lines like MCF7-Adr (Fig. 5-1, c) (Altan *et al.*, 1998). However, it is possible that other drug sequestration mechanisms are at work here. MCF7-Adr cells are known to express both MRP1 (see the following chapter) and Pgp. Inhibiting the activity of these two proteins with verapamil redistributes doxorubicin away from sub-cellular compartments and into the nucleus (Fig. 5-1, d), suggesting a role for one or both of these proteins in altering drug distribution. Moreover, doxorubicin in these cells is sequestered in the lysosomes, and may suggest that lysosomally-localized MRP1 and Pgp are both active and contribute to drug sequestration (Fig. 5-1,e). Finally, the expression of MRP1 in the MCF7 sensitive line is sufficient to redistribute the drug away from the nucleus into sub-cellular organelles (Fig. 5-2, a-f), in pH independent manner (Fig. 5-2, d-f), much like MCF7-Adr cells.

For all of these reasons, we wanted to determine whether MRP1 retained transport activity within sub-cellular organelles. In order to investigate this question, we asked the following questions: one, are drug substrates found to co-localize with MRP1-containing organelles; two, is this co-localization reversible upon the inhibition of MRP1 activity; three, is drug accumulation into MRP1 organelles affected by alterations in organellar pH; and four, if the activity of cell surface MRP1 is blocked, will drug accumulation in MRP1-positive organelles still occur? In this fashion, we would test if patterns of intracellular drug accumulation correlated with intracellular MRP1 activity, and not with other cellular phenomena frequently associated with drug resistance.

5.2 Doxorubicin localizes to MRP1-ECFP containing vesicles

We first compared the drug accumulation patterns of cells transfected with MRP1-ECFP to those expressing only endogenous MRP1 (Fig. 5-3). We found that HeLa cells with only endogenous MRP1 accumulated doxorubicin in the nucleus, and to a lesser extent, in vesicle-like structures around the nucleus (Fig. 5-3, a-c). For the most part, these structures did not co-localize with a marker for the lysosomes (Fig. 5-3, d-f); however, this conclusion is suggested only by epifluorescence microscopy, and extensive studies have not been conducted regarding this question using either confocal or deconvolution microscopy. However, the expression of MRP1-ECFP in HeLa cells resulted in a dramatic redistribution of doxorubicin fluorescence, with almost no visible fluorescence emanating from the nucleus, and an enriched accumulation of the drug in a perinuclear region (Fig. 5-3, h) that co-localizes with perinuclear MRP1 (Fig. 5-3, g, i).

To determine whether doxorubicin in this peri-nuclear compartment was indeed accumulating in MRP1-containing organelles, we examined the localization of both using deconvolution microscopy. We found that the peri-nuclear region positive for both doxorubicin and MRP1-ECFP (Fig. 5-4, a-c) was composed of what looked like individual vesicles containing both fluorophores (Fig. 5-4, d-f). In this case, the merge of the two images (Fig. 5-4, f) did not always result in yellow where the vesicles co-localized. Because these images represent living cells with rapidly moving vesicles, one second time delays between the acquisition of the images sometimes precluded absolute spatial co-localization. Additionally, the relative intensities of the two fluorophores are not matched, and vesicles labeled with more of one reporter than another do not appear yellow.

Infrequently, MRP1-ECFP was localized anomalously in HeLa cells; that is, it was found in regions other than the plasma membrane and the perinuclear region. This observation was not unexpected, as HeLa cells are not clonal, but a genotypically heterogeneous, transformed cell line. In an extremely rare instance, for example, MRP1-ECFP accumulated in what appeared to be large aggregates within the endo-membrane system (Fig. 5-4, g). Surprisingly, in this same multi-nucleated MRP1-ECFP expressing cell, doxorubicin was also found distributed throughout the endo-membrane system (Fig. 5-4, h) in a pattern very similar to the distribution of MRP1-ECFP (Fig. 5-4, i). Doxorubicin only assumed this dispersed sub-cellular distribution when MRP1-ECFP was likewise dispersed, and never in a cell that was not transfected with an MDR protein. Despite this anomalous localization pattern for MRP1, the protein was still active in the cell, and the expression of MRP1-ECFP still resulted in the exclusion of the drug from

the nucleus (Fig. 5-4, h). The observation that the intracellular distribution of doxorubicin varies with the intracellular distribution of MRP1-ECFP is suggestive that the protein has sub-cellular activity.

Moreover, in instances when the MRP1-ECFP plasmid was poorly expressed in HeLa cells, the protein was found only in intracellular compartments, and not at the plasma membrane at all (Fig. 5-4, j). This result suggests that the intracellular localization of the protein is not an artifact of an over-expression system. However, despite weak expression of this protein, cells like this one still accumulated the drug in MRP1-ECFP expressing vesicles, even if expression of the protein was not sufficient to exclude the drug from the nucleus (Fig. 5-4, k-l).

Therefore, in addition to the plasma membrane, MRP1-ECFP localized to intracellular compartments that were peripheral to the nucleus. Within these vesicles, MRP1-ECFP fluorescence was coincident with doxorubicin fluorescence, a finding which would be consistent with MRP1-mediated sequestration of the drug away from the nucleus. In rare instances, when a cell exhibited an altered pattern of intracellular MRP1 distribution, doxorubicin also assumed this altered pattern, arguing strongly that intracellular MRP1 actively transports doxorubicin.

5.3 Doxorubicin sequestration in MRP1-vesicles is dependent on MRP1 activity

We next wanted to determine if doxorubicin accumulation in MRP1-containing vesicles was dependent upon MRP1 activity, or simply a result of altered pH in MRP1-vesicles. If intracellular MRP1 is to be found predominantly

in the lysosomal compartment, then the lysosomal accumulation of a weakly basic chemotherapeutic like doxorubicin could simply be a function of acidification in these compartments. We therefore assayed the effect of concanamycin A on the sub-cellular distribution of doxorubicin in MRP1-ECFP expressing cells. Concanamycin A inhibits organellar acidification, as assayed by the pH sensitive dye acridine orange, which fluoresces in the red in a low pH environment (Fig. 5-5, a-b). In the absence of concanamycin A, acridine orange staining in the organelles peripheral to the nucleus is red (Fig. 5-5, a); after the addition of concanamycin A, red fluorescence is significantly reduced (Fig. 5-5, b), suggesting the reagent is inhibiting organellar acidification in these cells. We then added doxorubicin to concanamycin A-treated cells, and found that doxorubicin-sequestration was unaffected (Fig. 5-5, c-e). Thus, in HeLa cells over-expressing MRP1, alterations in cellular pH were unable to alter doxorubicin distribution, a finding in contrast with MCF7-Adr cells (Fig. 5-1, c) which have no doubt developed many different mechanisms of drug resistance during their protracted drug selection.

To determine whether the co-localization of doxorubicin and MRP1 in intracellular compartments was mediated by MRP1 activity, we inhibited MRP1 activity with verapamil, and then observed the distribution of doxorubicin. As expected, verapamil-treated cells accumulated doxorubicin primarily in the nucleus (Fig. 5-5, f-h), regardless of the degree to which they expressed MRP1-ECFP. More interesting however was the almost total absence of peri-nuclear doxorubicin in these cells (Fig. 5-5, g). As a result of inhibiting MRP1 activity, doxorubicin accumulation in the nuclear periphery was also blocked, and MRP1-ECFP cells treated with verapamil had no more vesicular doxorubicin

accumulation than cells not transfected with MRP1-ECFP (Fig. 5-5, i).

These results suggest that the expression of MRP1-ECFP alone is responsible for the peri-nuclear accumulation of doxorubicin.

We had now established that intracellular MRP1-ECFP co-localizes with doxorubicin and that this co-localization is mediated by MRP1 activity. We next wanted to determine whether this intracellular MRP1 activity alone was sufficient to promote the classic doxorubicin-resistant phenotype: exclusion of the drug from the nucleus. We have seen that there are two pools of MRP1, one at the cell surface, and one at the periphery of the nucleus. It is possible that the nuclear drug exclusion found in MRP1-ECFP expressing cells is a result of MRP1 activity at the surface of the cell. Although FACS analysis did suggest that MRP1 expression only minimally, if at all, reduced the total doxorubicin uptake in HeLa cells (see chapter 4, Fig. 4-6, c), these data represent relationships on a log scale; less dramatic, but perhaps still physiologically relevant, decreases might be missed. Thus, it was still possible that MRP1 at the plasma membrane was reducing intracellular drug accumulation and this reduction alone was responsible for nuclear drug exclusion. Intracellular MRP1 activity may have been unrelated to the decreased nuclear accumulation of the drug in MRP1-expressing cells.

To investigate this possibility, we needed a way of inhibiting MRP1 activity only at the cell surface. With MRP1 blocked at the cell surface, we could then assay whether intracellular MRP1 could still sequester the drug in MRP1-containing vesicles, and whether this activity was sufficient to decrease drug accumulation in the nucleus. For this purpose, we employed the help of two cysteine-based cross linking reagents, BM[PEO]₄ and BMH. The first is a cell-impermeable reagent which, if it blocked MRP1 activity, would do so only at the

cell surface, and in this way we would be able to isolate the activity of intracellular MRP1. The second would block both pools of MRP1, if it inhibited MRP1 at all. However, before using either cross-linking reagent, we needed to be sure that these reagents would block MRP1 activity without impairing cell viability. If cells were viable after the administration of the cross-linkers, and if MRP1 activity were inhibited by their administration, then these reagents would provide us a way of investigating the role of intracellular MRP1 activity in nuclear drug exclusion.

MRP1 sensitivity to these reagents was gauged with the compound tetramethyl rhodamine ester (TMRE). TMRE is a fluorescent MDR substrate that does not accumulate inside MRP1-expressing cells, but instead, is effluxed from the cell in an MRP1-dependent manner. TMRE is also a live stain dye; drug entry is dependent on the maintenance of plasma membrane potential, and upon cell entry, TMRE accumulates in the mitochondria (Farkas *et al.*, 1989). With TMRE, we could assay the effects of the cross-linking reagents on both cell viability and MRP1 activity at the same time. If after addition of these reagents, TMRE entered all cells regardless of the degree to which they expressed MRP1, the cross-linking reagents could next be used to assay intracellular MRP1 activity on doxorubicin.

When cells were exposed to TMRE (Fig. 5-6, a-c), the MRP1-expressing cell (Fig. 5-6, a) accumulated little to none of the drug, while cells that did not express detectable levels of the MRP1-ECFP took up the drug in the mitochondria (Fig. 5-6, b-c). Treatment with the MRP1 inhibitor verapamil rendered MRP1-ECFP cells incapable of effluxing TMRE (Fig. 5-6, d-e), and all cells accumulated the dye in the mitochondria comparably (Fig. 5-6, f). These results

suggest that TMRE exclusion from the cell is mediated by MRP1.

Crosslinking with the cell impermeable reagent BM[PEO]₄ affected MRP1-ECFP expressing cells much as verapamil did; all cells accumulated TMRE to the same extent, regardless of the degree to which they expressed MRP1 (Fig. 5-6, g-i).

Likewise, when cells were cross-linked with the cell permeable reagent BMH, MRP1-dependent efflux of TMRE was also inhibited (Fig. 5-6, j-l). The fact that cells accumulated TMRE after the addition of either BMH or BM[PEO]₄ suggests that cross-linking did not compromise cell viability. The fact that addition of these reagents inhibited MRP1-dependent TMRE transport suggests that cross-linking is sufficient to block MRP1 activity. Moreover, if BM[PEO]₄ is only reacting with MRP1-ECFP at the cell surface, then these results indicate that MRP1 activity at the plasma membrane is responsible for the absence of TMRE in cells.

In order to determine whether BM[PEO]₄ was inhibiting MRP1 selectively at the plasma membrane, we next tested the effect of BM[PEO]₄ addition on sub-cellular pools of MRP1-ECFP. Because doxorubicin accumulates in MRP1- containing vesicles (Fig. 5-4, d-f), we tested the effect of BM[PEO]₄ treatment on the intracellular distribution of the drug. Used in concert with BMH treatment, this experiment would test if BM[PEO]₄ was inhibiting primarily plasma membrane MRP1 and what role, if any, intracellular MRP1 activity played in doxorubicin sequestration.

When BM[PEO]₄ treated cells were exposed to doxorubicin (Fig. 5-7, a-c), doxorubicin did not accumulate in the nucleus of a cell expressing MRP1-ECFP even though MRP1 activity against TMRE is blocked with this treatment. Indeed, the MRP1-ECFP expressing cell (Fig. 5-7, a) continued to be

characterized by perinuclear doxorubicin staining (Fig. 5-7, b) which corresponds to the localization of intracellular MRP1 (Fig. 5-7, a, c). In contrast, when cells were exposed to the cell permeable cross-linker BMH, prior to doxorubicin incubation (Fig. 5-6, d-f), all cells accumulated the drug within the nucleus, much as they did when treated with verapamil. These results reveal that BM[PEO]₄ affected the activity of MRP1-ECFP primarily at the plasma membrane, whereas BMH inhibited MRP1 throughout the cell.

From these experiments, we can safely make the following observations. First, BMH and BM[PEO]₄ do not affect cell viability. Second, MRP1 activity at the surface of cells is responsible for the absence of TMRE accumulation in MRP1-expressing cells, and the addition of the cell impermeable BM[PEO]₄ blocks cell surface activity. Third, loss of cell surface MRP1 activity upon BM[PEO]₄ addition only marginally effects nuclear doxorubicin accumulation in MRP1-expressing cells. Finally, only the additional loss of intracellular MRP1 activity is sufficient to redistribute doxorubicin to the nucleus. These results then strongly suggest that intracellular MRP1 is responsible for intracellular doxorubicin sequestration, a drug resistance phenotype.

5.4 BM[PEO]₄ and BMH cross-link MRP1-ECFP

We next tested whether BMH and BM[PEO]₄ are affecting MRP1 activity by directly cross-linking MRP1-ECFP; if so, the electrophoretic mobility of MRP1 should be altered by treatment with either reagent. When cell lysates of MRP1-ECFP transfected cells were immunoblotted with the anti-MRP1 antibody MRPr1, the antibody recognized a doublet that migrated near a 250kDa protein standard. However, when cell lysates of BM[PEO]₄ treated cells were similarly

probed, the antibody recognized a much more slowly migrating species of the protein, suggesting that the reagent was cross-linking MRP1 directly. Likewise, when cell lysates of BMH treated cells were probed with the anti-MRP1 antibody, we see similar changes in the electrophoretic mobility of the protein (Fig. 5-8, a). We have reason therefore to believe that cross-linking with either reagent inhibits MRP1 as a result of direct protein modification.

5.5 BM[PEO]₄ and BMH do not increase cell permeability to MRP1 substrates

Even if MRP1 is being directly modified by these cross-linking reagents, it is possible that treatment with BM[PEO]₄ or BMH is not inhibiting MRP1, but simply increasing cell permeability to TMRE. In order to investigate this possibility, we determined the average TMRE accumulation in a population of cells as a function of MRP1 expression, and we determined whether this average was altered by the addition of cross-linker (Figure 5-8, b). When we calculated these averages, we found that neither BM[PEO]₄ nor BMH had any effect on TMRE accumulation in cells that expressed MRP1-ECFP at background levels. We did find, however, that BM[PEO]₄ was able to block MRP1 activity on TMRE almost entirely; all BM[PEO]₄ treated cells accumulated TMRE equivalently, even at high levels of MRP1 expression. On the other hand, BMH inhibition of MRP1 activity was not complete at the concentration of BMH used (Figure 5-8, b). However, since BMH enters cells and is free to interact with many intracellular cysteines, it might be more difficult to inhibit MRP1 activity with BMH at a concentration that would not at the same time be lethal to the cells.

We next performed statistical analyses on BM[PEO]₄-treated cells that were exposed to doxorubicin. We found that the concentration of the cell impermeable crosslinker that was able to block MRP1 activity on TMRE had a marginal effect on doxorubicin distribution. After treatment with BM[PEO]₄, MRP1-ECFP expressing cells still showed a statistically significant reduction in nuclear drug accumulation, if not as much as untreated MRP1-ECFP cells (Fig. 5-8, c). In contrast, when cells were treated with BMH, the nuclear fluorescence of the drug was not reduced by the expression of MRP1-ECFP, as it was in control cells (Fig. 5-8, c). Thus, at a concentration of BMH that was only partially able to block MRP1-mediated TMRE efflux, MRP1 activity against doxorubicin was inhibited. Since BM[PEO]₄ treatment completely inhibited MRP1-ECFP activity at the plasma membrane, as assayed by loss of TMRE efflux, but had little effect on the sub-cellular localization of doxorubicin, we have reason to believe that the intracellular pool of MRP1-ECFP unaffected by BM[PEO]₄ treatment is responsible for doxorubicin sequestration.

5.6 Expression of Pgp and BCRP also results in analogous doxorubicin sequestration

If the intracellular activity of MRP1 is capable of mediating drug sequestration and thus presenting a drug-resistance phenotype, we wondered whether other MDR proteins would also be able to function in this way. We have already seen that BCRP and Pgp, for example, are expressed in compartments peripheral to the nucleus, in regions that are positive for lysosomal markers (Fig. 5-9, a-c, and Fig. 5-9, g-i). Therefore, we decided to test the effect of expressing these proteins on doxorubicin accumulation. When BCRP-ECFP-transfected cells

were incubated in the drug, we found once again that doxorubicin accumulated in the nucleus of non-expressing HeLa cells. However, the expression of BCRP-ECFP (Fig. 5-9, d) redistributed the drug away from the nucleus into BCRP-positive vesicles (Fig. 5-9, e-f). In a similar fashion, Pgp-expressing vesicles that were positive for lysosomal markers (Fig. 5-9, g-i) also accumulated doxorubicin (Fig. 5-9, j-l), and this accumulation correlated with loss of nuclear doxorubicin fluorescence. For these reasons, we suspect that intracellular Pgp and BCRP also function to sequester doxorubicin from the nucleus in peri-nuclear vesicles. However, more thorough examinations of the intracellular activity of Pgp and BCRP have yet to be performed.

5.7 Discussion

We have demonstrated that the plasma membrane transporter MRP1 has a sub-cellular localization from which it can promote a drug resistance phenotype. This phenotype is reversible upon inhibition of MRP1 by verapamil but unaffected by alterations in intracellular pH. Using fluorescent markers for the ER, the Golgi, the recycling endosomes, and the lysosomes, we have shown in the previous chapter that this intracellular MRP1 activity most likely originates from the lysosomes. Moreover, Pgp and BCRP also localize to lysosomal membranes from which they also transport doxorubicin.

Of course, MRP1 activity does not stem entirely from the intracellular organelles; TMRE, for example, is effluxed by MRP1 before it can accumulate in the cell, presumably by plasma membrane localized versions of the transporter. Strangely, the dominant activity of the protein on doxorubicin is on intracellular membranes. Our results suggest that MRP1 may have different activity profiles at

different membranes, a difference that could be a function of environment (lipids, cholesterol) or post-translational modifications (e.g., phosphorylation) that occur at some sub-cellular compartments. Alternatively, these sub-cellular compartments may contain other transport mechanisms that act synergistically with MRP1 activity.

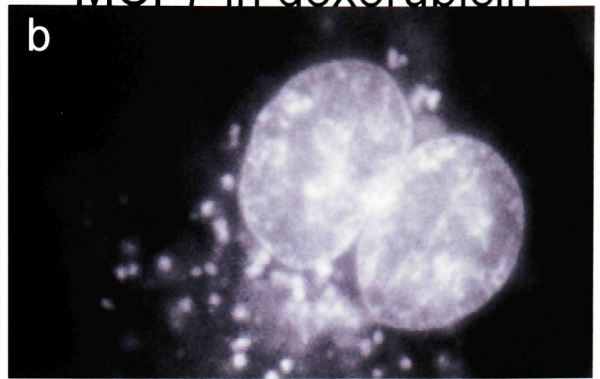
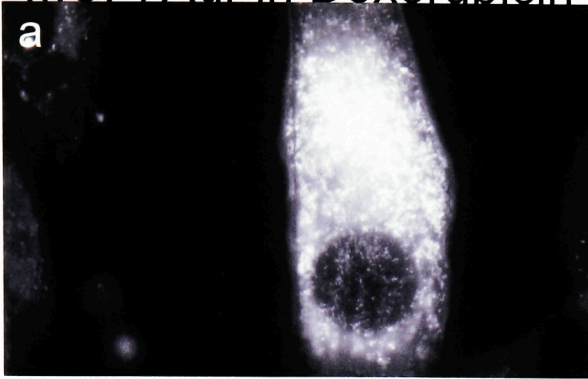
Intracellular localization and activity for MRP1 and for other members of the MDR transporter family may suggest different strategies for chemotherapeutic regimens in a clinical setting. To date, inhibitors for these MDR transporters have been selected presumably on the assumption of plasma membrane based efflux mechanisms. MRP1-mediated intracellular drug sequestration may necessitate alternate strategies in the search for MDR inhibitors.

Figure 5-1 Doxorubicin sequestration in MCF7-Adr cells. a-b. Doxorubicin is sequestered away from the nucleus, the target of doxorubicin toxicity, into acidified organelles in drug resistant MCF7-Adr cells (a), but not in the drug sensitive parent cell line MCF7 (b). c. Disrupting organellar acidification with concanamycin A, an inhibitor of vacuolar-type proton ATPases, redistributes doxorubicin into the nucleus of MCF7-Adr cells, suggesting the involvement of pH in drug sequestration. d. Inhibiting MRP1 and Pgp with verapamil also redistributes doxorubicin into the nucleus of MCF7-Adr cells, perhaps suggesting the additional involvement of these proteins in drug sequestration. e. In MCF7 Adr cells, doxorubicin (first micrograph) accumulates in regions positive for the lysosomal marker synaptotagmin VII (second micrograph), an observation made clear in the merge of the two images (third micrograph).

MCF7Adr in Doxorubicin

MCF7 in doxorubicin

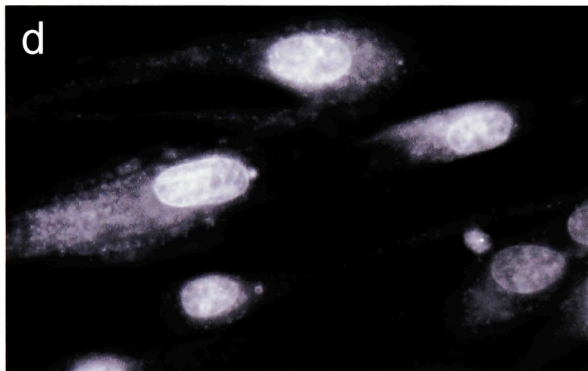
Control



Concanamycin A

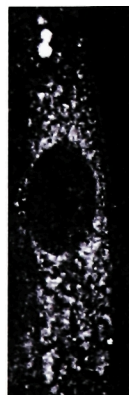


Verapamil



e MCF7Adr in Doxorubicin

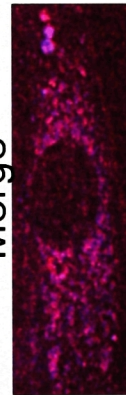
Synaptotagmin VII



Doxorubicin



Merge



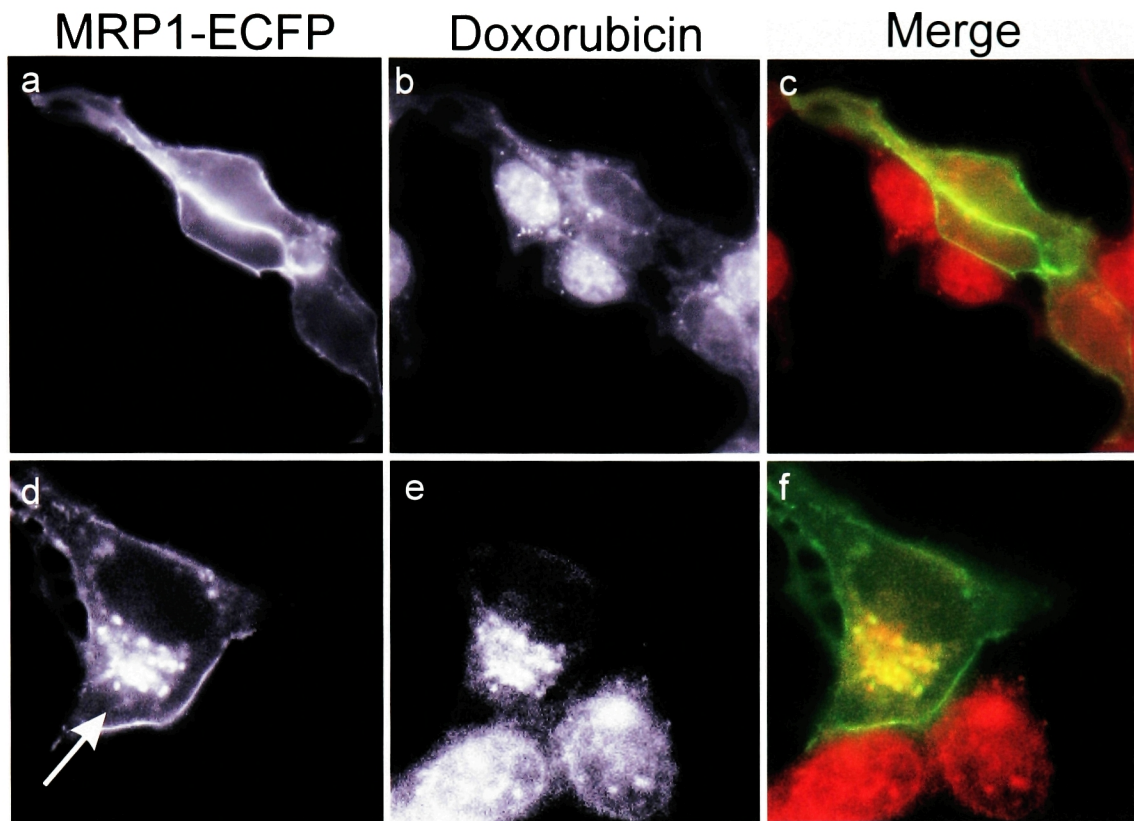


Figure 5-2 The expression of MRP1 in drug sensitive MCF7 cells. a-c. The expression of MRP1-ECFP redistributes doxorubicin away from the nucleus and mimics a drug resistance phenotype in this drug-sensitive MCF7 line. d-e. An enlarged view of MCF7 cells expressing MRP1; note the accumulation of the drug in MRP1-positive regions of the cell (arrow).

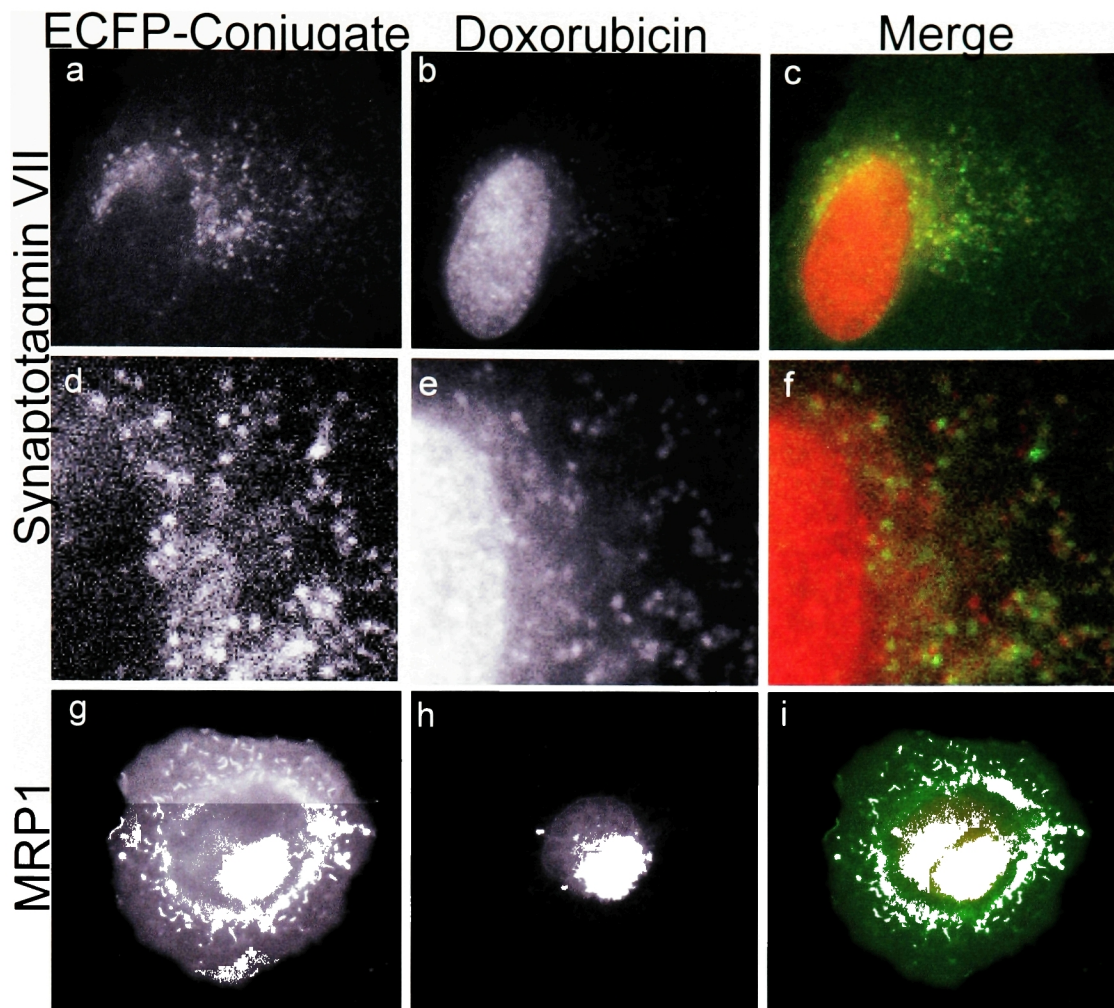


Figure 5-3. Doxorubicin redistribution upon the expression of MRP1.

a-c. HeLa cells transfected with the lysosomal marker synaptotagmin VII are imaged after doxorubicin incubation. Doxorubicin accumulates in the nucleus and, to a much lesser extent, in vesicles at the periphery of the nucleus. d-f. A close up of the cell presented in (a-c), showing doxorubicin accumulation in peri-nuclear vesicles. These vesicles do not appear to co-localize with the lysosomal marker; however, this is just a preliminary assessment, and the question needs further investigation. g-i. Significant enrichment of doxorubicin occurs in the peri-nuclear region of the cell as a result of MRP1-ECFP expression, and this enrichment appears to be in regions positive for MRP1-expression.

Figure 5-4 Doxorubicin localizes to MRP1-ECFP-positive vesicles. a. ECFP fluorescence reveals that a transiently transfected HeLa cell expresses MRP1 both at the plasma membrane and in a juxtanuclear region. The scale bar is 10µm. b. Doxorubicin fluorescence demonstrates that the drug likewise accumulates in a peri-nuclear region in an MRP-ECFP expressing cell, while the non-expressing cells surrounding it accumulate the drug in the nucleus. c. The merge of MRP1-ECFP fluorescence (green) and doxorubicin fluorescence (red) shows the co-localization of doxorubicin and peri-nuclear localized MRP1-ECFP (yellow). d-f. An enlarged image of the cell depicted in (a-c) reveals individual MRP1-ECFP containing vesicles that also contain doxorubicin. The scale bar is 1µm. g-i. In rare instances when MRP1-ECFP aberrantly collects in the endo-membrane system, doxorubicin accumulation is not peri-nuclear but is likewise dispersed. The scale bar is 10µm. j-l. A cell expressing low levels of MRP1-ECFP has little to no plasma membrane ECFP fluorescence and accumulates doxorubicin in a pattern that coincides with intracellular MRP1-ECFP. The scale bar is 5µm.

MRP1-ECFP

Doxorubicin

Merge

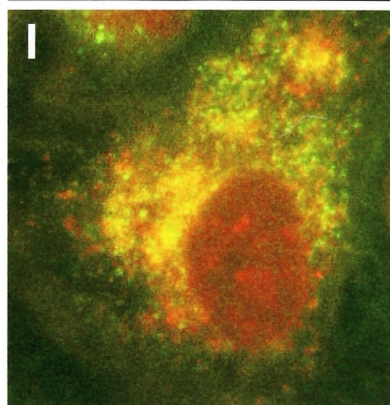
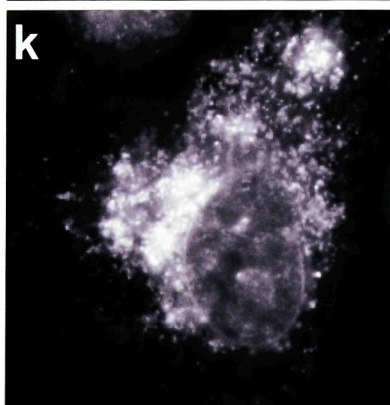
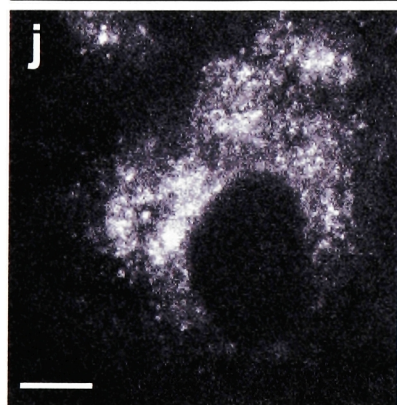
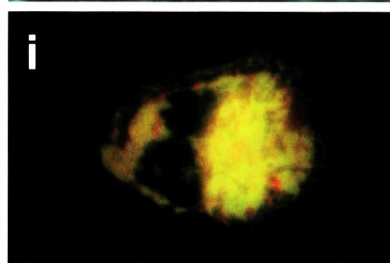
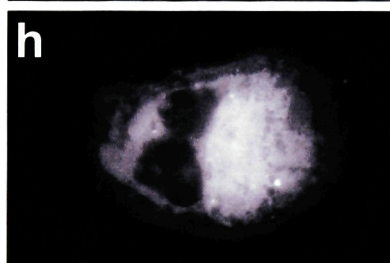
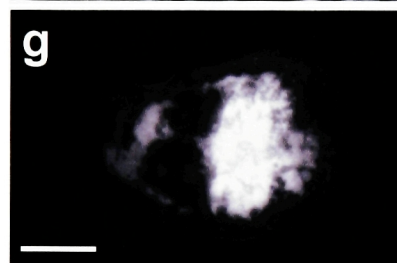
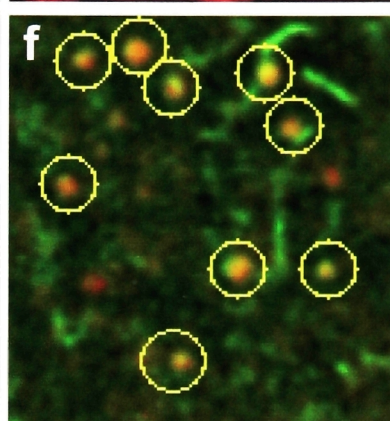
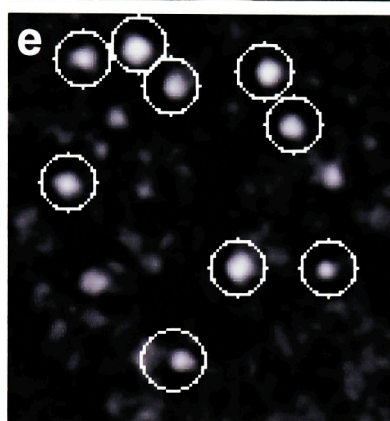
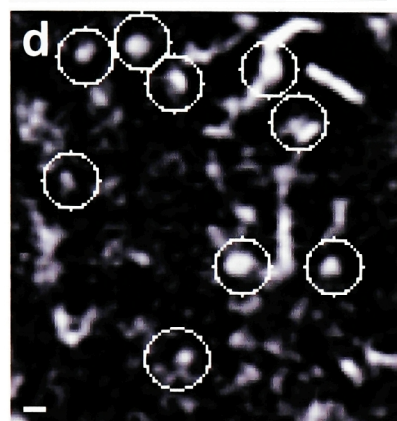
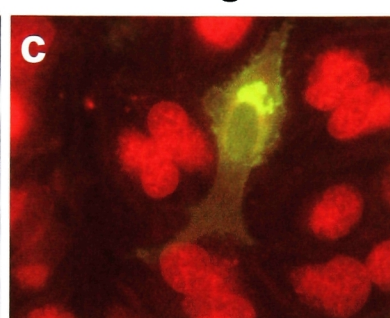
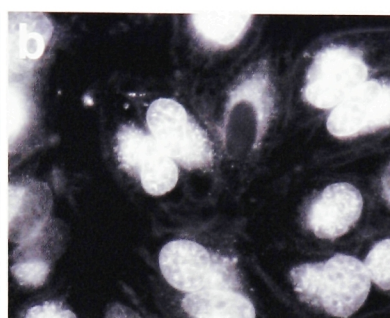
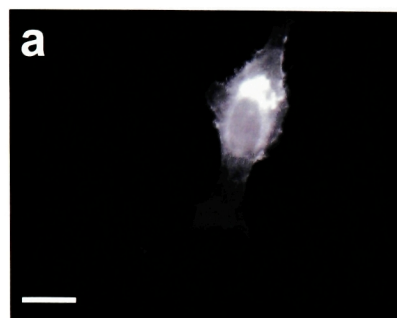


Figure 5-5 Accumulation of doxorubicin in MRP1-positive regions is dependent on MRP1 activity, and not pH. a-b. Acridine orange staining reveals concanamycin A-dependent disruption of organellar acidification. Acridine orange fluoresces red in low pH environments. Upon the addition of concanamycin A, an inhibitor of V-type proton ATPases, HeLa cells show significant decreases in red fluorescence (acidified compartments). c-e. The disruption of organellar acidification with concanamycin A has no discernable effect on the distribution of doxorubicin in MRP1-ECFP expressing HeLa cells. f-h. Inhibiting MRP1 activity with verapamil redistributes doxorubicin into the nucleus of MRP1-ECFP expressing HeLa cells, and substantially reduces perinuclear accumulation of the drug. i. A non-transfected HeLa cells accumulates doxorubicin in a pattern very similar to MRP1-ECFP expressing cells treated with verapamil (f-h). There is very little perinuclear accumulation of the drug in either case.

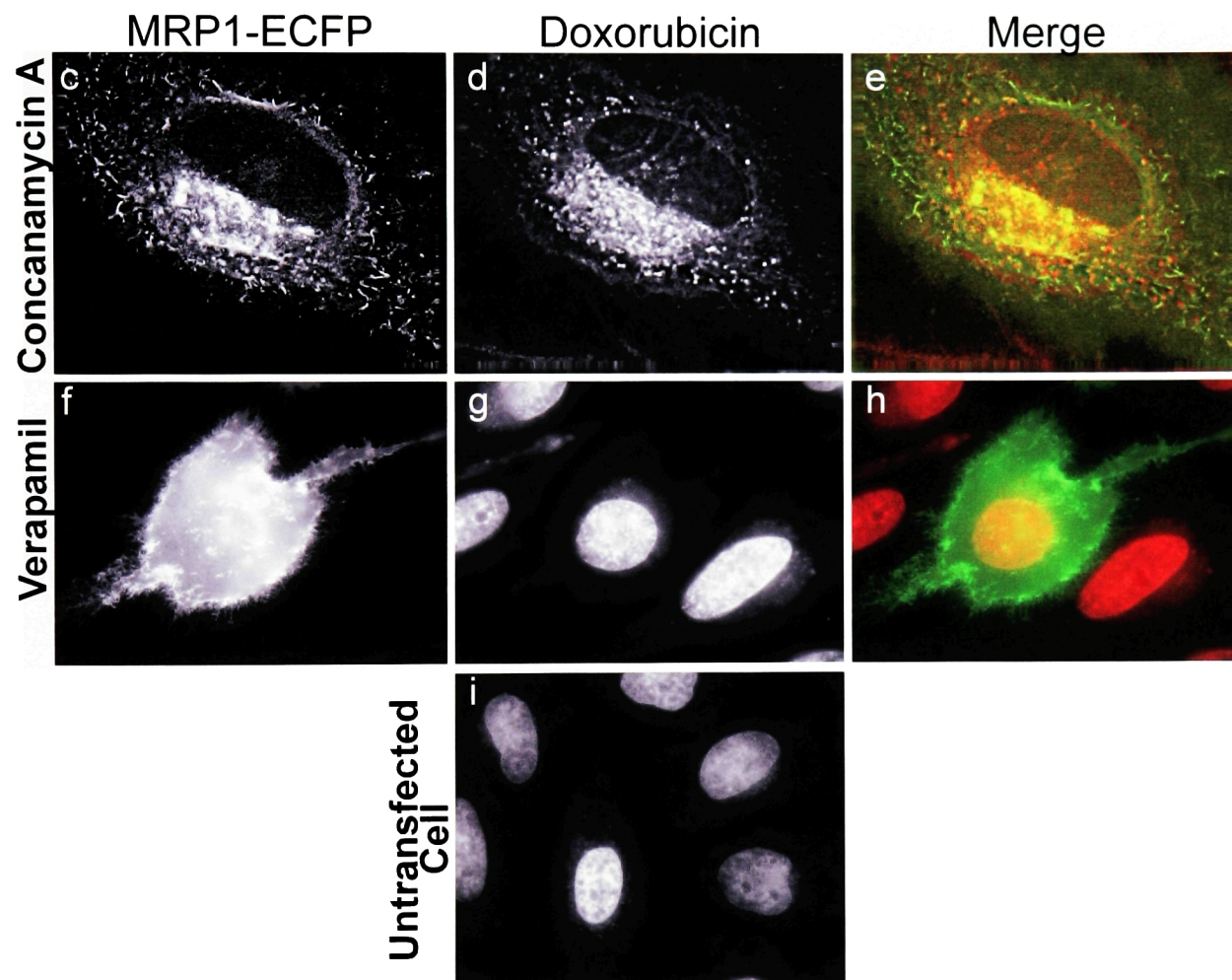
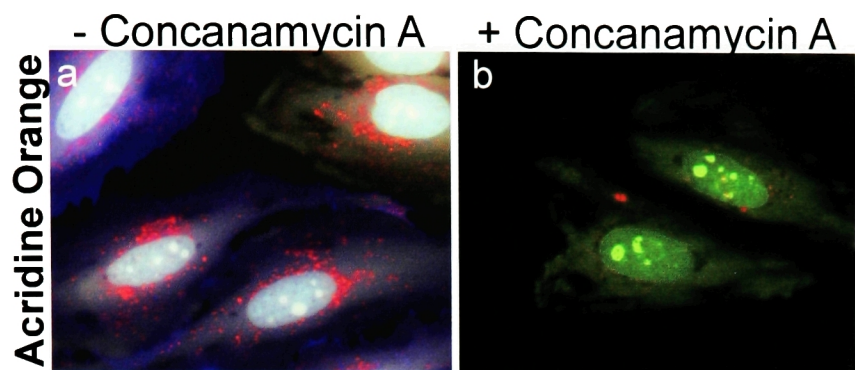
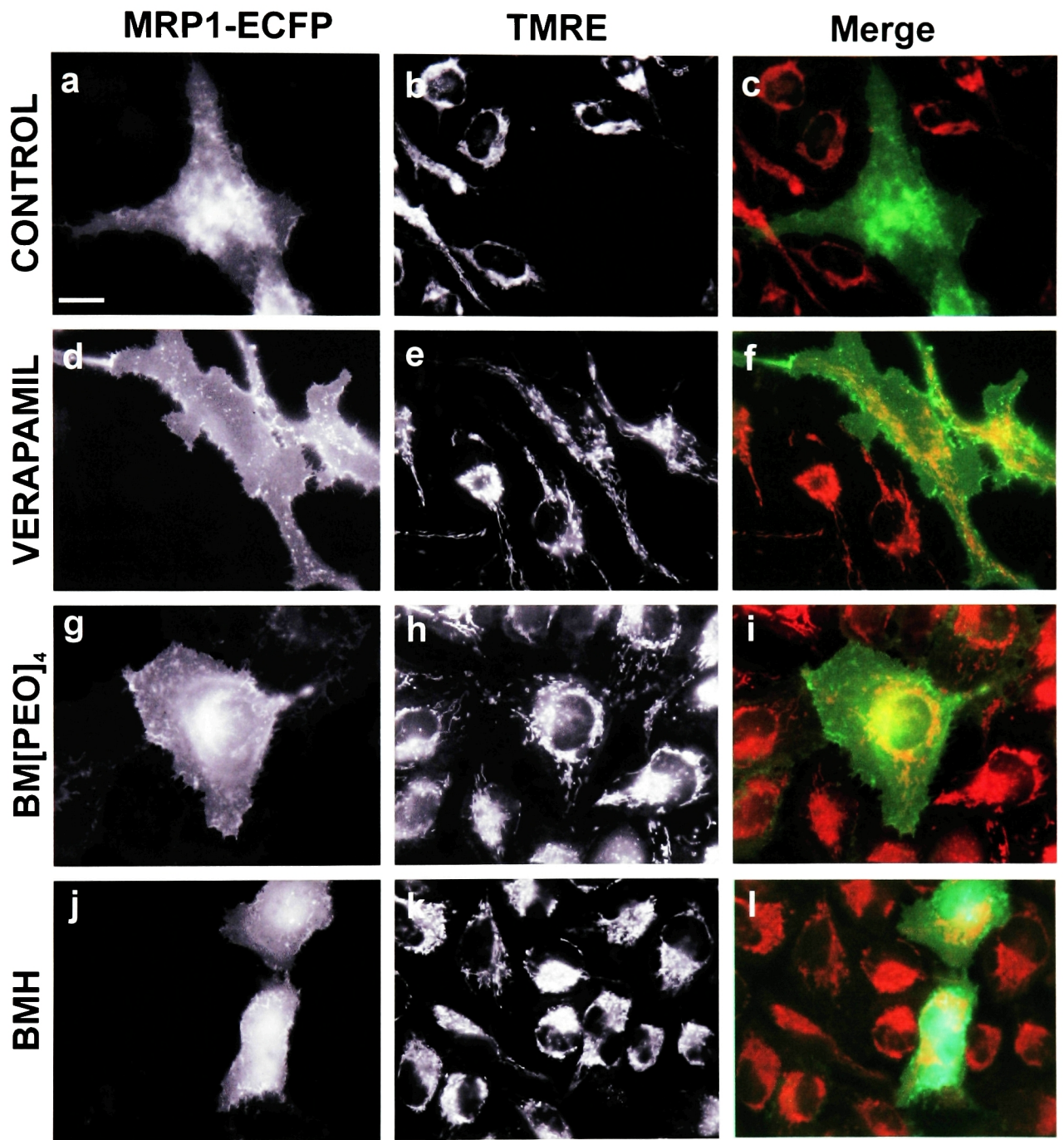


Figure 5-6. Crosslinking MRP1-ECFP interferes with its ability to transport substrates at the plasma membrane, as assayed by TMRE accumulation. a-c. MRP1-ECFP expression prevents the intracellular accumulation of TMRE, so that the MRP1 positive cell is not visible under TMRE fluorescence. d-f. Inhibiting MRP1 with verapamil prevents MRP1-mediated TMRE transport, and the two MRP1-ECFP expressing cells in this field now accumulate the drug. g-i. Crosslinking cells with the cell-impermeable reagent BM[PEO]4 prevents MRP1-mediated TMRE transport so that the MRP1 positive cell accumulates TMRE just like its non-expressing counterparts. j-l. Addition of the cell permeable crosslinker BMH also inhibits MRP1 transport of TMRE. The scale bar for the micrographs is 10 μ m.



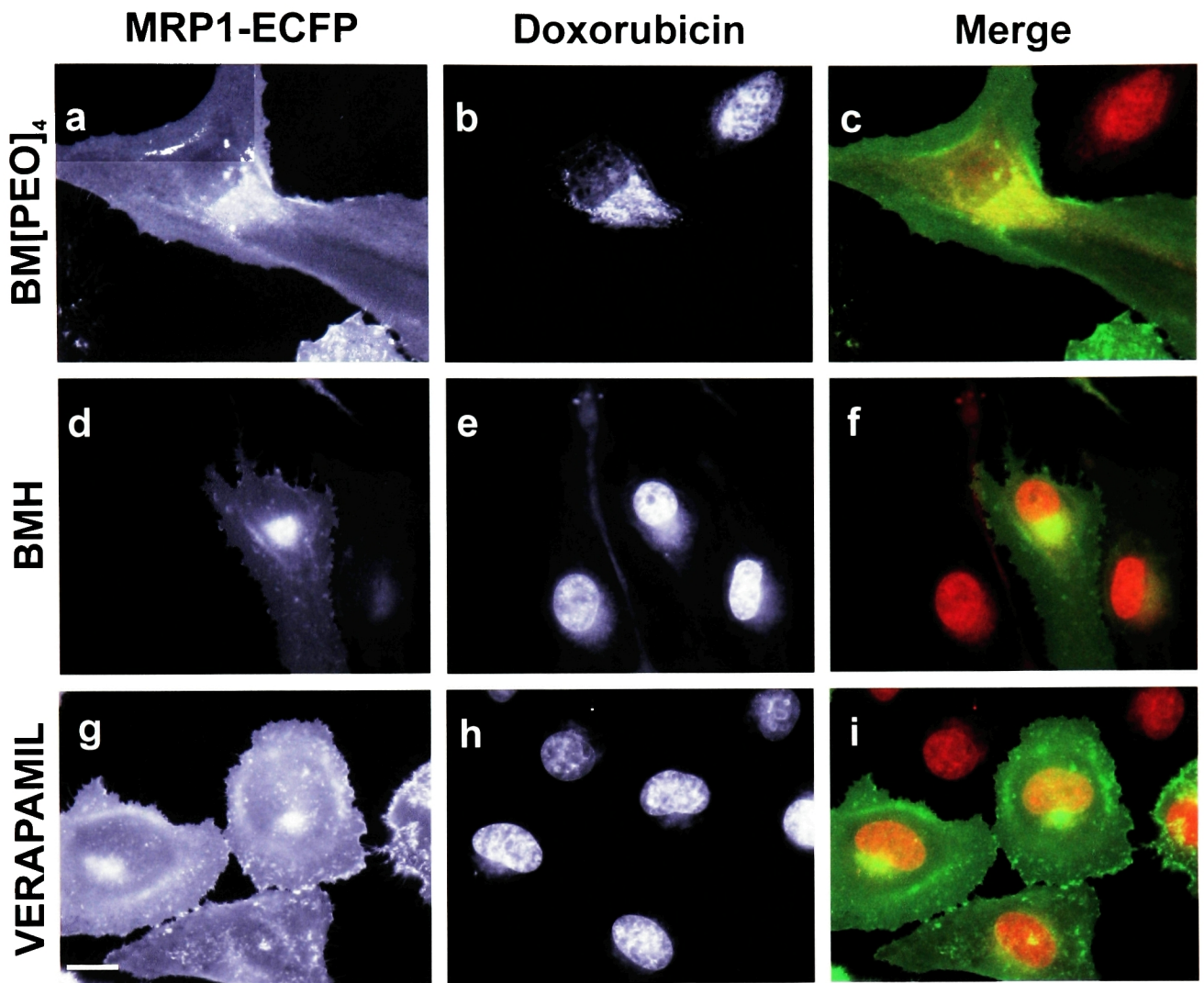


Figure 5-7 MRP1-ECFP actively sequesters doxorubicin in internal compartments. a-c. Addition of the cell-impermeable cross-linker BM[PEO]₄ has no effect on the sub-cellular distribution of doxorubicin in MRP1-ECFP expressing cells; the drug is still to be found in peri-nuclear regions positive for MRP1-ECFP. d-f. Addition of the cell-permeable crosslinker BMH redistributes doxorubicin to the nucleus of MRP1-ECFP expressing cells, much as the MRP1 inhibitor verapamil does (g-i).

Figure 5-8 The effect of crosslinking on the electrophoretic mobility and transport activities of MRP1-ECFP. a. In an immunoblot of MRP1-ECFP transfected cell lysates, an anti-MRP1 antibody recognizes a doublet whose molecular mass migrates below the 250kDa protein marker. However, addition of BM[PEO]₄ significantly retards the mobility of MRP1-ECFP. An immunoblot of BMH treated cells likewise reveals a changed mobility of the protein after crosslinking. b. MRP1-ECFP activity can be quantified by relating how much TMRE a cell accumulates to how much MRP1-ECFP a cell expresses. Fluorescence functions as a reporter for both MRP1 expression and TMRE accumulation. Neither BM[PEO]₄ nor BMH increase the permeability of cells to TMRE, since all cells with background MRP1 fluorescence accumulate comparable levels of TMRE. Moreover, cells treated with BM[PEO]₄, regardless of the degree to which they express MRP1, accumulate as much TMRE as untreated, non-MRP1 expressing cells. c. MRP1-ECFP activity against doxorubicin can be quantified by relating MRP1 expression to the doxorubicin fluorescence inside the nucleus. In BM[PEO]₄ treated cells, MRP1-ECFP still reduces the relative amount of doxorubicin accumulated in the nucleus. For both BM[PEO]₄ treated and untreated cells, MRP1-mediated reduction in nuclear fluorescence is statistically significant ($P < 0.01$ and $P < 0.0001$, respectively). However, all BMH treated cells have similar amounts of doxorubicin in the nucleus, whether they express MRP1-ECFP or not.

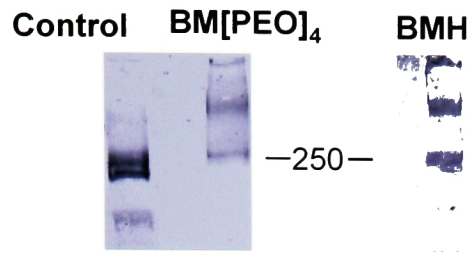
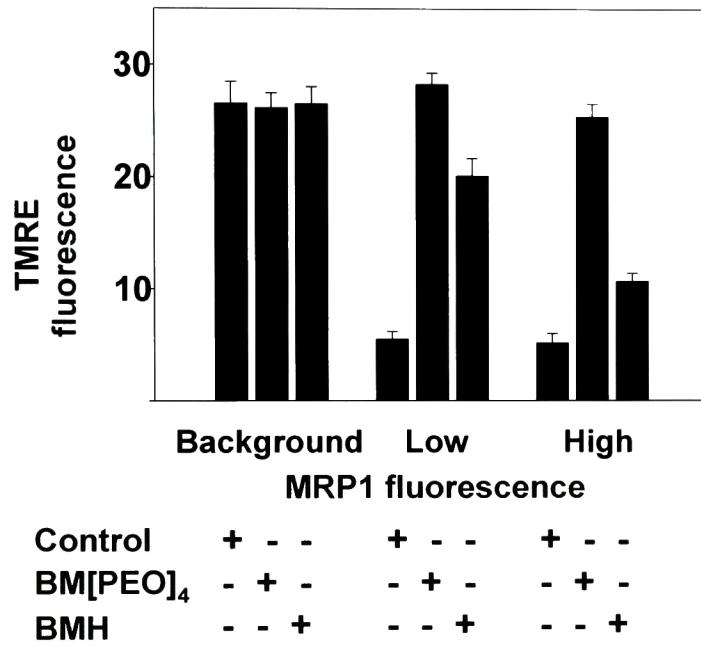
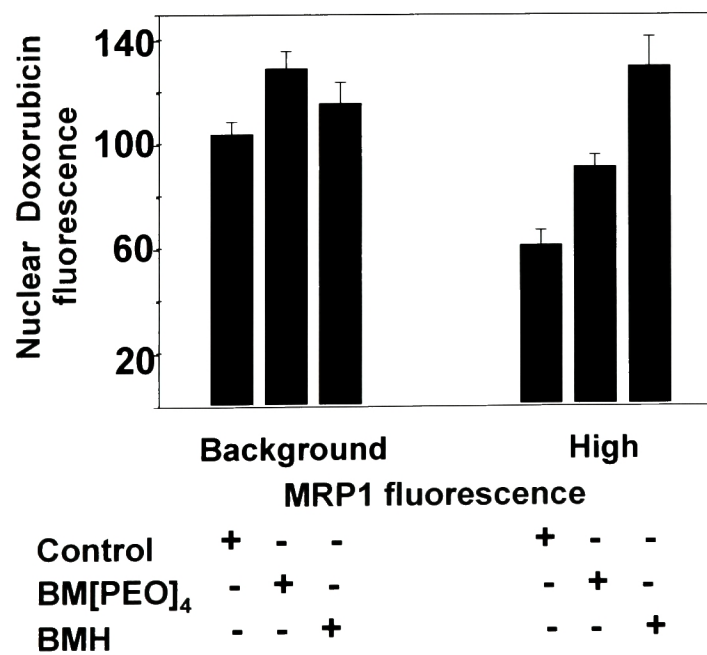
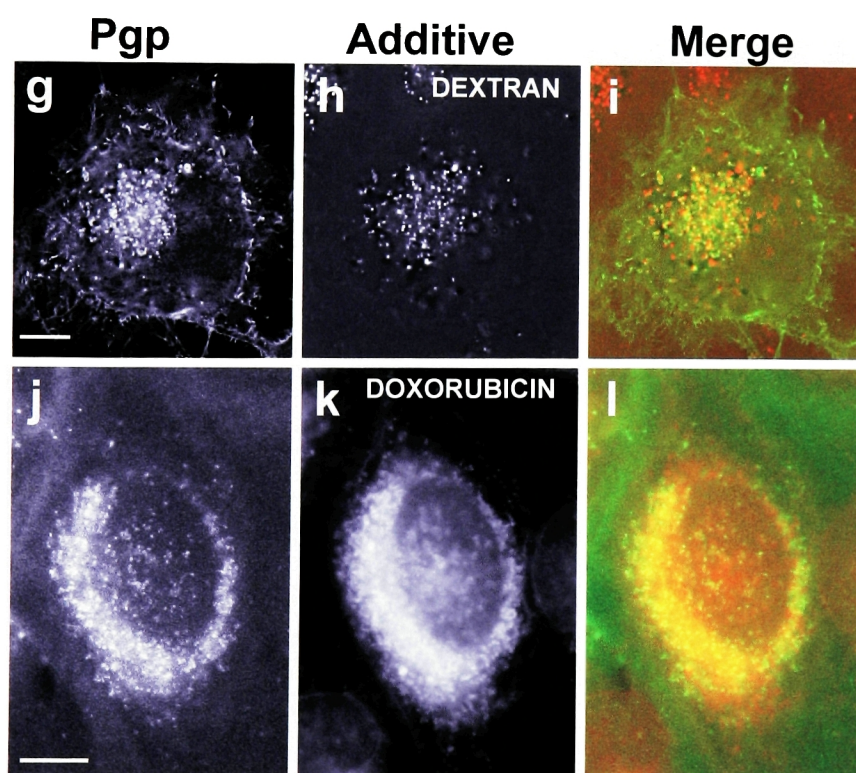
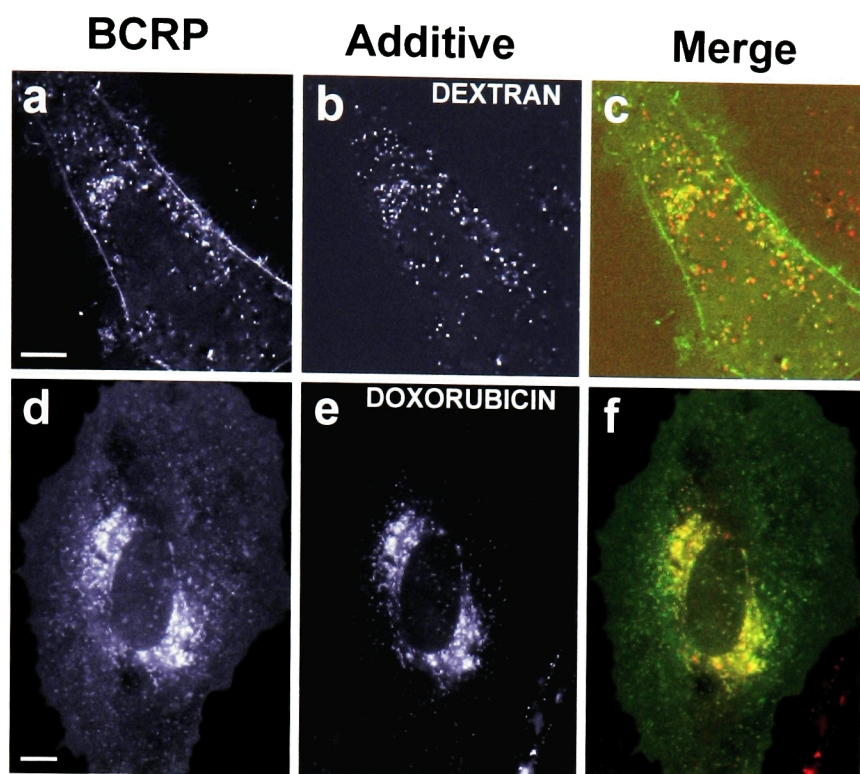
a**b****c**

Figure 5-9 Pgp and BCRP co-localize with a lysosomal marker and accumulate doxorubicin in regions positive for either Pgp or BCRP. All scale bars represent 10 μ m. a. A cell transfected with BCRP-ECFP expresses the protein at the plasma membrane and in intracellular regions. The image is a deconvolved fluorescent section of a cell. b. Fluorescent dextrans chased into the lysosomes of the cell in a accumulate in intracellular vesicles. c. The merge of (a) and (b) shows the degree to which BCRP-ECFP (green) colocalizes with the lysosomal marker (red). d-f. Panel shows the degree of colocalization of BCRP-ECFP in (d) and doxorubicin in (e). g-i. Panel shows the degree to which Pgp-ECFP accumulates in intracellular vesicles (g) that are positive for fluorescent dextrans chased into the lysosomes (h). j-l. Panel shows the localization patterns of Pgp-ECFP and doxorubicin.



6 Chapter 6 MRP1 activity and glutathione

6.1 Glutathione co-transport model

Previously published reports have suggested that MRP1-mediated transport of chemotherapeutic agents is dependent upon the presence of reduced glutathione. A number of lines of enquiry have suggested glutathione involvement in MRP1 activity: *in vitro* studies with membrane vesicles derived from MRP1-expressing cells, *in vitro* transport assays with MRP1 reconstituted into proteo-liposomes, as well as whole cell drug sensitivity assays with the glutathione-depleting agent BSO. These assays have all suggested that MRP1, a protein belonging to an organic anion transport family, needs the organic anion glutathione to activate the transport of hydrophobic, cationic chemotherapeutic drugs like daunorubicin or vincristine. In their protein reconstitution studies of MRP1, Mao *et al.*, for example, found that glutathione stimulated the transport of radio-labeled vincristine by over 4 fold (Mao *et al.*, 2000). In their examination of MRP1 transfected cells, Zaman *et al.* observed that glutathione depletion with BSO resulted in a significant reduction in the IC₅₀ values of doxorubicin and daunorubicin, 5 fold and 3 fold decreases, respectively (Zaman *et al.*, 1995). Glutathione has been shown to stimulate the ATPase activity of the reconstituted protein (Hooijberg *et al.*, 2000), and a photo-activatable derivative of glutathione, azido-phenacyl-glutathione, photo-labels the protein specifically (Qian *et al.*, 2002). In addition, enhanced glutathione transport has been measured in MRP1-containing cells and membrane vesicles, especially in the presence of a drug substrate.

This data has led many to suggest a model of MRP1 activity in which reduced glutathione promotes high affinity drug binding to MRP1. Upon binding to MRP1 in the presence of glutathione, the drug is then co-transported from the cell with glutathione. This glutathione co-transport model has been evoked to explain MRP1-mediated transport of the xenobiotics frequently used in chemotherapeutic regimens. For endogenous molecules speculated to be the physiological substrates of MRP1 transport, however, the protein is not always thought to require glutathione for its activity. LTC₄, for example, has been shown to be transported in the absence of glutathione, both in membrane vesicles and in proteoliposomes. The conjugated estrogen derivative 17- β -Estradiol 17-(β -D-Glucuronide), also a putative physiological substrate for MRP1, is also not thought to require glutathione for its transport. These observations have led some to speculate that reduced glutathione is necessary to activate the transport of hydrophobic, cationic substances (Feller *et al.*, 1995a). Indeed, the observation that calcein, itself an MRP1 substrate, does not depend on reduced glutathione for its efflux from the cell, suggested this functional difference: glutathione activates the transport of only those substances that are non-anionic and not conjugated to organic anions (Feller *et al.*, 1995a)

However, there are some problems with this assessment of MRP1 activity. Recent studies involving the conjugated estrogen estrone-3-sulfate (Qian *et al.*, 2001), as well as a β -O-Glucuronide conjugate of 4-(Methylnitrosamino)-1-(3-pyridyl)-1-butanol (NNAL) (Leslie *et al.*, 2001), have suggested that these anion conjugates also require glutathione for MRP1-dependent transport. In the case of estrone-3-sulfate, transport at V_{\max} was stimulated a little over 4 fold by the

presence of 1 mM glutathione; in the case of NNAL-O-glucoronide, maximal stimulation occurred at 3mM glutathione, both of which are within the range of intracellular glutathione for the average mammalian cell, 1-5mM. While MRP1 shows a glutathione requirement for estrone-3-sulfate transport (Qian *et al.*, 2001), the protein does not need glutathione to transport the anionic estrogen conjugate, 17- β -Estradiol 17-(β -D-Glucoronide) (Loe *et al.*, 1996a). Why would MRP1 require the presence of reduced glutathione to transport some conjugated anions and not others? No model of MRP1 activity to date has been able to address this question. Moreover, in the case of those anionic conjugates that are transported only in the presence of glutathione, no glutathione co-transport was observed. Neither estrone-3-sulfate nor NNAL-O-glucoronide were able to stimulate the transport of glutathione. If the glutathione co-transport model is correct, and glutathione is being effluxed out of the cell with MRP1 substrates, then these substrates should reciprocally stimulate glutathione transport. Why glutathione would stimulate one class of substrates in accordance with the co-transport model, and stimulate other drugs without being co-transported has not been addressed or resolved.

6.2 Glutathione co-transport: evaluating the data

A number of other questions also arise in reviewing the model of glutathione-dependent substrate transport. Much of the data supporting the model has been derived from kinetic measurements of protein activity in membrane vesicles or in proteo-liposomes. The assessment that glutathione is required for MRP1 transport of chemotherapeutic agents, for example, is based on the finding that reduced glutathione increases transport rates several fold. However, even in

the presence of reduced glutathione, these transport rates are themselves quite low, and do not reflect transport rates found for other transport proteins. Moreover, the transport rates suggested for high affinity substrates are also extremely low and are not within a physiological range. Mao et al., for example, report that purified MRP1 reconstituted into liposomes transports its high affinity substrate LTC₄ with a V_{\max} of 125 pmol/mg MRP1/min. At this rate, one molecule of MRP1 would transport one molecule of LTC₄ every 42 minutes (Table 6-1). Moreover, the rate for vincristine transport in the presence of glutathione is 19 pmol/mg MRP1/min, a rate that would correspond to one molecule of MRP1 transporting one molecule of vincristine every 4.6 hours (Table 6-1). The rate provided for vincristine transport is not suggested to be the maximal velocity of the protein, but it is the only one provided. These transport rates are not comparable to the transport rates of other ATPases or even other ABC transporters like P-glycoprotein (Table 6-2). Moreover, the rates of ATP hydrolysis derived for purified MRP1 are either also low (Table 6-3, Cole), or correspond to non-physiological rates of substrate transport (Table 6-3 Riordan). Transporters that couple substrate transport to ATP hydrolysis are generally believed to transport 1 to 1,000 substrate molecules/sec. The transport rates available for MRP1 in proteoliposomes seem to suggest then that the protein being studied has lost substantial activity during purification and reconstitution.

The transport rates provided for MRP1 in membrane vesicles are more difficult to interpret. Although each transport rate is provided at maximal velocity (V_{\max}), no attempt is made to assess the total MRP1 concentration in the assays. Assessments of transport are instead provided in terms of transport velocity per total milligram of vesicle protein (Table 6-4). Therefore, we cannot determine

whether estimated transport rates could be within a physiological range. However, if we were to estimate that MRP1 protein levels in their over-expression system constitute between 0.1 and 1% of the total vesicle protein (a conservative estimate for an over-expression system), then their transport rates would be non-physiological for many of the substrates assayed, including those used to invoke the glutathione co-transport model (Table 6-4).

Whole cell studies which conclude that MRP1 is dependent on glutathione for its activity are problematic, as well. For example, in their study of MRP1-mediated drug resistance in S1 cells over-expressing MRP1, Zaman et al. do report a reduction in the IC_{50} values of both doxorubicin and daunorubicin upon the addition of the glutathione-depleting agent BSO (Zaman *et al.*, 1995). However, similar reductions in the IC_{50} values for these two drugs were seen in Pgp-over-expressing S1 cells in the presence of BSO, and this pattern was also evident in the S1 background cell line. This discrepancy is noted in their study; however, no attempt was made to reconcile the non-specific effects of BSO with the model of MRP1 glutathione dependence.

6.3 Methods of studying glutathione dependence *in vivo*

For all of these reasons, we have decided to investigate further the role of glutathione in modulating MRP1 activity, using our fluorescent model system. Two ways of assessing glutathione dependence were available to us. The first was to examine the effect of BSO on cells over-expressing MRP1-ECFP. The second was to examine the effects of over-expressing MRP1 on cells that had no endogenous glutathione biosynthetic pathway. Both assays would study the effect of glutathione depletion on MRP1 activity; the former would examine the

question pharmacologically, the latter genetically, with a cell line generated from a mouse homozygous for a disruption in the gene encoding γ glutamylcysteine synthetase (γ -GCS). The γ -GCS enzyme catalyzes the first step in glutathione synthesis (Fig. 6-1 a), and the loss of this gene product results in the complete loss of intracellular glutathione, as determined by HPLC (Shi *et al.*, 2000). Although disruption of the γ -GCS promoter and the first exon is homozygous lethal in the mouse, cell lines were established from the homozygous embryo at embryo day 3.5, five days prior to the average time of death (see Fig. 6-1 b). These cell lines could only survive in the presence of exogenously added GSH or the reducing agent N-acetyl cysteine (NAC). Those cell lines maintained in NAC were dubbed GCS-NAC by Shi *et al.*, indicating both the loss of the γ -GCS gene product, as well as supplementation with NAC.

To assess the activity of MRP1 in the absence of cellular glutathione, we obtained the GCS2-NAC cell line and continued to maintain it in culture media supplemented with NAC. To ensure that this cell line had a disruption in the gene encoding the heavy subunit of γ -GCS, we performed nested PCR on genomic DNA isolated from GCS2-NAC, using primers suggested by Shi *et al.* In this fashion, we confirmed that this cell line did contain a disruption in the γ -GCS gene (Fig. 6-2, a). Next, we wanted to ensure that this disruption would result in the loss of glutathione production, as previously reported. For this purpose, we employed thin layer chromatography (TLC) to detect intracellular glutathione, using an assay commercially available from Molecular Probes. This glutathione detection assay chemically conjugates cellular glutathione to a fluorescent probe that can be visualized with TLC. The assay is sensitive to concentrations of

reduced glutathione within 10 μ M. When samples from GCS2-NAC cells were dotted onto the TLC plate, we found there to be no detectable glutathione, in accordance with the previously published report (Shi *et al.*, 2000) (Fig. 6-2, b).

6.4 Testing human MRP1 activity in mouse

Before expressing MRP1-ECFP in this glutathione null background, we wanted to ensure that the human gene encoding MRP1 would be expressed and properly localized in a mouse embryonic stem cell line. For these sets of experiments, we used the BDC1 cell line, a mouse cell line derived from a wild-type embryo, also at embryonic day 3.5 (Shi *et al.*, 2000). The expression of MRP1-ECFP in this mouse line resulted in a sub-cellular protein distribution pattern similar to that seen in HeLa cells (see chapter 4). MRP1-ECFP localized to the plasma membrane (Fig. 6-3, a-b), and to an intracellular region that was predominantly perinuclear (Fig. 6-3, c-d, see also Fig. 5-2). To ensure that MRP1-ECFP retained activity in a mouse cell line, we incubated BDC1 cells expressing MRP1-ECFP in the MRP1 substrate TMRE. Cells expressing the protein (Fig. 6-3, e) were able to exclude the drug and were negative for TMRE fluorescence (Fig. 6-3, f-g), indicating that the protein retained activity in this genetic background.

6.5 MRP1 is active in GCS2-NAC cells, in the absence of glutathione

We could now test the activity of MRP1-ECFP in the GCS2-NAC cell line and thereby assess the glutathione dependence of MRP1. We began with TMRE, a positively-charged, MRP1 substrate that is also an indicator of cell viability.

When GCS2-NAC cells were exposed to TMRE, cells that did not express MRP1-ECFP readily took up the drug (Fig. 6-4, a). The observation that GCS2-NAC cells could be positive for TMRE indicates that the loss of glutathione had not compromised cell viability. Only the cell expressing MRP1-ECFP was characterized by reduced TMRE accumulation (Fig. 7-4, b-c). This MRP1-dependent reduction is made clear in a line scan of the fluorescent intensities of the field, where red represents TMRE and green represents MRP1-ECFP fluorescence (Fig. 6-4, d). The observation that MRP1-ECFP expression is sufficient to reduce TMRE accumulation in GCS2-NAC cells suggests that MRP1 can function in the absence of glutathione on at least one of its cationic substrates. The glutathione co-transport model has been evoked to explain MRP1-mediated transport of non-anionic substrates (Feller *et al.*, 1995b).

We next assayed the activity of MRP1 against daunorubicin, a substrate previously thought to require glutathione for its transport from the cell (Zaman *et al.*, 1995; Renes *et al.*, 1999). Once again, GCS2-NAC cells showed MRP1-dependent daunorubicin exclusion (Fig. 6-4, e-g), and had significantly reduced levels of intracellular daunorubicin relative to neighboring cells (Fig. 6-4, h). These experiments suggested that MRP1 did not require glutathione to transport daunorubicin either.

Finally, we tested the activity of MRP1-ECFP against vincristine, the substrate whose transport had been originally used to suggest the model of glutathione co-transport. Because vincristine is not fluorescent, we assayed drug transport by the degree to which microtubules were depolymerized after incubation in vincristine. We have seen previously that the expression of MRP1-ECFP protects the cell from vincristine-induced microtubule loss (Chapter 4).

When GCS2-NAC cells were incubated in vincristine, MRP1-ECFP expression substantially mitigated the effects of the drug. MRP1-ECFP cells retained visible microtubule structure, with the microtubule organizing center readily identifiable (Fig. 6-4, i-k).

In order to make a more statistical appraisal of MRP1 activity in the absence of glutathione, we next quantified the accumulation of MRP1-substrates as a function of drug fluorescence, this time using large populations of GCS2-NAC cells. We found that MRP1 over-expression led to a statistically significant reduction in the accumulation of TMRE (Fig. 6-5, a) ($P < 0.001$). On average, TMRE fluorescence was reduced by a little over 71% in this glutathione-deficient cell line by the expression of MRP1-ECFP. Similarly, the expression of MRP1-ECFP also led to a statistically significant reduction in the accumulation of daunorubicin in these cells ($P < 0.001$), decreasing daunorubicin fluorescence in ECFP-positive cells by slightly over 50%. Although these fluorescence-based assays may not correspond to direct assessments of intracellular drug concentrations, as a result of intracellular drug metabolism or fluorescence-quenching, these assays do suggest that there is a pattern of differential drug accumulation upon MRP1-expression, and this pattern exists both in the presence and absence of intracellular glutathione.

6.6 MRP1 is active in cells pharmacologically depleted of glutathione

We next sought to investigate the glutathione dependence of MRP1 in cells treated with BSO, an irreversible inhibitor of the GCS holoenzyme. After incubation in BSO for prolonged periods of time, the glutathione bio-synthetic pathway is blocked and cells become depleted of their intracellular pools of

glutathione. BSO incubation protocols typically result in 80-90% reduction in intracellular glutathione after at least 24 hours of BSO exposure (Mans *et al.*, 1992). In one study in which MRP1 activity was said to be dependent upon glutathione, BSO treatment resulted in the loss of, on average, over 82% of intracellular glutathione stores (Zaman *et al.*, 1995). When we incubated both HeLa and wild-type mouse embryonic stem cells in BSO following a similar protocol (see Chapter 2), we found that glutathione stores were likewise effected. HeLa cells, as well as BDC1 cells, experienced a greater than 80% reduction in intracellular glutathione after BSO treatment (Fig. 6-6 a, b).

We next assayed MRP1 activity in BSO-treated HeLa cells against both TMRE and daunorubicin. The expression of MRP1-ECFP led to substantial decreases in the accumulation of TMRE, whether cells were treated with BSO or not (Fig. 6-7, compare a-d to e-h). Similarly, MRP1-ECFP expressing cells showed substantial reductions in daunorubicin accumulation relative to neighboring cells, despite the addition of BSO (Fig. 6-8, a-d vs. e-h). Statistical evaluations of large populations of MRP1-expressing cells also suggested that MRP1 retained activity against both TMRE and daunorubicin after glutathione depletion via BSO (Fig. 6-9). Interestingly enough, these statistical assessments of BSO-mediated effects also suggested that BSO-treated cells accumulated more of the MRP1 substrate, independent of MRP1 expression (Fig. 6-9, a and b, compare the first two bars). TMRE and daunorubicin accumulation increased in cells expressing background levels of MRP1-ECFP by 64.8 and 112.8%, respectively (see Table 6-5). These results are in accordance with previously published results demonstrating the non-MRP1-specific effects of BSO in

enhancing drug toxicity (Zaman *et al.*, 1995). In our case, it seemed as if BSO might be making the cell more permeable to MDR substrates like TMRE and daunorubicin.

6.7 BSO increases cell permeability to MDR substrates

To test this possibility, we examined the effects of BSO on drug accumulation in cells endogenously expressing varied levels of MRP1 (Fig. 6-10, a). The MCF-7 Adr cell line, for example, is multi-drug resistant, expresses both MRP1 and Pgp, and has been selected for elevated resistance to doxorubicin, an anthracycline closely related to daunorubicin in structure. When MCF7-Adr cells were incubated in daunorubicin, we found that these cells had significantly elevated levels of drug accumulation in response to BSO-treatment (Fig. 6-10, b-c). At the same light threshold levels, and under identical illumination conditions, BSO-treated cells had much greater daunorubicin fluorescence (Fig. 6-10, c) than untreated cells (Fig. 7-10, c). On average, daunorubicin fluorescence in MCF7-Adr cells increased by 181.6% as a result of BSO (Fig. 6-11, a). TMRE drug incubation assays were more difficult to interpret in this cell line, as MCF7-Adr cells did not uptake TMRE, perhaps indicating the toxic effects of continual selection under doxorubicin (Fig. 6-10, d-e). We also assayed the effects of BSO on the primary NHDF line, whose endogenous expression of MRP1 was the least elevated of the three cell lines tested (Fig. 6-10, a). When NHDF cells were incubated in TMRE, we found that TMRE fluorescence increased on average by 179% in response to BSO treatment (Table 7-5, Fig. 6-11, a). Finally, we attempted to assess the effect of BSO on drug uptake in non-transfected NIH 3T3 cells, but shortly after exposure to BSO, this cell line rounded up and died (Fig. 6-

11, c). We even examined the effect of BSO on the glutathione-null cell line, GCS2-NAC, and discovered that in this line, too, there was a BSO induced increase in drug accumulation (Table 7-5). Thus, in all cell lines tested, BSO had non-MRP1 mediated effects on drug uptake and toxicity.

6.8 Discussion

Well established as an organic anion transporter with broad specificity (Leier *et al.*, 1994; Loe *et al.*, 1996a; Loe *et al.*, 1996b; Hooijberg *et al.*, 1999), MRP1 has also been shown to transport cationic, and neutral hydrophobic compounds like the anthracyclines, vincristine, and TMRE (Cole *et al.*, 1994; Grant *et al.*, 1994; Paul *et al.*, 1996; Rajagopal *et al.*, 2002). Much speculation has surrounded the ability of the transporter to promote the cellular efflux of non-anionic substances, and it is generally believed that compounds that are cationic or neutral in nature are co-transported with reduced glutathione. The model for glutathione co-transport has been suggested primarily by protein reconstitution assays in membrane vesicles and proteoliposomes (Loe *et al.*, 1996b; Loe *et al.*, 1998; Mao *et al.*, 2000; Loe *et al.*, 2000), as well as by whole cell studies involving glutathione depletion via BSO (Zaman *et al.*, 1995). Glutathione is speculated to facilitate the high affinity transport of non-anionic substances, either by inducing conformational changes in the protein (Qian *et al.*, 2001) or by a mechanism that invokes positive co-operativity between drug binding and glutathione binding (Borst *et al.*, 1999).

When we examined the ability of MRP1 to transport cationic substances in the absence of glutathione, however, we found that MRP1 still retained activity against three of its substrates, TMRE, daunorubicin, and vincristine, substrates

which previously were thought to require glutathione for transport. In GCS2-NAC cells deficient in the production of γ -glutamyl cysteine synthetase, a gene necessary for glutathione production, MRP1 expression resulted in protein-dependent reduction of cationic substrates. Moreover, in BSO-treated HeLa cells, as well as in BSO-treated NHDF cells, MRP1 expression also resulted in the cellular reduction of cationic substrates. Our data is not in accord with previous assessments of MRP1 activity, and the basis for this disagreement is not clear. However, data published to date regarding the glutathione dependence of MRP1 has been collected either in cell-free systems, in proteoliposomes or inside-out membrane vesicles, or in BSO-treated cells depleted of cellular glutathione. *In vitro* assessments of MRP1 activity, though certainly indispensable for gathering basic biochemical data, may not represent the transport abilities of the protein *in vivo*. Moreover, our data indicate that when whole cells are depleted of their glutathione stores by treatment with BSO, these cells appear to be more permeable to MRP1 substrates, an increase that cannot be explained by glutathione depletion alone, as GCS2-NAC cells also experienced this increase once treated with BSO.

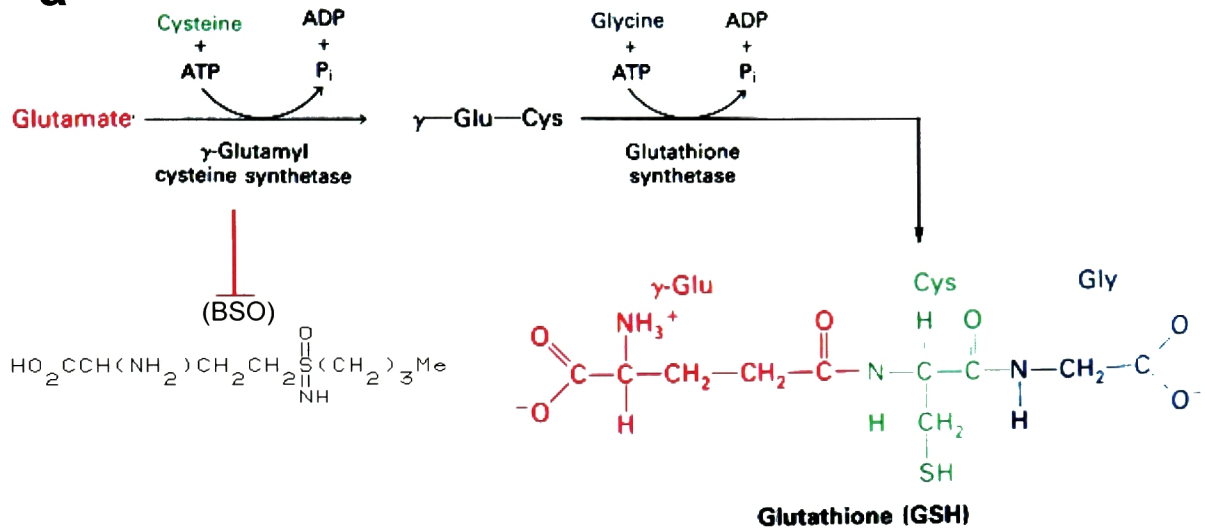
This BSO-mediated increase in cellular drug accumulation might help explain previously published observations that MRP1 is inhibited by BSO. Indeed, comparison of drug accumulation in MRP1-expressing HeLa cells with and without BSO treatment (Fig. 6-9, a, bars 3-4 and Fig. 6-9, b, bars 3-4), might lead to the conclusion of an MRP1-specific effect; however, reference to the change in drug accumulation experienced by non-MRP1 expressing cells (Fig. 6-9, a, bars 1-2, and Fig. 6-9, b, bars 1-2) makes this possibility less likely. Non-specific increases in drug accumulation were found in all four cell lines treated

with BSO, including GCS2-NAC cell lines. It is therefore also difficult to conclude that BSO is increasing cell permeability by depriving endogenous MRP1 of glutathione, as GCS2-NAC cells have never biosynthesized glutathione.

In demonstrating that MRP1 can function in the absence of glutathione, we cannot discount the possibility that, if present, glutathione does support MRP1-mediated transport. It is entirely possible that under conditions in which glutathione is depleted, another cellular compound functionally substitutes for glutathione in enabling MRP1 activity. This compound may facilitate conformational changes in MRP1 that are redox dependent or it may be co-transported with MRP1 substrates. Whether another compound might be able to functionally substitute for glutathione or whether MRP1 activity is independent of glutathione entirely should prove to be an important area of research for future investigation.

Figure 6-1 Glutathione bio-synthetic pathway and generation of a glutathione deficient mouse line. a. Glutathione biosynthesis is catalyzed by two enzymes, γ -glutamylcysteine synthetase (γ -GCS) and glutathione synthetase. Loss of the γ -GCS enzyme or inhibition of enzyme activity via BSO results in the loss of glutathione production. This figure is adapted from Stryer's Biochemistry. b. A mouse embryo homozygous for the loss of the gene encoding the heavy subunit of γ -GCS was generated by Shi et al. with a disruption in the TATA box and the first exon of the gene. The disruption was embryo lethal by embryo day 8.5, but cell lines were rescued at embryo day 3.5. Arrow pairs in the figure indicate primers used to confirm the gene disruption (see Fig. 6-2). This figure has been taken from Shi et al, 2000.

a



b

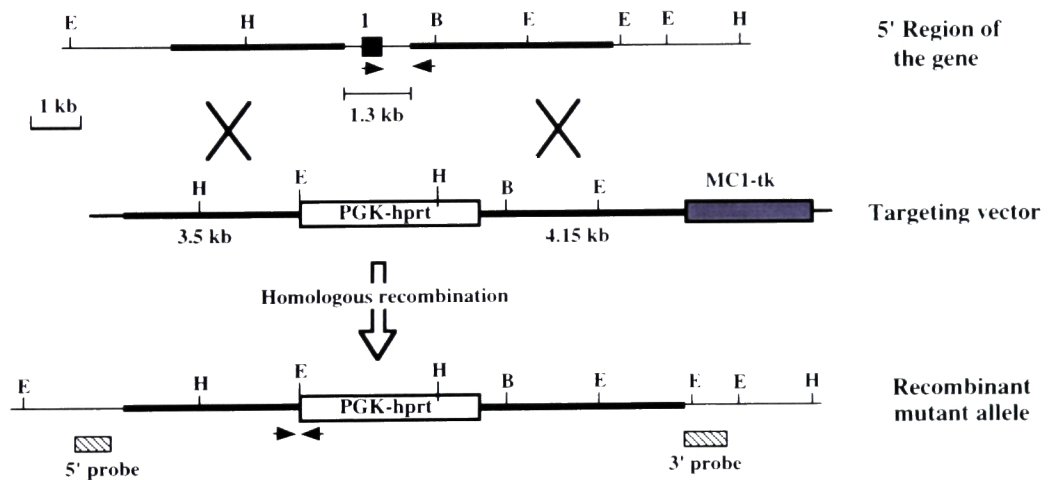
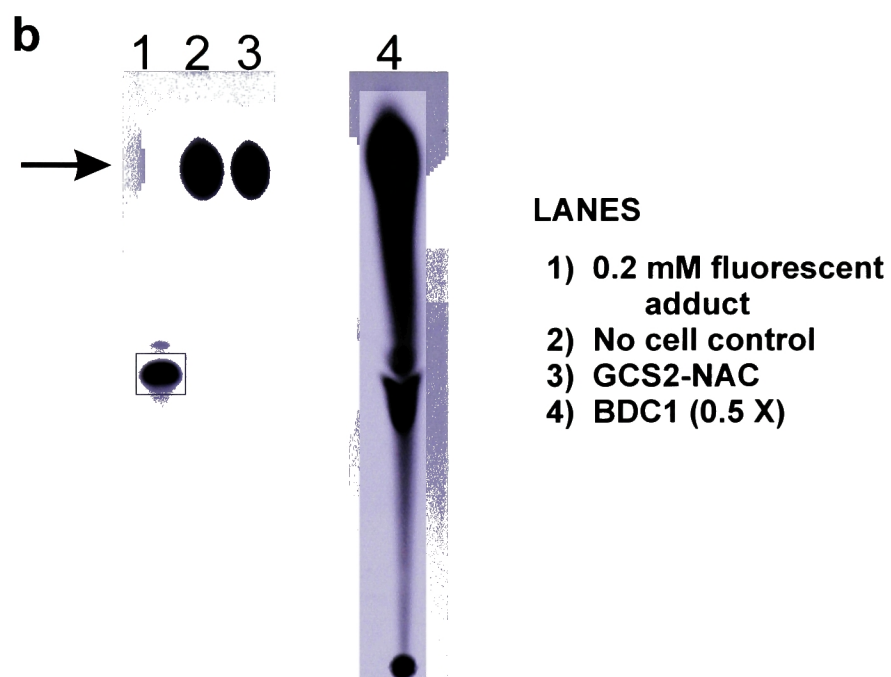
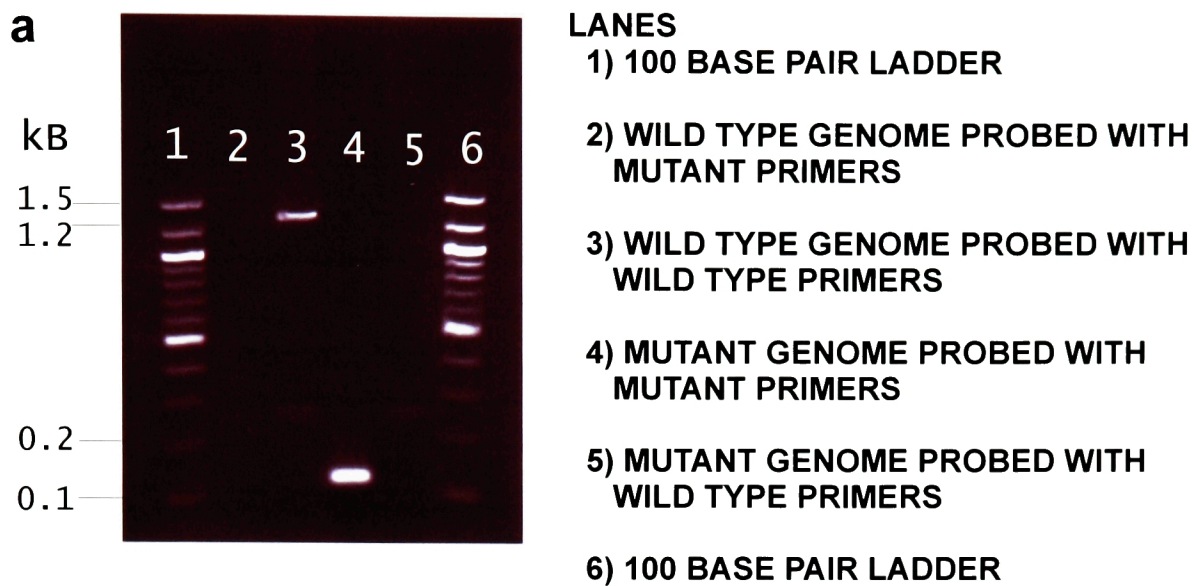


Figure 6-2 Confirmation of the disruption in γ -GCS in GCS2-NAC cells. a. To confirm that the GCS2-NAC cells used in our experiments were deficient for glutathione synthesis, we performed nested PCR on genomic GCS2-NAC and wild type BDC1 cells. The primers used for the results of the PCR reaction shown here are indicated as arrow pairs in Figure 6-1. Lanes 1, 6 are loaded with a 100 bp DNA ladder. Lane 2 is the wild type BDC1 genome probed with primers for the gene disruption. Lane 3 is the wild type BDC1 genome probed with primers for the wild-type sequence (removed by the gene disruption in mutant alleles). Lane 4 is the mutant GCS2-NAC genome probed using mutant primers. Lane 5 is the mutant GCS2-NAC genome probed using wild-type primers. b. Thin layer chromatography was performed on GCS2-NAC and BDC1 cells to confirm that the former was deficient in glutathione production. The assay detects glutathione after chemical conjugation of reduced glutathione to a fluorescent substrate. Lane 1 (box) was loaded with glutathione that was pre-conjugated to the fluorescent substrate. Lane 2 was loaded with cell culture media and lysis buffer alone. Lane 3 was loaded with GCS2-NAC cell lysates. Lane 4 was loaded with BDC1 cell lysates. Sample size of lane 4 was half of that of lane 3. Arrow indicates non-conjugated fluorescent-substrate.



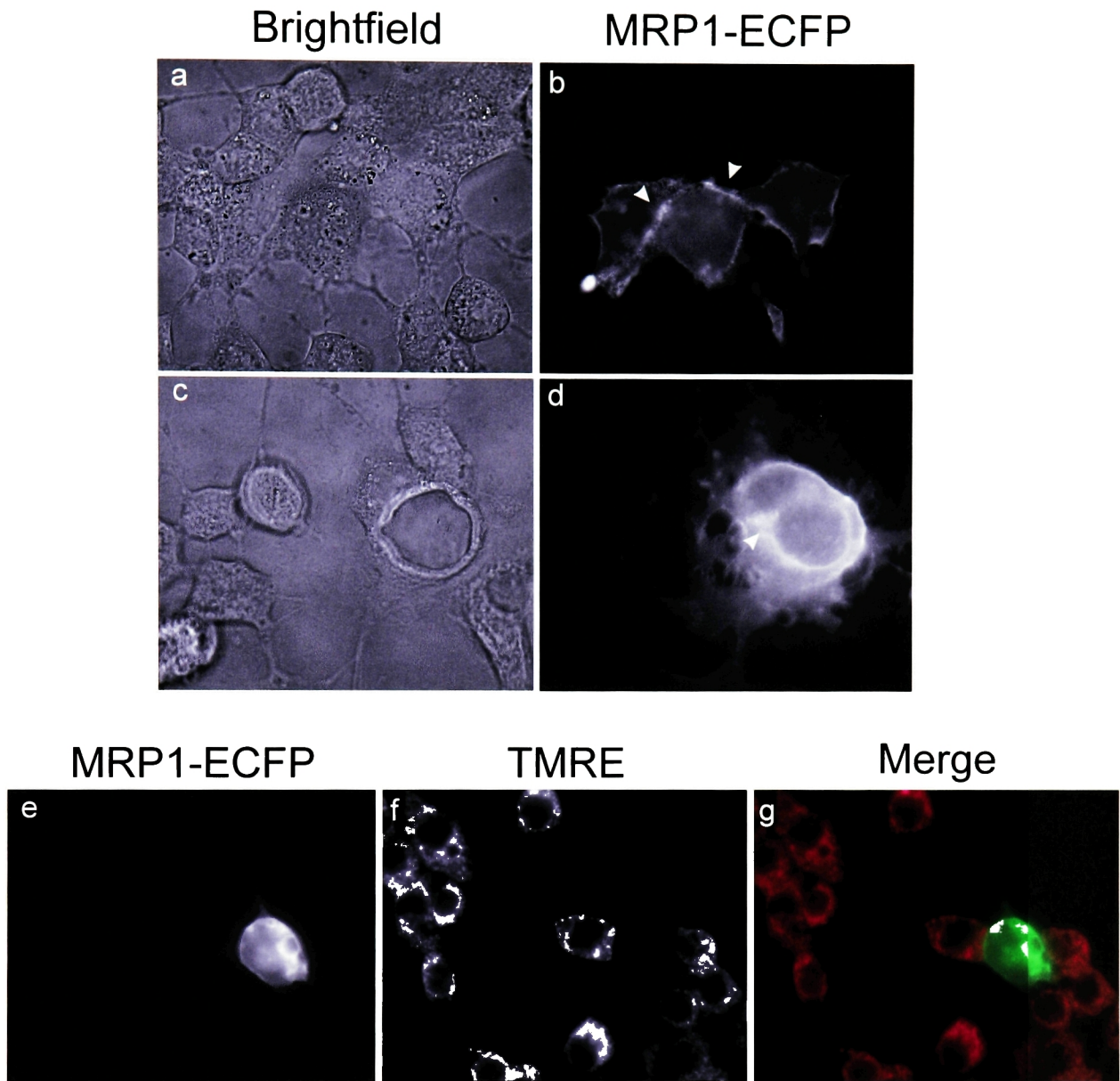


Figure 6-3 MRP1-ECFP is expressed, properly targeted, and functional in a mouse cell line. a-b. MRP1-ECFP is targeted to the plasma membrane in BDC1 mouse cells. Arrows indicate the rim-staining characteristic of proteins localized to the plasma membrane. c-d. MRP1-ECFP is also found in a peri-nuclear region in BDC1 mouse cells. e-g. MRP1-ECFP expressing cells (e) have substantially reduced TMRE fluorescence (f) compared to neighboring cells.

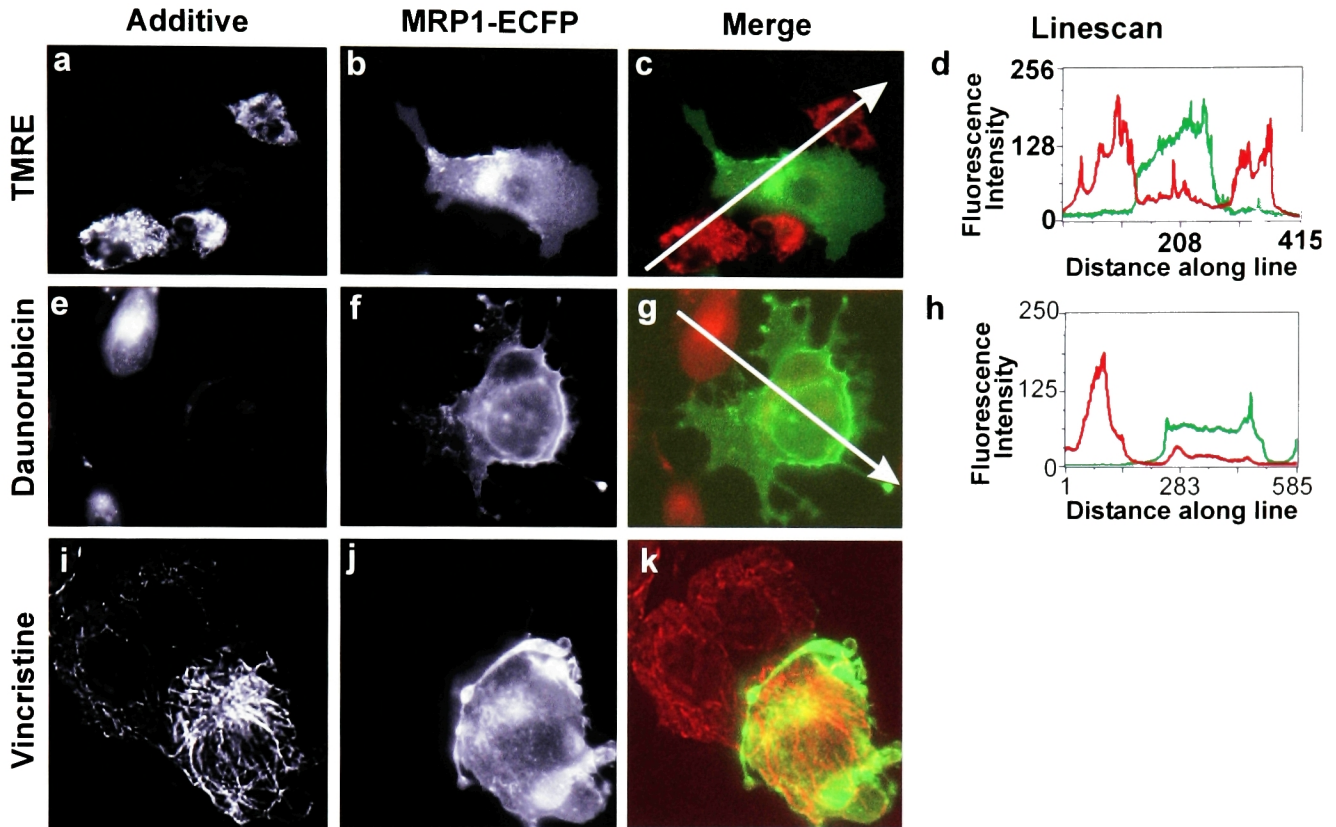


Figure 6-4 MRP1 is active in GCS2-NAC cells. a. Transiently transfected GCS2-NAC cells incubated in TMRE showed cellular drug accumulation as a function of rhodamine fluorescence. The cell in the center showed decreased TMRE accumulation. b. An MRP1-ECFP expressing cell in this same field is revealed by ECFP fluorescence. c. The merge of ECFP fluorescence (green) and rhodamine fluorescence (red) revealed that MRP1 expression correlated with decreased TMRE accumulation. d. A line scan of the fluorescent intensities in the merged image (c) illustrated MRP1-dependent TMRE reduction in these cells. e-h. MRP1-ECFP transfected cells showed decreased daunorubicin accumulation as a function of MRP1-expression. i-k. MRP1-expression correlated with chemo-protection against vincristine-mediated microtubule damage.

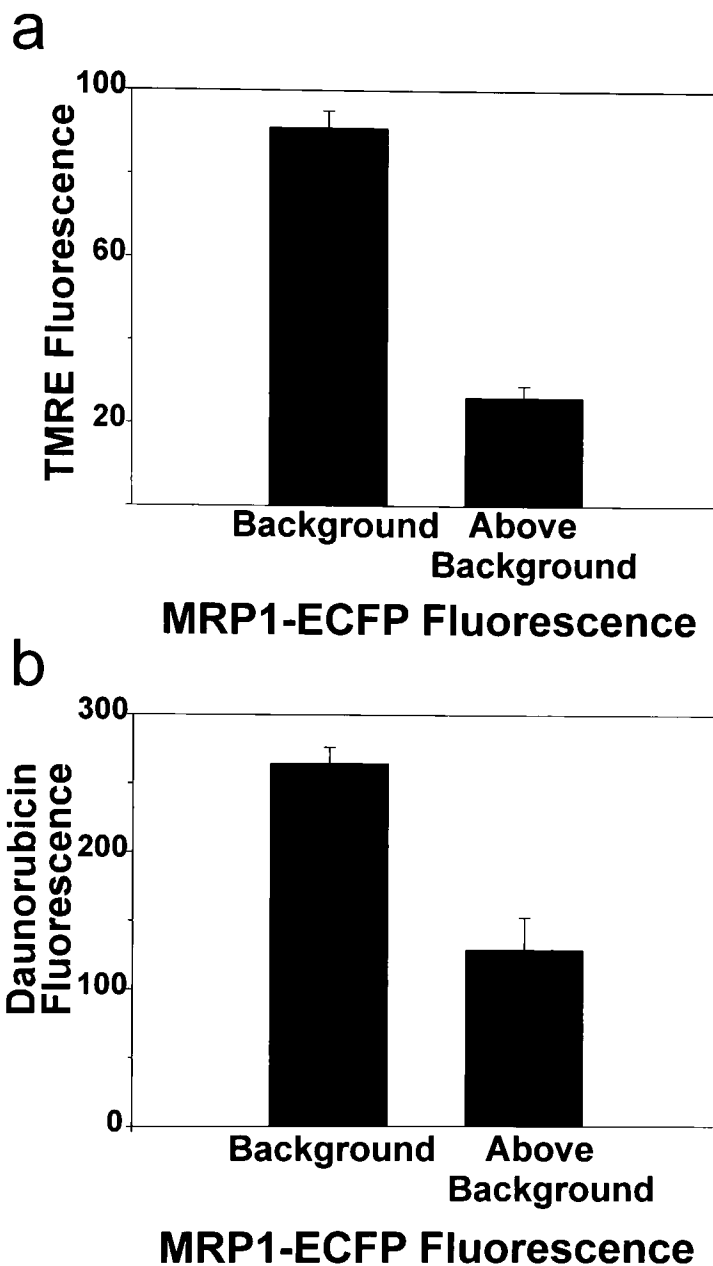


Figure 6-5. Quantification of MRP1-dependent drug transport in glutathione depleted cells. a. MRP1-ECFP transfected GCS2-NAC cells showed MRP1-dependent TMRE reduction, where cells expressing MRP1 are identified by "above background" ECFP fluorescence. b. GCS2-NAC cells also showed an MRP1-dependent reduction in daunorubicin accumulation. The reduction in drug accumulation seen with MRP1-expression was statistically significant for both TMRE and daunorubicin, with $P < 0.001$ in each case.

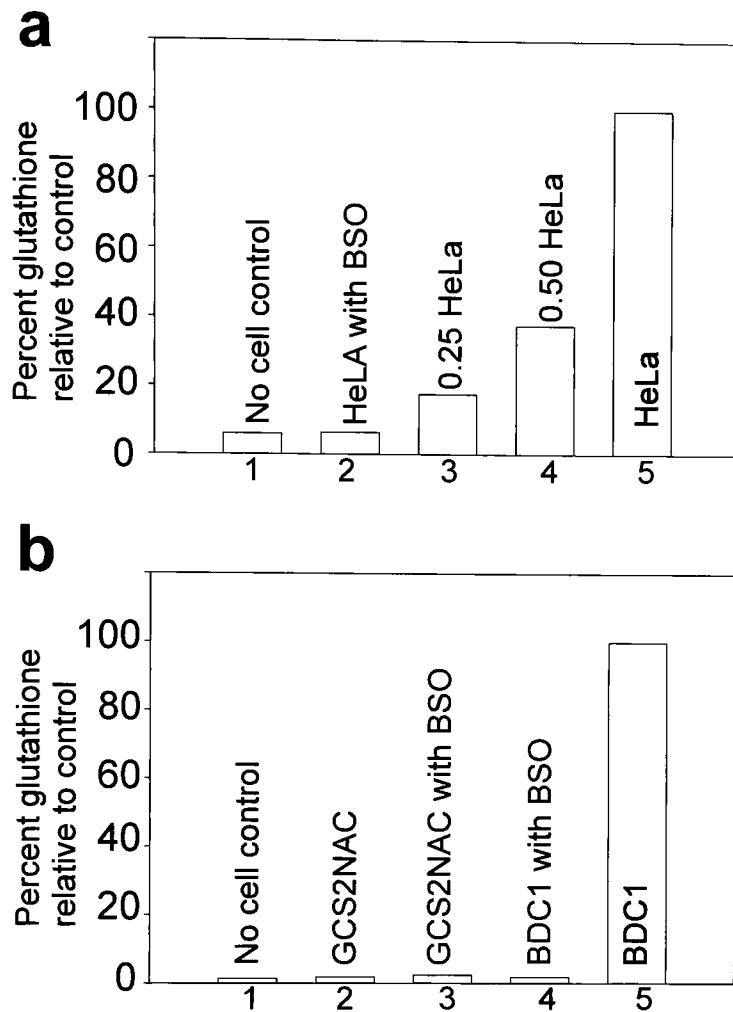


Figure 6-6 BSO incubation depleted intracellular glutathione stores by more than 80%. a. HeLa cells were assayed by TLC for intracellular glutathione stores, both with and without treatment with BSO. Treatment with BSO decreased glutathione stores in these cells to nearly undetectable levels, comparable to the no cell control (compare bars 1 and 2). Glutathione levels are presented as a percentage of non-treated HeLa cells of a fixed sample size (bar 5). Glutathione levels decrease in non-treated samples with sample size (bar 3, bar 4). b. BDC1 cells were also assayed by TLC for glutathione both with and without BSO treatment. BSO reduced glutathione levels in BDC1 cells (bar 4) to levels comparable to the no cell control (bar 1) or GCS2-NAC cells (bar 2-3). BSO had no effect on glutathione levels in GCS2-NAC cells (bars 2-3). Glutathione levels are expressed as a percentage of those found in wild type cells of a fixed sample size (bar 5).

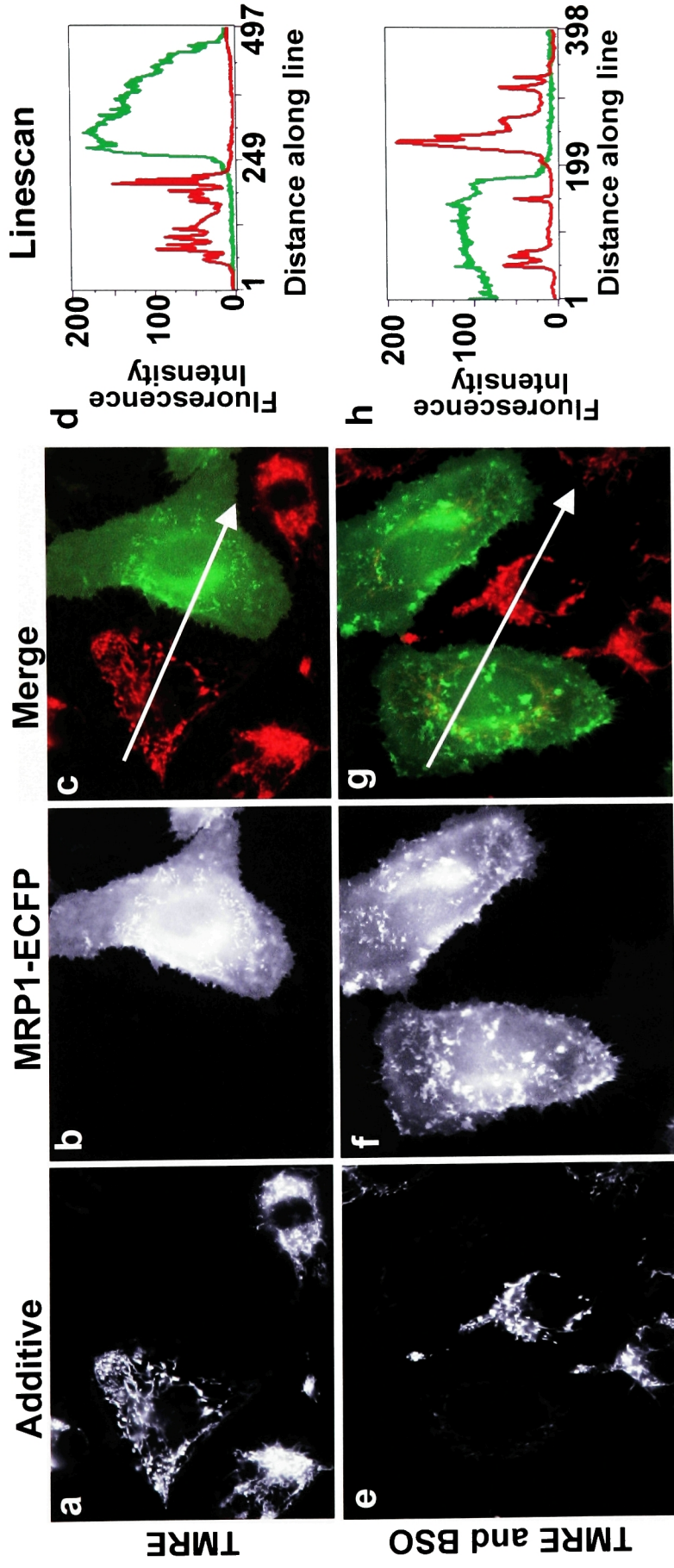


Figure 6-7 MRP1 is active against TMRE in HeLa cells depleted of cellular glutathione via BSO. a-d. An MRP1 expressing HeLa cell (b) has reduced TMRE accumulation compared to neighboring, non-MRP1 expressing cells (a), an observation made evident in the merge of CFP and rhodamine fluorescence (c), as well as in a line scan of the fluorescent intensities of the field (d). e-h, BSO treated HeLa cells incubated in TMRE also showed MRP1-dependent reduction in TMRE accumulation.

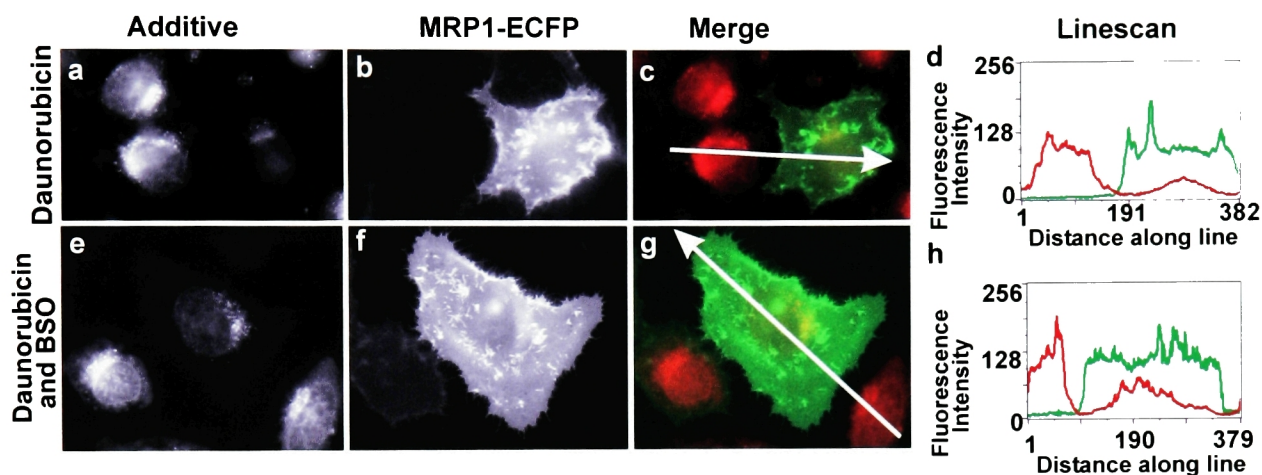


Figure 6-8 MRP1 is active against daunorubicin in HeLa cells depleted of cellular glutathione via BSO. a-d. An MRP1-expressing HeLa cell (b) incubated in daunorubicin showed reduced drug accumulation compared to two non-MRP1 expressing cells (a), as seen in the merged image (c) and in the line scan (d). e-h. BSO treated HeLa cells incubated in daunorubicin still showed MRP1-dependent daunorubicin reduction, a reduction clear in the line scan (h) of the merged image (g).

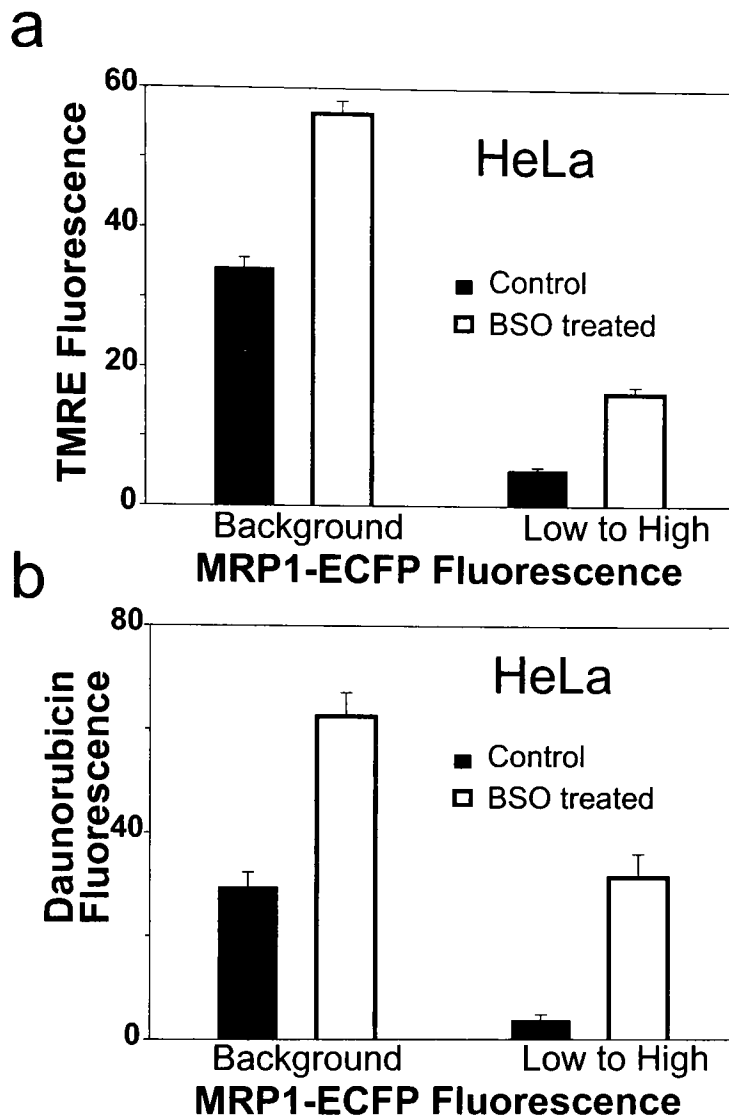


Figure 6-9. Quantification of MRP1-dependent drug transport in HeLa cells depleted of glutathione via BSO. a. BSO-treated HeLa cells transfected with MRP1 showed MRP1-dependent TMRE reduction (bars 2 and 4), just as non-BSO treated HeLa cells did (bars 1 and 3). BSO treatment increased TMRE accumulation in both MRP1-ECFP and non-MRP1-ECFP expressing cells (compare bars 1 and 2) b. Both BSO-treated and non-BSO treated HeLa cells showed an MRP1-dependent reduction in daunorubicin. BSO addition increased cellular accumulation of daunorubicin in cells independent of MRP1 expression (compare bars 1 and 2).

a

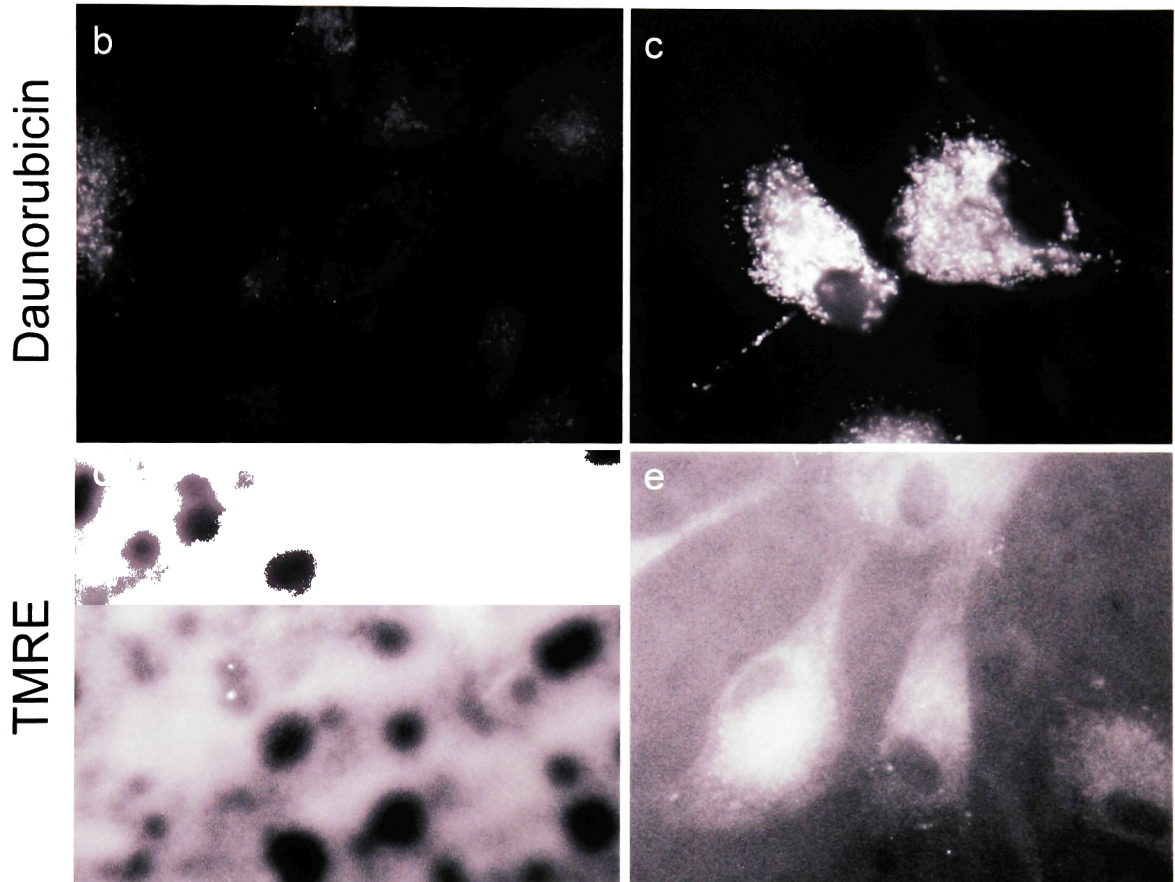
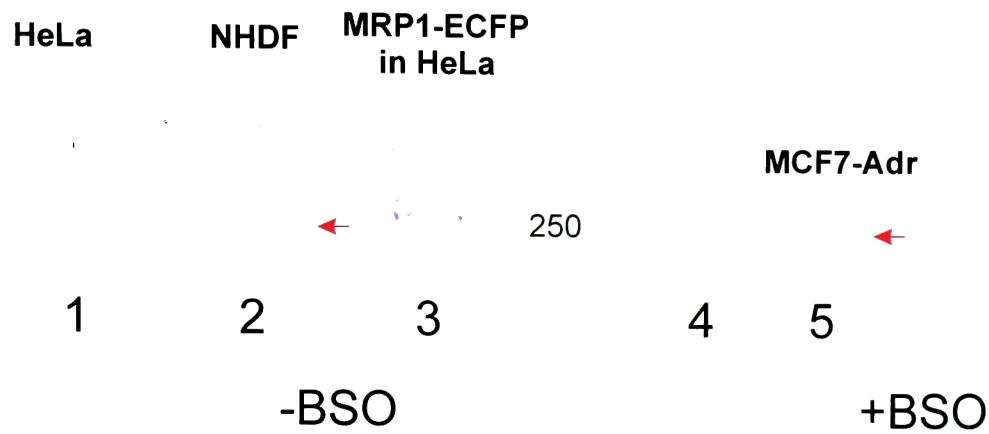
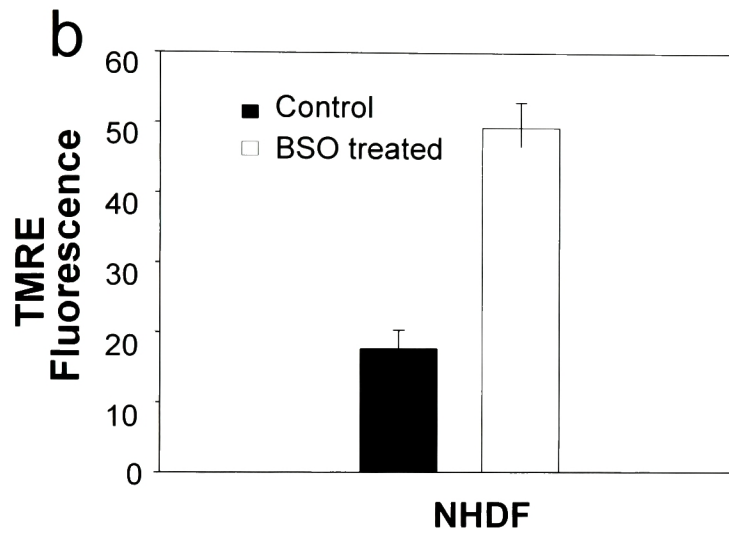
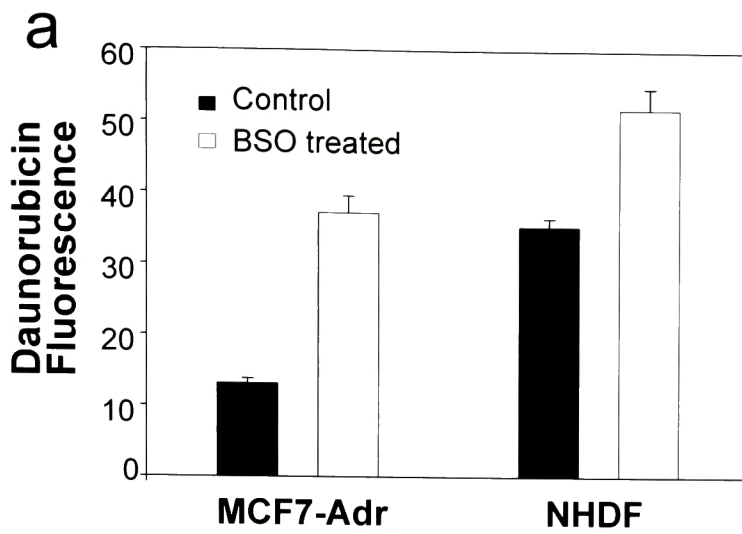


Figure 6-10. Evaluation of the effect of BSO on cells expressing varied levels of MRP1. a. Western blots of HeLa (lane 1), NHDF (lane 2), and MCF7-Adr (lane 5) cell lines reveal varied degrees of endogenous MRP1 expression, compared to MRP1-ECFP transfected HeLa cells (lane 3). Similar sample sizes were loaded. Arrows indicate position of MRP1. Lane 4 is a protein weight standard. b-c. BSO increases the permeability of MCF7-Adr cells to doxorubicin; micrographs are set to identical light threshold values, with identical exposure times. d-e. The effect of BSO on the permeability of MCF7-Adr cells to TMRE cannot be assessed, as TMRE does not enter these cells.

Figure 6-11. BSO increases cellular drug accumulation and has cytotoxic effects in NIH3T3 cells. a. A multidrug resistant tumor cell line (MCF7-Adr) and a primary cell line (NHDF) showed BSO-dependent increases in daunorubicin accumulation. b. NHDF cells also showed BSO-dependent increases in TMRE accumulation. c. The cytotoxicity of BSO in NIH 3T3 cells is demonstrated by the sudden decrease of adherent cells after BSO addition.



c NHDF cells with and without BSO

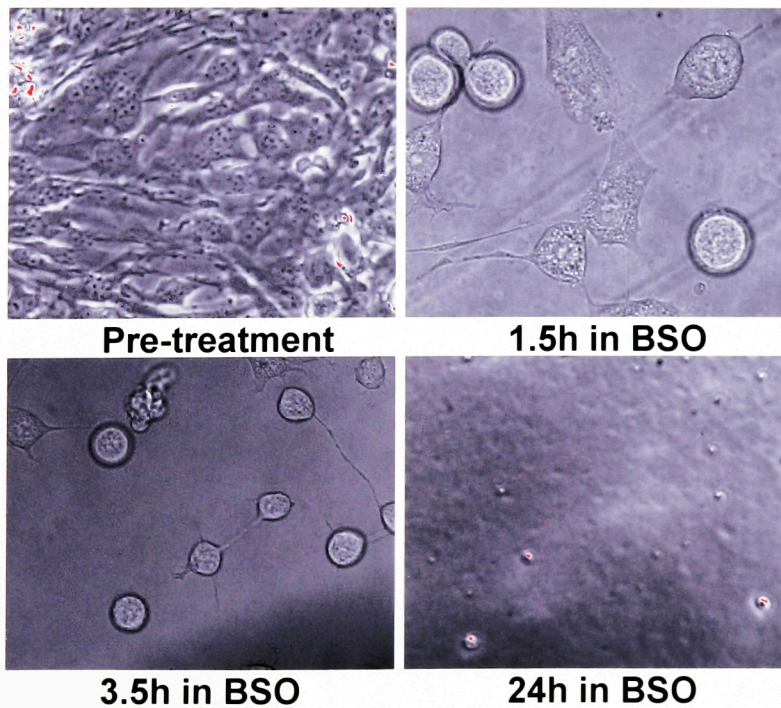


Table 6-1

Putative Substrate	Proteoliposomes (pmol/mg MRP1/min)	Time for 1 protein to transport 1 substrate molecule
LTC ₄	V _{max} 125	42 minutes
VCR* + GSH	19	4.6 hours
VCR alone	5	17.5 hours
GSH alone	30	2.9 hours
GSH* + VCR	60	1.67 hours

Table 6-2

Transporter	V _{max} of ATPase (nmol /mg/min)	ATP hydrolyzed/sec	Substrate turn over rates (substrate/sec)
Na+/K+ ATPase	800 (Bear)	100.0	Na+ : 500 (Hille)
Ca2+ ATPase	600 (Bear)		Ca2+: 200 (Hille)
Glucose transporter			Glucose: 10,000 (Hille)
P-glycoprotein: unstimulated stimulated by drug	(Ramachandra) 1000 6500	2.83 18.44 1.4	Vinblastine: 1.1 (Ambudkar)
CFTR	50-250 (Bear)	1.0	

Ambudkar,S.V., Cardarelli,C.O., Pashinsky,I., Stein,W.D. (1997). Relation between the turnover number for vinblastine transport and for vinblastine-stimulated ATP hydrolysis by human P-glycoprotein. J.Biol.Chem. 272, 21160-21166.

Hille, B. Ion Channels of Excitable Membranes. Sinauer Associates, 2001.

Li,C., Ramjeesingh,M., Wang,W., Garami,E., Hewryk,M., Lee,D., Rommens,J.M., Galley,K., Bear,C.E. (1996). ATPase activity of the cystic fibrosis transmembrane conductance regulator. Journal of Biological Chemistry 271, 28463-28468.

Mao,Q., Deeley,R.G., Cole,S.P. (2000). Functional reconstitution of substrate transport by purified multidrug resistance protein MRP1 (ABCC1) in phospholipid vesicles. Journal of Biological Chemistry 275, 34166-34172.

Ramachandra,M., Ambudkar,S.V., Chen,D., Hrycyna,C.A., Dey,S., Gottesman,M.M., Pastan,I. (1998). Human P-glycoprotein exhibits reduced affinity for substrates during a catalytic transition state. Biochemistry 37, 5010-5019.

Table 6-5

Cell Type	[GSH] after BSO treatment	MRP1-mediated drug reduction (%)		MRP1-mediated drug reduction in BSO treated cells		increase in drug uptake upon BSO treatment (%)	
		TMRE	Daun	TMRE	Daun	TMRE	Daun
Gcs-Nac	Non-detectable	71.2	51.0	NT	26.0	NT	28.5
HeLa	Non-detectable	84.8	87.4	65.3	49.9	64.8	112.8
NHDF	Non-detectable	78.9	84.5	71.1	48.3	179.0	46.6

Chapter 7 Conclusion

In the previous chapters, we have presented an *in vivo* examination of MRP1 activity which has, for the first time, investigated the role of the localization, substrate specificity, and co-factor dependence of MRP1 on a single cell basis. With the construction of our fluorescent MRP1-EGFP reporter, we have been able to address specific questions about the effects of expressing the protein in living cells, without the use of drug selection. In the absence of drug selection, our model system has avoided up-regulating other drug response mechanisms whose contributions to drug resistance might easily be conflated with the activity of MRP1. In this way, we have been able to examine the effect of expressing only MRP1 under different conditions: when using different cell lines or when using different putative substrates, in the absence of glutathione or in the presence of BSO. Our model system also allowed us to examine the effect of expressing other MDR-conferring proteins, either singly or pairs of them together, in the same cellular background and under the same culture conditions, and thus enabled more careful comparisons of the activity profiles of these proteins. Finally, the use of a fluorescent construct in single-cell assays allowed us to correlate degrees of protein expression to transport efficiencies on a cell per cell basis, an ability important for understanding thresholds of protein activity.

This single cell approach was especially useful in studying the sub-cellular localization and activity of MRP1. Using this technique, we were able to discern differences in the sub-cellular distribution of MRP1 in single cells expressing different levels of the protein. We saw cells for which the protein was predominantly in sub-cellular compartments, and cells for which the protein was

also significantly expressed at the plasma membrane. Using fluorescent markers for sub-cellular organelles, we were then able to identify MRP1-positive compartments during one stage in the trafficking history of the protein, and we were able to extend this localization to other multi-drug resistance proteins. Furthermore, we were able to correlate the sub-cellular expression of these proteins with patterns of drug accumulation, a task out of the range of other detection techniques (radio-labeled transport studies, immunocytochemistry and protocols requiring cell fixation). And, more importantly, with the use of cross-linking reagents, we were able to show, on a single cell level, that the activity from these sub-cellular compartments was sufficient to mimic a drug resistance phenotype.

Our model system was also useful in examining the dependence of MRP1 activity on glutathione. We were able to compare the activity profiles of the protein in cell lines depleted for glutathione with cells whose glutathione biosynthesis pathways were not disrupted. Single-cell examinations of transfected cells incubated in BSO revealed to us that the addition of this glutathione depleting agent increased cell permeability to MDR substrates. We saw that this BSO-mediated increase was independent of MRP1 activity, as GCS2-NAC cells genetically depleted of their glutathione stores also had increased cell permeability to MDR drugs upon BSO addition. These direct, side by side comparisons of cells both over-expressing and not over-expressing MRP1, of cells both treated and not treated with BSO, facilitated a more direct examination of MRP1 dependence upon glutathione. As a result, we have seen that in multiple cell lines, and with different modes of disrupting glutathione synthesis, MRP1 retains activity in the absence of glutathione.

This assessment of glutathione independence for MRP1 runs counter to many previously published examinations of MRP1 activity, and we have no ready explanation for this disagreement. It is possible that in the absence of glutathione, the cell employs other organic anions to catalyze MRP1-mediated transport. There are reports, for example, that ophthalmic acid can functionally substitute for glutathione in this capacity (Leslie *et al.*, 2001). It is also possible that the *in vitro* activity of MRP1, as revealed by protein reconstitution studies and membrane vesicle transport assays, is not representative of the activity of the protein in whole cells. In the process of purifying and reconstituting the protein, for example, MRP1 may have lost some of its activity; certainly, the transport rates reported for the protein would be consistent with this hypothesis.

Other interesting avenues of investigation also remain open at the end of this study. It has not been determined, for example, whether the functional re-expression of the GCS holoenzyme would affect MRP1-mediated transport in GCS2-NAC cells. We are of the opinion that any changes in MRP1 activity would be attributable to enhanced cell viability in the presence of glutathione. However, these questions could be tested by using another MDR protein like BCRP in conjunction with MRP1. Additionally, it would be interesting to determine whether in GCS2-NAC cells, MRP1 could transport conjugated organic anions, especially those conjugated anions that were previously thought to require glutathione for transport. Thus far, we have only tested the transport of cationic, hydrophobic substances like TMRE and daunorubicin in this cell line. Conjugated organic anions like estrone-3-sulfate nor NNAL-O-glucoronide may respond differently in this background. It might also be interesting to examine patterns of doxorubicin sequestration in these glutathione deficient cells, and test

whether glutathione could play any role in the metabolism or vesicular accumulation of the drug.

A number of questions are yet to be addressed with respect to the sub-cellular localization and activity of MRP1, too. We have seen that in one period in its trafficking history, the protein resides in the lysosomal compartment. What secretory path does the protein follow to arrive at this compartment? Has lysosomal MRP1 recently been endocytosed from the plasma membrane or has it followed the alternate ER-to-Golgi path to the lysosomes? Are there, then, two separate pools of the protein, one directed to the plasma membrane, and another to the lysosomes? Are there post-translational differences in these two pools or any other discernable method of segregating them? If there is only one pool of MRP1 in these cells, is the lysosomal pool derived from recently endocytosed plasma membrane MRP1 or is the plasma membrane MRP1 derived from recently exocytosed lysosomal MRP1? And with respect to the pool of lysosomal MRP1, does the protein reside in multi-vesicular bodies within the compartment or is the protein capable of halting the multi-vesicularization associated with lysosomal degradation?

We have seen that when MRP1-ECFP is weakly expressed in HeLa cells, MRP1 is to be found primarily in sub-cellular compartments, and not at the plasma membrane at all. Is this sub-cellular MRP1 also lysosomal or could it simply be protein associated with the Golgi or the ER? Moreover, we have only identified the sub-cellular compartment in one period in the trafficking history of the protein. Is the protein found predominantly in other sub-cellular compartments at other times? And is this trafficking history shared with other members of the MRP family? The apically-localized MRP2, for instance, has

been found to reside in a novel sub-cellular organelle in non-polarized hepatic cells (Tuma *et al.*, 2002); to what extent would the baso-laterally localized MRP1 also be found there if expressed in these cells? How much of the sub-cellular trafficking history of MRP1 is dependent upon cell and tissue type? Would the distribution of sub-cellular MRP1 be dependent upon polarization? And in tissues, would protracted drug exposure have any effect on the localization of the protein?

Questions also arise with respect to protein localization and doxorubicin resistance. It has been suggested, for example, that doxorubicin resistance in human MRP1 is dependent upon a specific residue in the protein (glutamate at amino acid 1089). Mutations in MRP1 at this residue sensitize otherwise resistant cells to doxorubicin, and the mouse ortholog, *mrp1*, which does not confer resistance to doxorubicin, also does not contain glutamate in the orthologous position. Moreover, mutations in mouse *mrp1* that result in glutamate conversions at this critical residue confer doxorubicin resistance (Zhang *et al.*, 2001). It would be interesting to see whether this residue, and patterns of doxorubicin resistance, are linked in any way to MRP1 targeting and sub-cellular localization. If drug sequestration is an important means of conferring MRP1-mediated resistance to doxorubicin, maybe residues in this region relay protein targeting information. Perhaps there are differences in the sub-cellular localization of mouse *mrp1* and human MRP1 that affect drug sensitivity.

Of course, there are a host of other problems and questions not directly addressed by the work presented in this thesis, such as the function of the protein in normal physiology, and the many changes that must occur, both in promoter regulation, and in protein trafficking, as a result of cellular transformation and

acquired drug resistance in whole organisms. Much work also remains to be done in the field addressing effective means of inhibiting MRP1-mediated drug resistance in a clinical setting. In all, the work presented in this thesis has addressed questions about MRP1 trafficking and activity, substrate specificity and co-factor dependence, and has at the same time, served to elicit many more and interesting questions along the way.

Bibliography

Altan,N., Chen,Y., Schindler,M., Simon,S.M. (1998). Defective acidification in human breast tumor cells and implications for chemotherapy. *Journal of Experimental Medicine* 187, 1583-1598.

Bakos,E., Hegedus,T., Hollo,Z., Welker,E., Tusnady,G.E., Zaman,G.J., Flens,M.J., Varadi,A., Sarkadi,B. (1996). Membrane topology and glycosylation of the human multidrug resistance- associated protein. *Journal of Biological Chemistry* 271, 12322-12326.

Bakos,E., Evers,R., Szakacs,G., Tusnady,G.E., Welker,E., Szabo,K., de Haas,M., van Deemter,L., Borst,P., Varadi,A., Sarkadi,B. (1998). Functional Multidrug Resistance Protein (MRP1) Lacking the N-terminal Transmembrane Domain. *Journal of Biological Chemistry* 273, 32167-32175.

Borst,P., Elferink,R.O. (2002). Mammalian ABC transporters in health and disease. *Annu.Rev.Biochem.* 71, 537-592.

Borst,P., Evers,R., Kool,M., Wijnholds,J. (1999). The multidrug resistance protein family. *Biochimica et Biophysica Acta* 1461, 347-357.

Borst,P., Evers,R., Kool,M., Wijnholds,J. (2000). A Family of Drug Transporters: the Multidrug Resistance-Associated Proteins. *J.Natl.Cancer Inst.* 92, 1295-1302.

Cabrita,M.A., Hobman,T.C., Hogue,D.L., King,K.M.,
Cass,C.E. (1999). Mouse transporter protein, a membrane protein that regulates cellular multidrug resistance, is localized to lysosomes. *Cancer Res.* 59, 4890-4897.

Chan,H.S., Haddad,G., Thorner,P.S., DeBoer,G., Lin,Y.P., Ondrusek,N.,
Yeger,H., Ling,V. (1991). P-glycoprotein expression as a predictor of the outcome of therapy for neuroblastoma. *N.Engl.J.Med.* 325, 1608-1614.

Chang,X.B., Hou,Y.X., Riordan,J.R. (1997). ATPase Activity of Purified Multidrug Resistance-associated Protein. *Journal of Biological Chemistry* 272, 30962-30968.

Chen,Y., Simon,S.M. (2000). In situ biochemical demonstration that P-glycoprotein is a drug efflux pump with broad specificity. *The Journal of Cell Biology* 148, 863-870.

Cole,S.P., Bhardwaj,G., Gerlach,J.H., Mackie,J.E., Grant,C.E.,
Almquist,K.C., Stewart,A.J., Kurz,E.U., Duncan,A.M., Deeley,R.G. (1992). Overexpression of a transporter gene in a multidrug-resistant human lung cancer cell line. *Science* 258, 1650-1654.

Cole,S.P., Chanda,E.R., Dicke,F.P., Gerlach,J.H., Mirski,S.E. (1991). Non-P-glycoprotein-mediated multidrug resistance in a small cell lung cancer cell line: evidence for decreased susceptibility to drug-induced DNA damage and reduced levels of topoisomerase II. *Cancer Res.* 51, 3345-3352.

- Cole,S.P., Sparks,K.E., Fraser,K., Loe,D.W., Grant,C.E.,
Wilson,G.M., Deeley, RG (1994). Pharmacological characterization of multidrug resistant MRP-transfected human tumor cells. *Cancer Research* 54, 5902-5910.
- Doyle,L.A., Yang,W., Abruzzo,L.V., Krogmann,T., Gao,Y., Rishi,A.K.,
Ross,D.D. (1998). A multidrug resistance transporter from human MCF-7 breast cancer cells. *Proceedings of the National Academy of Sciences* 95, 15665-15670.
- Evers,R., Zaman,G.J., van Deemter,L., Jansen,H., Calafat,J., Oomen,L.C.,
Oude Elferink,R.P., Borst,P., Schinkel,A.H. (1996). Basolateral localization and export activity of the human multidrug resistance-associated protein in polarized pig kidney cells. *J.Clin.Invest* 97, 1211-1218.
- Farkas,D.L., Wei,M.D., Febroriello,P., Carson,J.H., Loew,L.M. (1989).
Simultaneous imaging of cell and mitochondrial membrane potentials. *Biophys.J.* 56, 1053-1069.
- Feller,N., Broxterman,H.J., Wahrer,D.C.R., Pinedo,H.M. (1995b). ATP-dependent efflux of calcein by the multidrug resistance protein (MRP): no inhibition by intracellular glutathione depletion. *FEBS Letters* 368, 385-388.
- Flens,M.J., Izquierdo,M.A., Scheffer,G.L., Fritz,J.M., Meijer,C.J.,
Scheper,R.J., Zaman,G.J. (1994). Immunochemical detection of the multidrug resistance-associated protein MRP in human multidrug-resistant tumor cells by monoclonal antibodies. *Cancer Res.* 54, 4557-4563.

Flens,M.J., Zaman,G.J., van,d., V, Izquierdo,M.A.,
Schroeijers,A.B., Scheffer,G.L., van der,G.P., de Haas,M., Meijer,C.J.,
Scheper,R.J. (1996). Tissue distribution of the multidrug resistance protein. *Am J Pathol.* 148, 1237-1247.

Gottesman,M.M. (2002). Mechanisms of cancer drug resistance.
Annu.Rev.Med. 53, 615-627.

Gottesman,M.M., Fojo,T., Bates,S.E. (2002). Multidrug resistance in
cancer: role of ATP-dependent transporters. *Nat.Rev.Cancer* 2, 48-58.

Grant,C.E., Kurz,E.U., Cole,S.P., Deeley,R.G. (1997). Analysis of the
intron-exon organization of the human multidrug- resistance protein gene (MRP)
and alternative splicing of its mRNA. *Genomics* 45, 368-378.

Grant,C.E., Valdimarsson,G., Hipfner,D.R., Almquist,K.C., Cole,S.P.,
Deeley,R.G. (1994). Overexpression of multidrug resistance-associated protein
(MRP) increases resistance to natural product drugs. *Cancer Res.* 54, 357-361.

Gros,P., Ben Neriah,Y.B., Croop,J.M., Housman,D.E. (1986). Isolation
and expression of a complementary DNA that confers multidrug resistance.
Nature 323, 728-731.

Hipfner,D.R., Deeley,R.G., Cole,S.P. (1999). Structural, mechanistic and
clinical aspects of MRP1. *Biochimica et Biophysica Acta* 1461, 359-376.

Hooijberg,J.H., Broxterman,H.J., Kool,M., Assaraf,Y.G., Peters,G.J.,
Noordhuis,P., Scheper,R.J., Borst,P., Pinedo,H.M., Jansen,G. (1999). Antifolate

resistance mediated by the multidrug resistance proteins MRP1 and MRP2. *Cancer Res.* 59, 2532-2535.

Hooijberg, J.H., Pinedo, H.M., Vrasdonk, C., Priebe, W., Lankelma, J., Broxterman, H.J. (2000). The effect of glutathione on the ATPase activity of MRP1 in its natural membranes. *FEBS Lett.* 469, 47-51.

Hurwitz, S.J., Terashima, M., Mizunuma, N., Slapak, C.A. (1997). Vesicular anthracycline accumulation in doxorubicin-selected U-937 cells: participation of lysosomes. *Blood* 89, 3745-3754.

Ito, K., Olsen, S.L., Qiu, W., Deeley, R.G., Cole, S.P. (2001). Mutation of a single conserved tryptophan in multidrug resistance protein 1 (mrp1/abcc1) results in loss of drug resistance and selective loss of organic anion transport. *Journal of Biological Chemistry* 276, 15616-15624.

Kartner, N., Riordan, J.R., Ling, V. (1983). Cell surface P-glycoprotein associated with multidrug resistance in mammalian cell lines. *Science* 221, 1285-1288.

Lampson, M.A., Schmoranz, J., Zeigerer, A., Simon, S.M., McGraw, T.E. (2001). Insulin-regulated release from the endosomal recycling compartment is regulated by budding of specialized vesicles. *Mol. Biol. Cell* 12, 3489-3501.

Lange, K., Gartzke, J. (2001). Microvillar cell surface as a natural defense system against xenobiotics: a new interpretation of multidrug resistance. *Am. J. Physiol Cell Physiol* 281, C369-C385.

Leier,I., Jedlitschky,G., Buchholz,U., Center,M., Cole,S.P.,
Deeley,R.G., Keppler,D. (1996). ATP-dependent glutathione disulphide transport
mediated by the MRP gene- encoded conjugate export pump. *Biochem.J.* *314* (*Pt*
2), 433-437.

Leier,I., Jedlitschky,G., Buchholz,U., Cole,S.P., Deeley,R.G., Keppler,D.
(1994). The MRP gene encodes an ATP-dependent export pump for C4 and
structurally related conjugates. *Journal of Biological Chemistry* *269*, 27807-
27810.

Leslie,E.M., Ito,K., Upadhyaya,P., Hecht,S.S., Deeley,R.G., Cole,S.P.
(2001). Transport of the beta -O-glucuronide conjugate of the tobacco-specific
carcinogen 4-(methylnitrosamino)-1-(3-pyridyl)-1-butanol (NNAL) by the
multidrug resistance protein 1 (MRP1). Requirement for glutathione or a non-
sulfur-containing analog. *J Biol.Chem.* *276*, 27846-27854.

Li,Z.S., Szczypka,M., Lu,Y.P., Thiele,D.J., Rea,P.A. (1996). The Yeast
Cadmium Factor Protein (YCF1) Is a Vacuolar Glutathione S-Conjugate Pump.
Journal of Biological Chemistry *271*, 6509-6517.

Lippincott-Schwartz,J., Donaldson,J.G., Schweizer,A., Berger,E.G.,
Hauri,H.P., Yuan,L.C., Klausner,R.D. (1990). Microtubule-dependent retrograde
transport of proteins into the ER in the presence of brefeldin A suggests an ER
recycling pathway. *Cell* *60*, 821-836.

Litman,T., Brangi,M., Hudson,E., Fetsch,P., Abati,A., Ross,D.D.,
Miyake,K., Resau,J.H., Bates,S.E. (2000). The multidrug-resistant phenotype

associated with overexpression of the new ABC half-transporter, MXR (ABCG2). *J. Cell Sci.* 113 (Pt 11), 2011-2021.

Llopis, J., McCaffery, J.M., Miyawaki, A., Farquhar, M.G., Tsien, R. Y. (1998). Measurement of cytosolic, mitochondrial, and Golgi pH in single living cells with green fluorescent proteins. *Proc. Natl. Acad. Sci. U.S.A* 95, 6803-6808.

Loe, D.W., Deeley, R.G., Cole, S.P. (1998). Characterization of vincristine transport by the M(r) 190,000 multidrug resistance protein (MRP): evidence for cotransport with reduced glutathione. *Cancer Research* 58, 5130-5136.

Loe, D.W., Deeley, R.G., Cole, S.P. (2000). Verapamil stimulates glutathione transport by the 190-kDa multidrug resistance protein 1 (MRP1). *J. Pharmacol. Exp. Ther.* 293, 530-538.

Loe, D.W., Almquist, K.C., Cole, S.P.C., Deeley, R.G. (1996a). ATP-dependent 17beta-Estradiol 17-(beta-D-Glucuronide) Transport by Multidrug Resistance Protein (MRP). *Journal of Biological Chemistry* 271, 9683-9689.

Loe, D.W., Almquist, K.C., Deeley, R.G., Cole, S.P.C. (1996b). Multidrug Resistance Protein (MRP)-mediated Transport of Leukotriene C(4) and Chemotherapeutic Agents in Membrane Vesicles. *Journal of Biological Chemistry* 271, 9675-9682.

Lu, Y.P., Li, Z.S., Drozdowicz, Y.M., Hortensteiner, S., Martinoia, E., Rea, P.A. (1998). AtMRP2, an Arabidopsis ATP binding cassette transporter able to transport glutathione S-conjugates and chlorophyll catabolites: functional comparisons with Atmrp1. *Plant Cell* 10, 267-282.

Lu,Y.P., Li,Z.S., Rea,P.A. (1997). AtMRP1 gene of *Arabidopsis* encodes a glutathione S-conjugate pump: Isolation and functional definition of a plant ATP-binding cassette transporter gene. *Proceedings of the National Academy of Sciences* 94, 8243-8248.

Mans,D.R., Schuurhuis,G.J., Treskes,M., Lafleur,M.V., Retel,J., Pinedo,H.M., Lankelma,J. (1992). Modulation by D,L-buthionine-S,R-sulphoximine of etoposide cytotoxicity on human non-small cell lung, ovarian and breast carcinoma cell lines. *Eur.J.Cancer* 28A, 1447-1452.

Mao,Q., Deeley,R.G., Cole,S.P. (2000). Functional reconstitution of substrate transport by purified multidrug resistance protein MRP1 (ABCC1) in phospholipid vesicles. *Journal of Biological Chemistry* 275, 34166-34172.

Morrow,C.S., Smitherman,P.K., Diah,S.K., Schneider,E., Townsend,A.J. (1998). Coordinated action of glutathione S-transferases (GSTs) and multidrug resistance protein 1 (MRP1) in antineoplastic drug detoxification. Mechanism of GST A1-1- and MRP1-associated resistance to chlorambucil in MCF7 breast carcinoma cells. *Journal of Biological Chemistry* 273, 20114-20120.

Muller, M. Human ABC transporters. 2003. Ref Type: Internet Communication.

Paul,S., Breuninger,L.M., Tew,K.D., Shen,H., Kruh,G.D. (1996). ATP-dependent uptake of natural product cytotoxic drugs by membrane vesicles establishes MRP as a broad specificity transporter. *Proceedings of the National Academy of Sciences* 93, 6929-6934.

Qian,Y.M., Grant,C.E., Westlake,C.J., Zhang,D.W.,
 Lander,P.A., Shepard,R.L., Dantzig,A.H., Cole,S.P., Deeley,R.G. (2002).
 Photolabeling of human and murine multidrug resistance protein 1 with the high
 affinity inhibitor [125I]LY475776 and azidophenacyl- [35S]glutathione. *Journal*
of Biological Chemistry 277, 35225-35231.

Qian,Y.M., Song,W.C., Cui,H., Cole,S.P., Deeley,R.G. (2001).
 Glutathione stimulates sulfated estrogen transport by multidrug resistance
 protein1. *Journal of Biological Chemistry* 276, 6404-6411.

Rajagopal,A., Pant,A.C., Simon,S.M., Chen,Y. (2002). In vivo analysis of
 human multidrug resistance protein 1 (MRP1) activity using transient expression
 of fluorescently tagged MRP1. *Cancer Research* 62, 391-396.

Renes,J., de Vries,E.G., Nienhuis,E.F., Jansen,P.L., Muller,M. (1999).
 ATP- and glutathione-dependent transport of chemotherapeutic drugs by the
 multidrug resistance protein MRP1. *Br.J.Pharmacol.* 126, 681-688.

Robbiani,D.F., Finch,R.A., Jager,D., Muller,W.A., Sartorelli,A.C.,
 Randolph,G.J. (2000). The leukotriene C(4) transporter MRP1 regulates CCL19
 (MIP-3beta, ELC)- dependent mobilization of dendritic cells to lymph nodes. *Cell*
103, 757-768.

Rybczynska,M., Liu,R., Lu,P., Sharom,F.J., Steinfels,E., Pietro,A.D.,
 Spitaler,M., Grunicke,H., Hofmann,J. (2001). MDR1 causes resistance to the
 antitumour drug miltefosine. *Br.J.Cancer* 84, 1405-1411.

Schindler,M., Grabski,S., Hoff,E., Simon,S.M. (1996).

Defective pH regulation of acidic compartments in human breast cancer cells (MCF-7) is normalized in adriamycin-resistant cells (MCF-7adr). *Biochemistry* 35, 2811-2817.

Schultz,M.J., Wijnholds,J., Peppelenbosch,M.P., Vervoordeldonk,M.J., Speelman,P., van Deventer,S.J., Borst,P., van der,P.T. (2001). Mice lacking the multidrug resistance protein 1 are resistant to *Streptococcus pneumoniae*-induced pneumonia. *J.Immunol.* 166, 4059-4064.

Shi,Z.Z., Osei-Frimpong,J., Kala,G., Kala,S.V., Barrios,R.J., Habib,G.M., Lukin,D.J., Danney,C.M., Matzuk,M.M., Lieberman,M.W. (2000). Glutathione synthesis is essential for mouse development but not for cell growth in culture. *Proc.Natl.Acad.Sci.U.S.A* 97, 5101-5106.

Tommasini,R., Evers,R., Vogt,E., Mornet,C., Zaman,G.J., Schinkel,A.H., Borst,P., Martinoia,E. (1996). The human multidrug resistance-associated protein functionally complements the yeast cadmium resistance factor 1. *Proceedings of the National Academy of Sciences* 93, 6743-6748.

Tuma,P.L., Nyasae,L.K., Hubbard,A.L. (2002). Nonpolarized cells selectively sort apical proteins from cell surface to a novel compartment, but lack apical retention mechanisms. *Mol.Biol.Cell* 13, 3400-3415.

Vincent De Vita,Jr., Samuel Hellman, Steven A Rosenberg (2001). *Cancer: Principles of Oncology*. Lippincott Williams & Wilkins.

Wijnholds,J., deLange,E.C., Scheffer,G.L., van den Berg,D.J., Mol,C.A., van,d., V, Schinkel,A.H., Scheper,R.J., Breimer,D.D., Borst,P. (2000). Multidrug resistance protein 1 protects the choroid plexus epithelium and contributes to the blood-cerebrospinal fluid barrier. *J.Clin.Invest* 105, 279-285.

Wijnholds,J., Evers,R., van Leusden,M.R., Mol,C.A., Zaman,G.J., Mayer,U., Beijnen,J.H., van,d., V, Krimpenfort,P., Borst,P. (1997). Increased sensitivity to anticancer drugs and decreased inflammatory response in mice lacking the multidrug resistance-associated protein. *Nature Medicine* 3, 1275-1279.

Wijnholds,J., Scheffer,G.L., van,d., V, van,d., V, Beijnen,J.H., Scheper,R.J., Borst,P. (1998). Multidrug resistance protein 1 protects the oropharyngeal mucosal layer and the testicular tubules against drug-induced damage. *Journal of Experimental Medicine* 188, 797-808.

Wioland,M.A., Fleury-Feith,J., Corlieu,P., Commo,F., Monceaux,G., Lacau-St-Guily,J., Bernaudin,J.F. (2000). CFTR, MDR1, and MRP1 immunolocalization in normal human nasal respiratory mucosa. *J Histochem.Cytochem.* 48, 1215-1222.

Yokomizo,A., Kohno,K., Wada,M., Ono,M., Morrow,C.S., Cowan,K.H., Kuwano,M. (1995). Markedly decreased expression of glutathione S-transferase pi gene in human cancer cell lines resistant to buthionine sulfoximine, an inhibitor of cellular glutathione synthesis. *Journal of Biological Chemistry* 270, 19451-19457.

Zaman,G.J., Lankelma,J., van Tellingen,O., Beijnen,J.,
Dekker,H., Paulusma,C., Oude Elferink,R.P., Baas,F., Borst,P. (1995). Role of
glutathione in the export of compounds from cells by the multidrug-resistance-
associated protein. *Proc.Natl.Acad.Sci.U.S.A* 92, 7690-7694.

Zhang,D.W., Cole,S.P., Deeley,R.G. (2001). Identification of an Amino
Acid Residue in Multidrug Resistance Protein 1 Critical for Conferring Resistance
to Anthracyclines. *Journal of Biological Chemistry* 276, 13231-13239.



THE LIBRARY



19010000484335

